C.3

SANDIA REPORT

SAND96–2031 • UC–742
Unlimited Release
Printed August 1996

Precision Linear Shaped Charge Analyses for Severance of Metals

Manuel G. Vigil

Prepared by
Sandia National Laboratories
Albuquerque, New Mexico 87185 and Livermore, California 94550
for the United States Department of Energy
under Contract DE-AC04-94AL85000

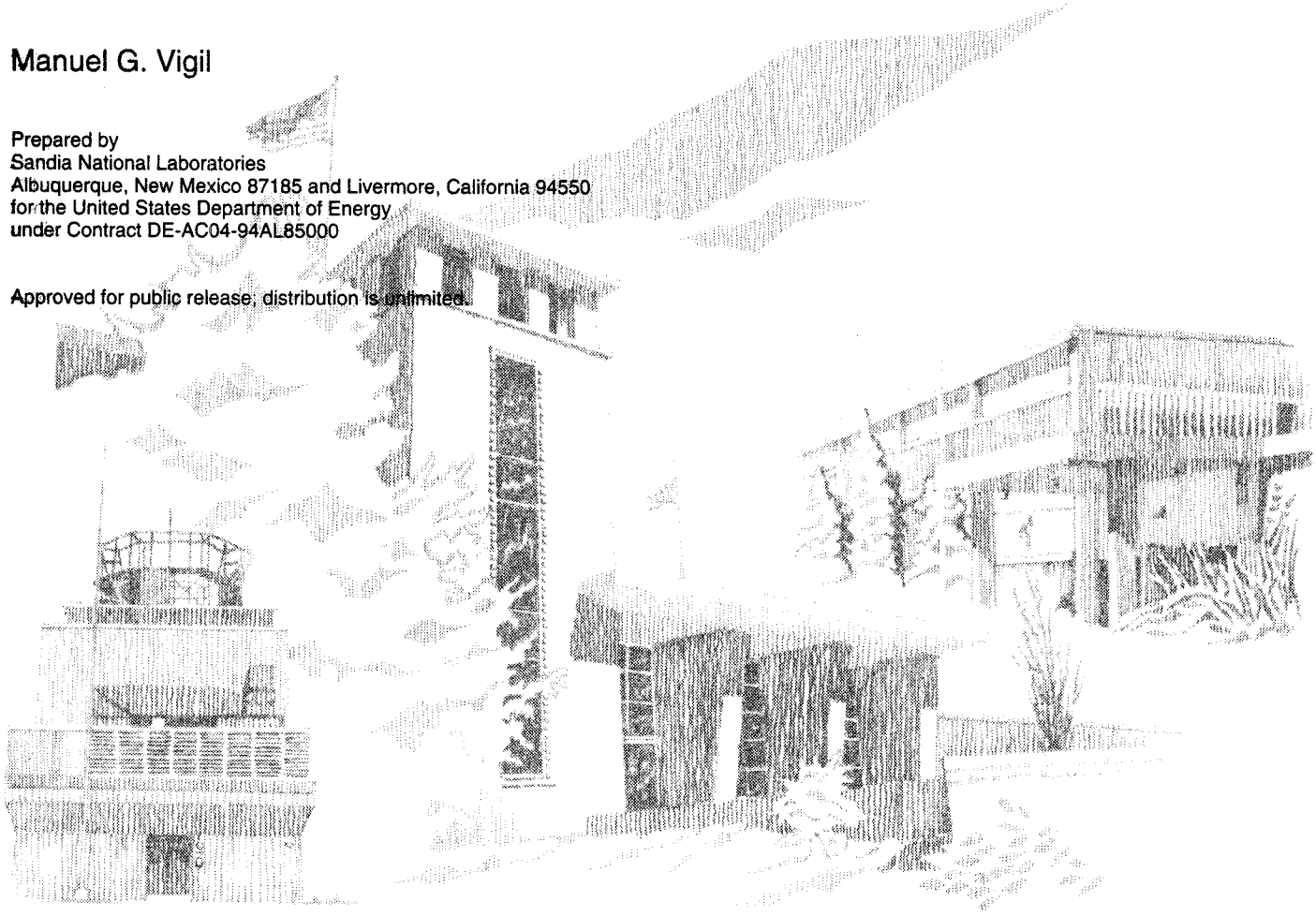

SF2900Q(8-81)

Issued by Sandia National Laboratories, operated for the United States Department of Energy by Sandia Corporation.

Available to DOE and DOE contractors from
Office of Scientific and Technical Information
PO Box 62
Oak Ridge, TN 37831

Prices available from (615) 576-8401, FTS 626-8401

Available to the public from
National Technical Information Service
US Department of Commerce
5285 Port Royal Rd
Springfield, VA 22161

NTIS price codes
Printed copy: A06
Microfiche copy: A01

SAND96-2031
Unlimited Release
Printed August 1996

Distribution
Category UC-742

PRECISION LINEAR SHAPED CHARGE ANALYSES FOR SEVERANCE OF METALS

Manuel G. Vigil
Explosive Components Department
Sandia National Laboratories
Albuquerque, New Mexico 87185

Abstract

The Precision Linear Shaped Charge (PLSC) design concept involves the independent fabrication and assembly of the liner (wedge of PLSC), the tamper/confinement, and explosive. The liner is the most important part of a linear shaped charge (LSC) and should be fabricated by a more quality controlled, precise process than the tamper material. Also, this concept allows the liner material to be different from the tamper material. The explosive can be loaded between the liner and tamper as the last step in the assembly process rather than the first step as in conventional LSC designs. PLSC designs have been shown to produce increased jet penetrations in given targets, more reproducible jet penetration, and more efficient explosive cross-section geometries using a minimum amount of explosive. The Linear Explosive Shaped Charge Analysis (LESCA) code developed at Sandia National Laboratories has been used to assist in the design of PLSCs. LESCA predictions for PLSC jet tip velocities, jet-target impact angles, and jet penetration in aluminum and steel targets are compared to measured data. The advantages of PLSC over conventional LSC are presented.

As an example problem, the LESCA code was used to analytically develop a conceptual design for a PLSC component to sever a three-inch thick 1018 steel plate at a water depth of 500 feet (15 atmospheres).

Intentionally Left Blank

Contents

Introduction 1
General Linear Shaped Charge 1
Conventional Linear Shaped Charge 2
Precision Linear Shaped Charge 3
Linear Explosive Shaped Charge Analysis (LESCA) Code 3
"Flange" Liner Configuration PLSC 4
"W" Liner Configuration PLSC 6
Conclusion 10
References 13

Appendix A Variable Standoff Configuration 79
Appendix B Constant Standoff Configuration 91

Tables

I LSCAP Versus Experimental PLSC Parameters 17
II PLSC Jet Penetration of Aluminum Target Data 18
III Example Problem PLSC Parameters 19
IV Example Problem Jet Penetration in Steel Data Summary 20

Figures

1 LSC Cross-Section Variables 23
2 Linear Shaped Charge Collapse and Jetting 24
3 Conventional LSC Fabrication 25
4 Conventional 25 gr/ft, Al Sheath, HNS Explosive 26
5 Test-to-Test Reproducibility of Conventional LSC 27
6 PLSC Components 28
7 LESCA Code Model of LSC Cross Section 29
8 LESCA Jet Penetration Graphics 30
9 Photographs of LSC Jet Tip Envelope Angle and Jet Particle Velocity Vector 31
10 LESCA Code Graphical Representation of Half of the LSC Liner Collapse Process 32
11 LESCA Code LSC Simulation with Detonator at Minimum versus Maximum Standoff 33
12 "Flange" Type 25 gr/ft PLSC 34
13 Conventional LSC Predicted Jet Penetration versus Standoff Compared to Experimental Data 35
14 Jet Penetration in Aluminum versus Standoff for PLSC versus Conventional LSC (Al Liner, 90 degree apex, Al Tamper) 36
15 65 gr/ft, PLSC7 Actual Cross Section 37

16 65 gr/ft, PLSC7 Cross Section and Jet Penetration into Aluminum 6061-T6 versus Standoff (LESCA versus Measured Data) 38
17 20 gr/ft PLSC Jet Penetration in 6061-T6 Aluminum versus Standoff (LESCA versus Measured Data) 39
18 30 gr/ft PLSC6 Jet Penetration versus Standoff (LESCA Code versus Measured Data) 40
19 Reproducibility of Measured 30 gr/ft PLSC Jet Penetration versus Standoff Data (Two Tests) 41
20 Reproducibility of 30 gr/ft PLSC6 Jet Penetration versus Distance Along Target (Constant Standoff, Foam Tamper) 42
21 PLSC Jet Penetration Depth (P) versus PLSC Explosive Loading (G) for Aluminum Targets 43
21A 5000 gr/ft PLSC Configuration 45
22 5000 gr/ft PLSC - Aluminum Target Configuration 47
23 Penetration versus Standoff/5000 gr/ft PLSC 48
24 Penetration versus Target Length/5000 gr/ft PLSC 49
25 Penetration and Fracture of Aluminum Target/5000 gr/ft PLSC, Side View, Test #3 51
26 Penetration and Fracture of Aluminum Target/5000 gr/ft PLSC, Top View, Test #3 53
27 Penetration and Fracture of Aluminum Target/5000 gr/ft PLSC, Side View, Test #5 55
28 Penetration and Fracture of Aluminum Target/5000 gr/ft PLSC, Top View, Test #5 57
29 600 gr/ft Cu Sheath, RDX Explosive LSC 59
30 1440 gr/ft Cu Sheath, RDX Explosive LSC 59
31 2000 gr/ft Cu Sheath, RDX Explosive LSC 59
32 Penetration vs. Standoff/600 gr/ft LSC 60
33 Penetration vs. Standoff/1440 gr/ft LSC 61
34 Penetration vs. Standoff/2000 gr/ft LSC 62
35 Jet Penetration and Fracture of 1018 Steel Target, Side View 63
36 Jet Penetration and Fracture of 1018 Steel Target, Edge View 65
37 Jet Penetration and Fracture of 1018 Steel Target, Top View 67
38 850 gr/ft PLSC Configuration 69
39 Penetration vs. Standoff/850 gr/ft PLSC 70
40 Example Problem Configuration 71
41 PLSC Cross-Section Geometry/10,740 gr/ft PBXN-301 Explosive 72
42 PLSC - Steel Target Variable Standoff Configuration 73
43 LSC - Steel Target Variable Standoff Configuration 74
44 Penetration versus Standoff/10,740 gr/ft PLSC 75

45 PLSC - Steel Target Constant Standoff Configuration 76
46 Penetration versus Parallel Standoff 77
47 Jet Tip Velocities versus Distance Along the Liner 78

Intentionally Left Blank

PRECISION LINEAR SHAPED CHARGE ANALYSES FOR SEVERANCE OF METALS

Introduction

Sandia National Laboratories (SNL)[1-9] is involved in the design of Linear Shaped Charges (LSC) varying in size from as small as 10 to larger than 11,000 grains/foot (gr/ft). These LSC components are required to perform such functions as rocket stage separation, parachute deployment, parachute system release, flight termination, system destruct, bridge destruction, severance of thick metallic barriers and system flight abort or disablement. Most of the LSC components for these systems require precise and reproducible jet penetration using the minimum explosive and component weights.

Sandia National Laboratories has conducted research and development work to design Precision Linear Shaped Charges (PLSC).[1-9] The sweeping detonation and three-dimensional collapse process of an LSC is a complex phenomenon. The Linear Shaped Explosive Charge Analysis (LESCA) code was developed at SNL to assist in the design of PLSC components. Analytical output from the LESCA code is presented and compared to experimental data for various LSC designs in the 16 to 5000 gr/ft explosive loading range. The LESCA code models the motion of the LSC liner elements due to explosive loading, jet and slug formation, jet breakup, and target penetration through application of a series of analytical approximations. The structure of the code is intended to allow flexibility in LSC design, target configurations, and in modeling techniques. The analytical and experimental data presented include LSC jet penetration in aluminum and steel targets as a function of standoff, jet tip velocities, and jet-target impact angles.

As an example problem, the LESCA code was used to analytically develop a conceptual design for a PLSC component to sever a three-inch thick 1018 steel plate at a water depth of 500 feet (15 atmospheres).

General Linear Shaped Charge

The parameters or variables for a general linear shaped charge cross section are illustrated in Figure 1. The large number of variables defining an LSC cross-section geometry makes the design of "the" optimum LSC a very difficult task primarily because it is not obvious as to which variables to initially hold constant in any given parametric study. Therefore, the scaling of LSCs is not a simple task. The larger core explosive loading (gr/ft) of similar conventional LSCs from the same manufacturer do not necessarily produce deeper jet penetrations in a given target. As shown in Figure 1, the LSC design depends on many variables other than just total explosive weight. The generic operational characteristics of an LSC are shown in Figure 2. For

conventional off-the-shelf LSCs, a metal tube or sheath containing explosive is swage-formed so that a wedge or cavity is created on one side. The LSC is typically point- or end-initiated and a detonation wave propagates along the longitudinal axis. The wedge collapses on itself and forms a high velocity sheet of jet particles. In general, because of the sweeping (propagating direction is 90 degrees from the desired jet cutting direction) detonation wave, the jet particles are not projected perpendicular to the original direction of the liner nor is the particle velocity perpendicular to the jet front (the jet angle relative to the target will be illustrated in later sections).

As illustrated in Figure 2(b), the LSC liner collapse produces two molten metal projectiles or jets. The leading, relatively high velocity (0.3 - 0.5 cm/us) main jet produces most of the jet penetration into the target. The slower (0.1 - 0.15 cm/us) rear jet or slug is sometimes found embedded in the cavity generated in the target by the main jet. Total severance of a finite thickness target can be a result from both the penetration of the main jet and the fracture of the remaining target thickness. The fracture portion of the severance thickness usually varies and can be as much as 50% of the thickness depending on the target strength parameters.

Conventional Linear Shaped Charge

Typically, for more than 50 years, conventional LSCs have been fabricated by loading a cylindrical tube with granular explosives, and then roll- or swage-forming the loaded tube to the familiar chevron configuration illustrated in Figure 3.

Some of the disadvantages of conventional LSC designs are as follows:

1. Nonsymmetrical cross-section geometries,
2. Nonuniform explosive density (neither within a plane at a given distance or along the length),
3. Nonoptimized explosive and sheath cross-section geometries,
4. Nonreproducible jet penetrations in target materials, and
5. Historically designed for nonprecise jet cutting.

Typical explosive and sheath (liner and tamper) cross-section geometries of a conventional 25 gr/ft, aluminum sheathed LSC loaded with HNS II explosive are shown in Figure 4 for polished and magnified (20X) sections from the same lot and a couple of feet apart. Conventional LSC disadvantages 1 - 3 listed above are very obvious in Figure 4. Figure 5 illustrates the test-to-test variations in jet penetration of an aluminum target for the 25 gr/ft conventional LSC shown in Figure 4. The reproducibility of this LSC is plus or minus 39%.

Precision Linear Shaped Charges (PLSC)

For a PLSC, the liner, explosive, and tamper materials can be assembled as illustrated in Figure 6. The liner, tamper, and explosive are manufactured independently to allow the required control of fabrication methods which result in a more precise component. The quality control of the liner is most important in the performance of LSC devices.

An extruded, machined, buttered, or cast explosive is loaded or assembled between the liner and tamper components after these other two components are fabricated. The explosive can be loaded using single or multiple extrusions, automated continuous feed injection techniques, or by a "buttering" manual technique, if necessary. Assembly aids, such as the use of vacuum, are also useful.

The LESCA code has been used to improve the PLSC parameters. The explosive charge to liner mass ratio can be designed to optimize the transfer of energy from the detonation wave through the liner to the high-velocity jet. The explosive charge to tamper mass ratio can be designed to optimize the tamper material and thickness. The maximum tamper thickness is defined as that thickness beyond which no additional gain in the liner collapse velocity is obtained. The tamper can be made of a different material than that selected for the liner in order to:

1. Fit different configurations,
2. Allow for explosive loading (buttering, etc.),
3. Allow selection of tamping characteristics in material,
4. Allow for built-in shock mitigation properties, and
5. Allow for a built-in standoff housing free of foreign materials and water which degrade jet formation.

Linear Explosive Shaped Charge Analysis (LESCA) Code

The original Linear Shaped Charge Analysis Program (LSCAP) was renamed the Linear Explosive Shaped Charge Analysis (LESCA) code. Therefore, throughout this report, LSCAP and LESCA code modeling, simulation, and predictions are interchangeable. The renaming of the code was necessary because of confusion with the Shaped Charge Analysis Program (SCAP) also developed at Sandia for the design of conical shaped charges.

The modeling capabilities of the LESCA code include:

1. Sweeping/tangential detonation propagation,
2. Jet-target impact angles,
3. Liner acceleration and velocity,

4. Jet formation process,
5. Jet penetration process including layered targets,
6. Jet breakup stress model, and
7. Target strength modeling.

The code is inexpensive relative to hydrocodes, can be easily used to conduct parametric studies, and is interactive (user friendly). The LESCA modeling of half of an LSC cross section (symmetry is assumed) is illustrated in Figure 7. Figure 8 shows sample LESCA output illustrating an LSC with a variable standoff to an aluminum target, sweeping detonation, a jet front envelope of 26.7 degrees, jet particle path relative to the target, and a comparison of the predicted and experimental target-jet penetration at 8 and 24 microseconds, respectively. The data of Figure 8 illustrate the code ability to predict the jet particle path relative to the target surface.

The measured jet tip envelope angle, q (defined in Figure 8), and jet particle velocity vector angle, a (defined in Figure 8), are shown in Figure 9 for two different LSCs. Measured data from Cordin rotating mirror camera film records were used in the angle comparisons with LSCAP (LESCA) code predictions listed in Table I.

Assuming a symmetrical liner collapse process, typical LESCA code graphical representations are shown in Figure 10 for two different LSCs. The LSC jet, slug, liner, tamper, and detonation product gases are shown in Figure 10.

LESCA code predicted jet penetration versus standoff data are shown in Figure 11 for configurations with the detonator at the minimum versus maximum standoff end of the LSC, as illustrated in the top half of Figure 11. Experimental jet penetration versus LSC standoff from the target data are also compared to the LESCA code predictions in Figure 11.

Aluminum Targets

This section includes PLSC design configurations and LESCA code predicted versus measured jet penetrations into aluminum targets versus standoff data.

"Flange" Liner Configuration PLSC

The "flange" type PSLC design shown in Figure 12 was designed to allow the extrusion of the LX-13 explosive from one end of the liner and tamper assembly. The length that can be extruded varies with the area or size of cavity between the liner and the tamper materials.

25 gr/ft PLSC

The LESCA code jet penetration versus standoff data are compared to measured data in Figure 13 for the conventional, 25 gr/ft, HNS explosive, aluminum liner, aluminum tamper LSC

cross-section geometry shown in the figure. A similar PLSC was designed to compare jet penetration performance with the conventional LSC shown in Figure 13. Aluminum liner and tamper materials were used. The liner apex angle was the same as the conventional LSC (90 degrees). The explosive was LX-13 for the PLSC and HNS II for the conventional LSC. The LX-13 and HNS II explosive metal driving ability is about the same. The measured jet penetration into an aluminum 6061-T6 target versus standoff data are compared in Figure 14. The PLSC maximum jet penetration was 40% greater than for the conventional LSC.

A parametric study was conducted incorporating the following variables into the 25 gr/ft, LX-13 explosive, flange PLSC designs similar to Figure 12:

1. Explosives
   a. LX-13/XTX-8003/PBXN-301

2. Liner materials
   a. Copper
   b. Aluminum
   c. Nickel

3. Tamper/confinement material
   a. Aluminum

4. PLSC Geometry
   a. Liner apex angles (ß): 70, 90 and 105 degrees
   b. Liner thicknesses (t): .004, and .010 inches

The PLSC materials, liner thickness (t), and apex angles (ß) were varied as listed in Table I. The PLSC jet tip velocity (V_j), jet envelope angle (q), jet-target impact angle (a), jet penetration into an aluminum 6061-T6 target (P), and optimum standoff (S.O.) are also listed in Table I. The LESCA predicted data are compared to the experimental measured values for most of the parameters. The effect on jet penetration versus standoff due to variations in some of the PLSC cross-section parameters were published in Reference 1.

65 gr/ft PLSC7

The 65 gr/ft "flange" liner configuration PLSC7 cross-section geometry is shown in Figure 15. The jet penetration into an aluminum (6061-T6) target versus standoff data predicted by the LESCA code are compared to experimental data in Figure 16. The PLSC7 configuration includes a 0.012 inch thick copper liner, LX-13 explosive, and an aluminum tamper.

"W" Liner Configuration PLSC

20 gr/ft PLSC5

The "W" liner configuration PLSC design, cross-section geometry shown in Figure 17 was designed to allow the explosive to be loaded using an automated feed injection technique or manually loaded in the liner in a buttering technique. These loading techniques are required for relatively small PLSC cross sections where long segments are desired. The 20 gr/ft PLSC5, LESCA code predicted, jet penetration versus standoff data are compared to measured data in Figure 17. The PLSC5 configuration includes a 0.008 inch thick copper liner, LX-13 explosive, and aluminum tamper. The apex angle was 75 degrees.

30 gr/ft PLSC6

The "W" liner configuration design, 30 gr/ft PLSC6 cross-section geometry, and copper liner actual cross-section geometry are shown in Figure 18. The LESCA-code-predicted jet penetration into an aluminum 6061-T6 target versus standoff data are compared to measured data in Figure 18. The PLSC6 configuration includes a 0.008 inch thick copper liner, LX-13 explosive, an aluminum tamper, and a 77 degree liner apex angle.

The test-to-test reproducibility for the PLSC6 design is illustrated in Figure 19. The measured jet penetration versus standoff data are compared for two different tests with a variable standoff LSC versus target configuration as illustrated in Figures 8 and 11. The LSC to large standoff varied from zero at one end to 0.225 inches as the other end. The measured jet penetration versus distance along the target data are shown in Figure 20 for two different tests and for a constant standoff (between the LSC and target) of 0.100 inches. For either variable (Figure 19) or constant (Figure 20) standoff LSC-target configurations, the test to test reproducibility of the jet penetration is very good.

5,000 gr/ft PBXN-301 Explosive/PLSC

Previously, the largest (5,000 gr/ft) PLSC design cross-section configuration is shown in Figure-21. This is a copper, W liner configuration with a copper tamper housing crimped around the liner after the explosive was loaded. This PLSC configuration includes a 0.067 inch thick copper liner, PBXN-301 explosive, a copper tamper, and a 76 degree liner apex angle.

The PLSC and aluminum target test configuration is shown in Figure 22. The minimum PLSC standoff was 1.0 inches and the maximum standoff was 2.0 inches as shown in Figure 22. The target dimensions were 6 x 6 x 12 inches. The detonator was located at the maximum standoff end. The LESCA-code-predicted jet penetration into an aluminum 6061-T6 target versus standoff data are compared to measured data in Figures 23 and 24. Measured data for untreated and for annealed (1300 degrees F), air quenched copper liners are compared in Figures 23 and 24. Post-test photographs of the aluminum targets are shown in Figures 25 (side view of half of target) and 26 (top view of both halves of target) for test number 3 (annealed liner). Post-test photographs of the aluminum targets are shown in Figures 27 (side view of half of target) and 28 (top view of both halves of target) for test number 5 (untreated liner).

Steel Targets

This section includes linear shaped charge design configurations and LESCA code predicted versus measured jet penetrations into mild steel targets versus standoff data. The modeling/simulation of the LESCA code were validated using measured jet penetrations in mild steel targets from data generated at Sandia for 600, 850, 1440, and 2000 gr/ft LSCs.

Conventional LSCs

The cross-section geometries for the 600, 1440, and 2000 gr/ft conventional LSCs are shown in Figures 29 through 31, respectively. These LSCs contain copper sheaths (liner and tamper housing). These LSCs include RDX explosive and total widths ranging from 1.02 to 1.15 inches.

The LESCA-code-predicted jet penetration into mild steel targets versus standoff data are compared to measured data in Figures 32 through 34. Post-test photographs of a typical steel target are shown in Figures 35 (side view of half of target), 36 (edge view), and 37 (top view of both halves of target).

850 gr/ft PLSC

The 850 gr/ft PLSC configuration is shown in Figure 38. This PLSC includes a 0.067 inch thick copper liner, a polyethylene tamper housing, and Octol explosive as shown in Figure 38. The LESCA-code-predicted jet penetration into a mild steel target versus standoff data are compared to measured data in Figure 39.

Example Problem

General

As an example problem, the LESCA code was used to analytically develop a conceptual design for a PLSC component to sever a three-inch thick 1018 steel plate at a water depth of 500 feet (15 atmospheres). The problem configuration is shown in Figure 40. The practical application of such a problem was assumed to be similar to what might be required to scrap or salvage the steel from a sunken ship. Therefore, the explosive charge could be lowered from a ship using a spooled cable on a jib crane. Divers could place the detonator lines and PLSC on the plate to be severed. Two detonators could be used for higher reliability and redundancy. The detonator and PLSC would be installed inside a pressure vessel or housing to withstand the 15 atmospheres (220.5 psia) external pressure. The required PLSC standoff (to allow the jet to form) from the target would be built into the pressure vessel housing with a minimum material thickness for the jet to penetrate before impacting the steel target.

LESCA Code Modeling/Simulation

The assumption was made that there are no constraints or limitations in the following:

1. PLSC size/geometry,
2. Explosive type,
3. Liner material,
4. Tamper/confinement material,
5. PLSC to steel target standoff,
6. Explosive weight, and
7. Total component weight.

PLSC Liner Material

The liner material is usually chosen from as high a density as the chosen explosive can accelerate efficiently and of a very ductile material. The higher densities produce the deeper jet penetration in a given target material. The higher ductility allows the jet to stretch to a longer length before breakup and this also produces deeper penetrations. Economics and practicality are factors to be considered in the liner material selection. Obviously, gold and platinum could be considered if only a couple of sets of hardware are required. Depleted uranium and lead are environmentally not acceptable. Tantalum and copper are the mostly likely candidates with all things considered. Copper was selected for this study simply based on costs and workability. Shear formed (spun) and stamped manufactured liners perform the best.

Explosive

The desired explosive for a PLSC is extrudable, castable, or one that can be injected by a continuous feed, automated technique. Explosives with higher metal driving or acceleration ability are desired. Secondary explosives with relatively high densities (implies higher detonation pressure, velocity, energy and Gurney velocity) are the best. Although PBXN-301 (LX-13 or XTX-8003) does not have all of the desired properties, it was chosen for this study simply because it is readily available and can be easily loaded into a PLSC design. It is also very stable and water resistant after it cures. This explosive also cures to a homogeneous density throughout the cross-section geometry and along the length of the PLSC. PBXN-301, LX-13, and XTX-8003 are all made of 80% PETN explosive and 20% SYLGARD binder. The three designations refer to products manufactured by the Navy, Lawrence Livermore National Laboratory, and Los Alamos National Laboratory, respectively. This explosive has the following properties that are required to run LESCA:

1. Density: 1.53 g/cc
2. Detonation velocity: 0.73 cm/us
3. Gurney velocity: 0.25 cm/us
4. Explosive exponent: 2.88

Tamper/Confinement Material

The tamper or confinement of the PLSC should be fabricated from the most dense material that is practical or economically feasible. Material properties are not important except those that are required to assemble the hardware. Copper was arbitrarily chosen for this study.

Pressure Vessel Material

The pressure vessel material is chosen simply to structurally withstand the external pressure of 15 atmospheres. Because the PLSC jet must penetrate the vessel, this wall thickness must be kept to a minimum and of material made of relatively lower density. Titanium material would be ideal because of the relatively high strength and low density. Cost considerations usually result in the selection of a steel material.

Assumptions

The large number of variables (Figure 1) defining an LSC cross-section geometry makes the design of "the" optimum LSC a very difficult task, primarily because it is not obvious as to which variables to hold constant in any given parametric study. Therefore, several optimized PLSC designs are possible to perform a given task depending on any of a number of selected approaches.

Because of our experience and success with the "W" liner configuration, this design was chosen for this task. A parametric study including the LSC variables shown in Figure 1, using the LESCA code, was conducted to find the minimum explosive weight to sever the three inches of 1018 steel.

The following assumptions were made:

1. The steel severance would be accomplished by the jet only penetration (no credit taken for fracture);
2. Minimize the explosive weight for a given cross-section geometry;
3. The liner material is copper;
4. The explosive is PBXN-301;
5. The tamper/confinement material is copper; and
6. The length of the PLSC is arbitrary.

Results

The selected PLSC cross-section geometry is shown in Figure 41. The explosive loading is 10,740 gr/ft (about 1.5 lb/ft). The total PLSC component weight is 66,504 gr/ft (about 9.4 lb/ft).

The PLSC and steel target variable standoff configuration shown in Figures 42 and 43 was arbitrarily selected. This variable standoff configuration will allow the prediction of the PLSC maximum jet penetration (3.22) in steel and also the determination of the optimum standoff (2.0 inches) for this cross-section geometry as shown in Figure 44.

The constant standoff configuration shown in Figure 45 was arbitrarily selected. The constant standoff configuration can also allow the prediction of the PLSC maximum jet penetration (3.5 inches) in steel and also the determination of the optimum standoff (1.74 inches) as shown in Figure 46. The maximum jet penetration and optimum standoff between the variable and constant configurations is due to the difference in the jet particle vector-target impact angles [(α), see Figures 8 and 43].

The axes (X and Z) defining the jet vector are shown in Figure 43. The jet tip X-axis (VX), Z-axis (VZ), and resultant vector (VMAG) velocities versus distance (XI) from the liner apex (XI = 0) to the liner base (XI = 1) are shown in Figure 47. The maximum resultant vector jet tip velocity was 0.47 cm/us. The jet envelope angle [(β), defined in Figures 8 and 43] was 38 degrees. The jet particle vector-target impact angle [(α), see Figures 8 and 43] for the variable standoff is 71 degrees.

The PLSC jet - steel target penetration graphics are shown in Appendix A in Figures A1 through A9 for the variable standoff configuration. The PLSC jet - steel target penetration graphics are shown in Appendix B in Figures B1 through B9 for the constant standoff configuration.

Conclusion

Precision Linear Shaped Charge liner, tamper, and explosive fabrication processes have been demonstrated to produce increased jet penetrations in aluminum and steel targets, more reproducible jet penetrations, and more efficient explosive cross sections compared to equivalent commercial LSCs.

The LESCA predicted jet tip velocities are within 20% of the experimental values (Table I). The predicted jet envelope angles (q) relative to the PLSC are within 20% of the photometrically measured values (Table I). The measured jet-target angles (a) are within 11% of the predicted values (Table I). Data for PLSC jet penetration into an aluminum target was presented demonstrating a 10% reproducibility for a given test (Figure 20). Data were presented to illustrate 40% improvement in maximum jet penetration for a PLSC design compared to an equivalent 25 gr/ft conventional LSC design (Figure 14).

Jet penetration versus explosive loading data are summarized in Figure 21 and Table II for the PLSC designs for most of the aluminum target data presented in this report. The target material was aluminum 6061-T6. The explosive was LX-13. The tamping material was aluminum, copper or Lexan. The data include both "flange" and "W" PLSC designs. Both "W" and "flange" PLSC designs performed equally well. Data for fracture[10], which is part of the total severance of a finite thickness target, was not included in the jet only penetration data presented throughout this report. Modeling/simulation of the fracture mechanism requires the use of a hydrocode like CTH[11-12] which was developed at Sandia.

The LESCA code predicted maximum jet penetrations in steel were in very good agreement with the measured data as shown in Figures 32- 34 and 39 for 600, 1440, 2000, and 850 gr/ft LSCs. The sample problem PLSC liner, explosive, tamper, and target parameters are summarized in Table III. The PLSC performance parameters are summarized in Table IV.

A parametric study with the LESCA code to determine "the" optimum PLSC design is very difficult because of the large number of interrelated variables. This does, however, emphasize the importance of the LESCA code in obtaining a more optimized design than is currently available from conventional LSC designs. For a given, new component, once the customer requirements are defined (constraining or fixing some PLSC parameters), then the LESCA code can be used to optimize the remaining parameters.

If a more detailed, three-dimensional shock wave physics modeling/simulation is desired, then the CTH hydrocode can be used. In addition to the problem geometries, the code requires the equations of state and Rankine-Hugoniot parameters for all of the different materials to generate the following information:

1. Material flow graphics,
2. Pressure/shock contours in the different material,
3 Shock and rarefaction wave tracking in the different material,
4. Material density contours,
5. Material velocity, temperature, density and pressure-time profiles in all materials,
6. Explosive initiation from single to multiple points,
7. LSC liner acceleration,
8. Jet formation,
9. Jet elongation,
10. Jet penetration in all target materials, and
11. A lot of other information.

The PLSC designs similar to those presented here have recently been incorporated in Sandia National Laboratory (SNL) systems. The Explosive Components Department plans to use PLSC designs in all future SNL systems requiring jet severance of materials, including metals, Kevlar parachute suspension lines, thick steel plates, and graphite-epoxy motor cases.

Intentionally Left Blank

References

1. M. G. Vigil, Design and Development of Precision Linear Shaped Charges, SAND89-0196C. Proceedings of the 9th International Symposium on Detonation, Portland, OR, August 28-September 1, 1989.

2. M. G. Vigil, J. G. Harlan, *Optimal Design and Fabrication of Reproducible Linear Shaped Charges*, SAND86-0982. Sandia National Laboratories, Albuquerque, NM, 1986.

3. M. G. Vigil, *Design of Linear Shaped Charges Using the LESCA Code*, SAND90-0243. Sandia National Laboratories, Albuquerque, NM, April 1990.

4. A. C. Robinson, *LESCA - A Code For Linear Shaped Charge Analysis - Users Manual*, SAND90-0150. Sandia National Laboratories, Albuquerque, NM, May 1990.

5. M. G. Vigil, Precision Linear Shaped Charge Jet Severance of Graphite-Epoxy Materials, SAND92-0610C. Proceedings of NASA Aerospace Pyrotechnic Conference, Houston, TX, June 9-10, 1992.

6. A. C. Robinson, M. G. Vigil, An Analytical-Experimental Comparison of 150 and 220 Grain Per Foot Linear Shaped Charge Performance. Tenth International Symposium on Ballistics, San Diego, CA, October 27-29, 1987.

7. A. C. Robinson, *Shaped Charge Analysis Program - Users Manual for SCAP 1.0*, SAND85-0708. Sandia National Laboratories, Albuquerque, NM, April 1985.

8. A. C. Robinson, *Asymptotic Formulas for the Motion of Shaped Charge Liners*, SAND84-1712. Sandia National Laboratories, Albuquerque, NM, September 1984.

9. A. C. Robinson, *Multilayered Liners for Shaped Charge Jets*, SAND85-2300. Sandia National Laboratories, Albuquerque, NM, December 1985.

10. M. G. Vigil, Linear Shaped Charge Jet Penetration and the Associated Fracture of Metallic Targets, Memorandum of Record, Sandia National Laboratories, March 1, 1993.

11. J. M. McGlaun, S. L. Thompson, and M. G. Elrick, *CTH User's Manual and Input Instructions*, SAND88-0523. Sandia National Laboratories, April 1988.

12. J. M. McGlaun, S. L. Thompson, L. N. Kmetyk, M. G. Elrick, *A Brief Description of the Three -Dimensional Shock Wave Physics Code CTH*, SAND89-0607. Sandia National Laboratories, July 1990.

Intentionally Left Blank

Tables

Intentionally Left Blank

Table 1 LSCAP* Versus Experimental PLSC Parameters
Liner: Flange design, phase 0
Tamper: Aluminum
Explosive: PBXN301, 25 gr/ft, Ensign Bickford
Target: Aluminum 6061-T6
Cordin Camera: 0.233 us interframe time

Liner Mat.	t(in)	β(deg)	V_j(cm/μs)		θ(deg)		α(deg)		P(in)		S.O.(in)		t_{bm} (μs)
			EXP.	LSCAP	EXP.	LSCAP	EXP.	LSCAP	EXP.	LSCAP	EXP.	LSCAP	
AL	.004	70	.57	.65	49	55	62	62	.18	.36	.14	.37	2.6
AL	.004	90	.41	.32	36	26	73	77	.11	.27	.09	.28	NM
AL	.004	105	.38	.46	31	26	84	77	.14	.22	.15	.27	NM
AL	.010	90	.32	.37	28	30	74	75	.14	.15	.17	.17	NM
AL	.010	105	.28	.32	24	26	74	77	.13	.11	.20	.16	3.1
CU	.004	70	.40	.41	22	24	67	78	.11	.41	.15	.16	3.3
CU	.004	90	.36	.33	27	21	77	79	.16	.28	.11	.12	3.1
CU	.004	105	.26	.28	24	19	78	80	.16	.21	.23	.09	NM
CU	.010	70	.23	.25	19	18	80	81	.15	.20	.18	.02	3.1
CU	.010	90	.25	.20	15	16	80	82	.13	.08	.19	.09	NM
CU	.010	105	.15	.17	13	13	85	84	.14	TBD	.23	TBD	NM
NI	.004	90	.33	.33	23	21	74	79	.18	.28	.10	.10	NM
NI	.010	90	.22	.20	15	15	81	83	.11	.09	.15	.08	NM

V_j = jet tip velocity
θ = jet envelope angle relative to PLSC
β = liner apex angle
t = liner thickness
P = jet penetration, maximum
α = jet target impact angle
S.O = standoff, optimum
Exp. = experimental data
JBREAK = LSCAP jet breakup stress model
TBCON = jet breakup constant
YLIN = dynamic yield stress/liner
Umin = minimum jet penetration velocity
AL = aluminum 6061T6
CU = oxygen free copper/annealed/soft
NJ = annealed/soft/nickel
NM = not measurable
t_{bm} = measured jet breakup time
α = 90 - θ/2

* - LSCAP CODE RENAMED LESCA

Table II. PLSC Jet Penetration of Aluminum Target Data

PLSC	(gr/ft)	Explosive	Tamper	Target	Al P (in)	S.O. (in)	Steel P (in)
0	25	LX-13	Aluminum	6061-T6	0.170	0.100	
3	16	LX-3	Aluminum	7075-T6	0.070	0.080	
5	20	LX-13	Aluminum	6061-T6	0.130	0.909	
6	30	LX-13	Cu/Lexan	6061-T6	0.190	0.100	
7	65	LX-13	Aluminum	6061-T6	0.320	0.137	
8	850	OCTOL	Copper	6061-T6	1.52	0.75	0.9
9	5000	PBXN-301	Copper	6061-7651	3.2		
10	10,740	LX-13	Copper	6061-T6	5.1*		3.0*

P - Jet Penetration Depth
S.O. - PLSC Standoff From Target
(gr/ft) - grain/foot Explosive Loading

* - LESCA Predicted

Table III. Example Problem PLSC Parameters

ITEM	PARAMETER VALUE
LINER:	
Material:	Copper
Thickness (in):	0.100
Density (g/cc):	8.96
Sound velocity (cm/us):	0.394
Apex angle (degrees):	76
Inside width (in):	2.48
Outside width (in):	2.68
Apex height (in):	1.70
EXPLOSIVE:	
Type:	PBXN-301
Density (g/cc):	1.53
Detonation velocity (cm/us)	0.73
Gurney velocity(cm/us):	0.25
Explosive exponent:	2.88
Height (in):	2.38
Maximum width (in):	3.22
Explosive weight (gr/ft):	10,740
TAMPER/CONFINEMENT:	
Material:	copper
Density (g/cc):	8.96
Inside width (in):	3.22
Outside width (in):	3.85
Height (in):	2.52
TARGET:	
Material:	1018 steel
Density (g/cc):	7.86
Thickness (in):	3.0

Table IV. Example Problem Jet Penetration in Steel Data Summary

Target: 3.0 inch thick 1018 steel plate

ITEM	PARAMETER VALUE
Jet:	
Material:	copper
Tip Velocity (cm/us)	0.47
Envelope angle (degrees):	38
Particle vector-target angle(degrees):	71 (variable standoff)
Target Penetration:	
Variable Standoff(in):	3.22
Constant Standoff(in):	3.50
PLSC - Target Optimum Standoff:	
Variable Standoff(in):	2.00
Constant Standoff(in):	1.74

Figures

Intentionally Left Blank

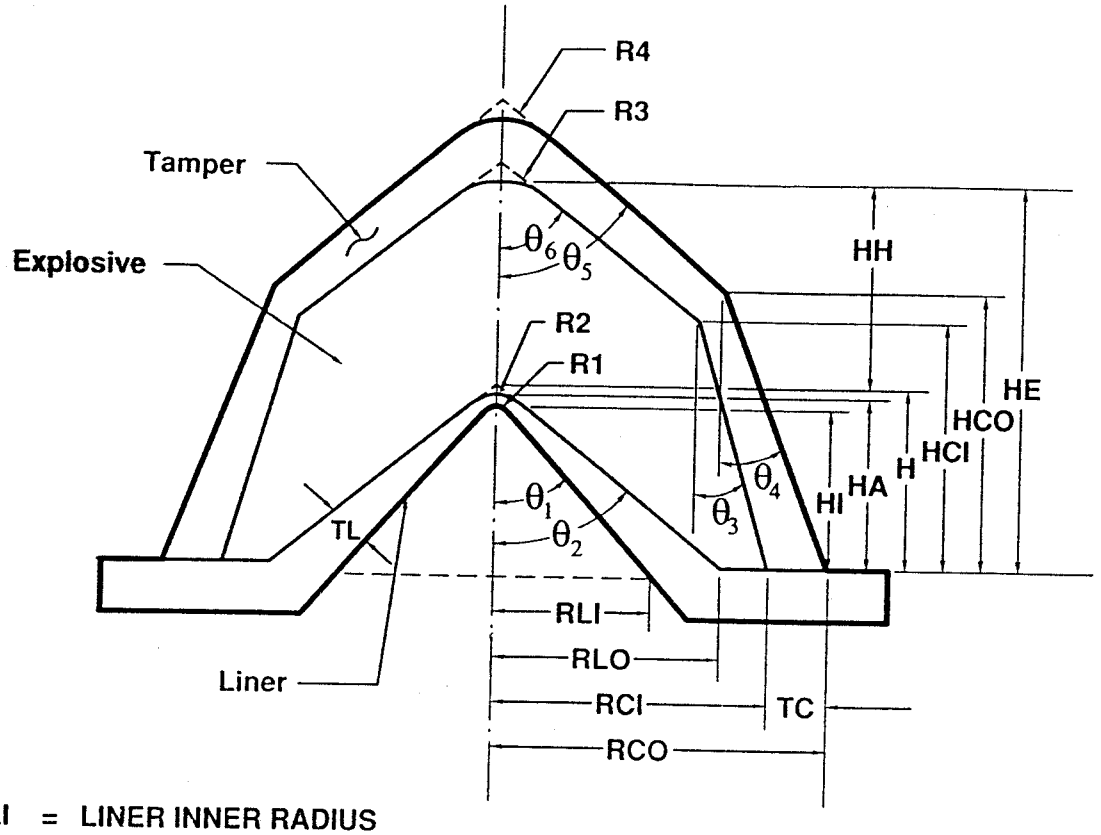

RLI = LINER INNER RADIUS
RLO = LINER OUTER RADIUS
RCI = CONFINEMENT/SHEATH INNER RADIUS
RCO = CONFINEMENT/SHEATH OUTER RADIUS
HI = LINER INNER HEIGHT
HA = LINER ACTUAL HEIGHT
H = LINER THEORETICAL APEX HEIGHT
HCI = CONFINEMENT/SHEATH INNER HEIGHT
HCO = CONFINEMENT/SHEATH OUTER HEIGHT
HE = EXPOSIVE HEIGHT
HH = EXPLOSIVE HEIGHT ABOVE APEX
TL = LINER THICKNESS
TC = CONFINEMENT/SHEATH THICKNESS
R1 = LINER INNER APEX RADIUS
R2 = LINER OUTER APEX RADUS
R3 = CONFINEMENT/SHEATH INNER APEX RADIUS
R4 = CONFINEMENT/SHEATH OUTER APEX RADIUS
θ_1 = LINER INNER APEX HALF ANGLE
θ_2 = LINER OUTER APEX HALF ANGLE
θ_3 = CONFINEMENT/SHEATH INNER APEX HALF ANGLE
θ_4 = CONFINEMENT/SHEATH OUTER APEX HALF ANGLE

FIGURE 1. LSC CROSS-SECTION VARIABLES

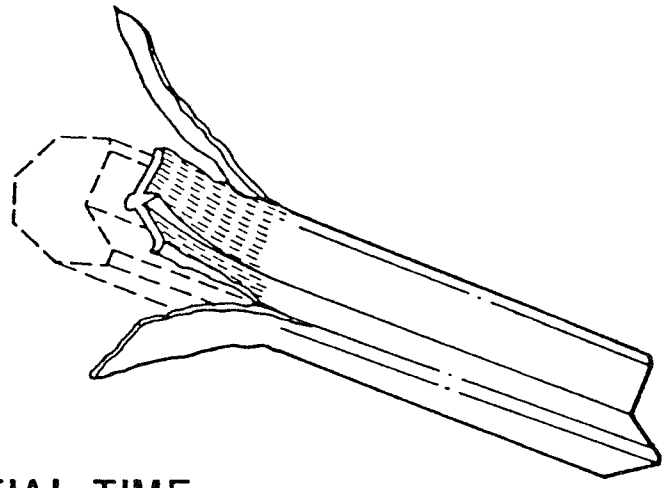

(a) INITIAL TIME

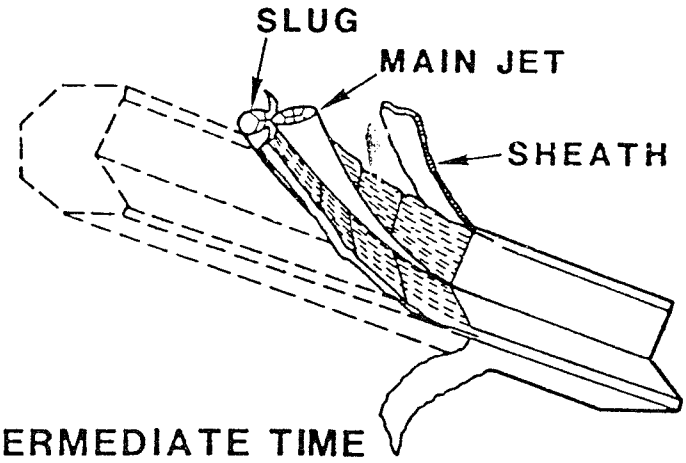

(b) INTERMEDIATE TIME

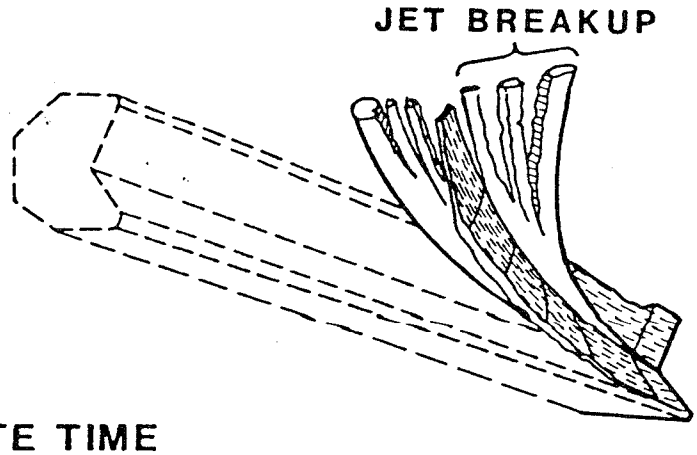

(c) LATE TIME

FIGURE 2. LINEAR SHAPED CHARGE COLLAPSE & JETTING

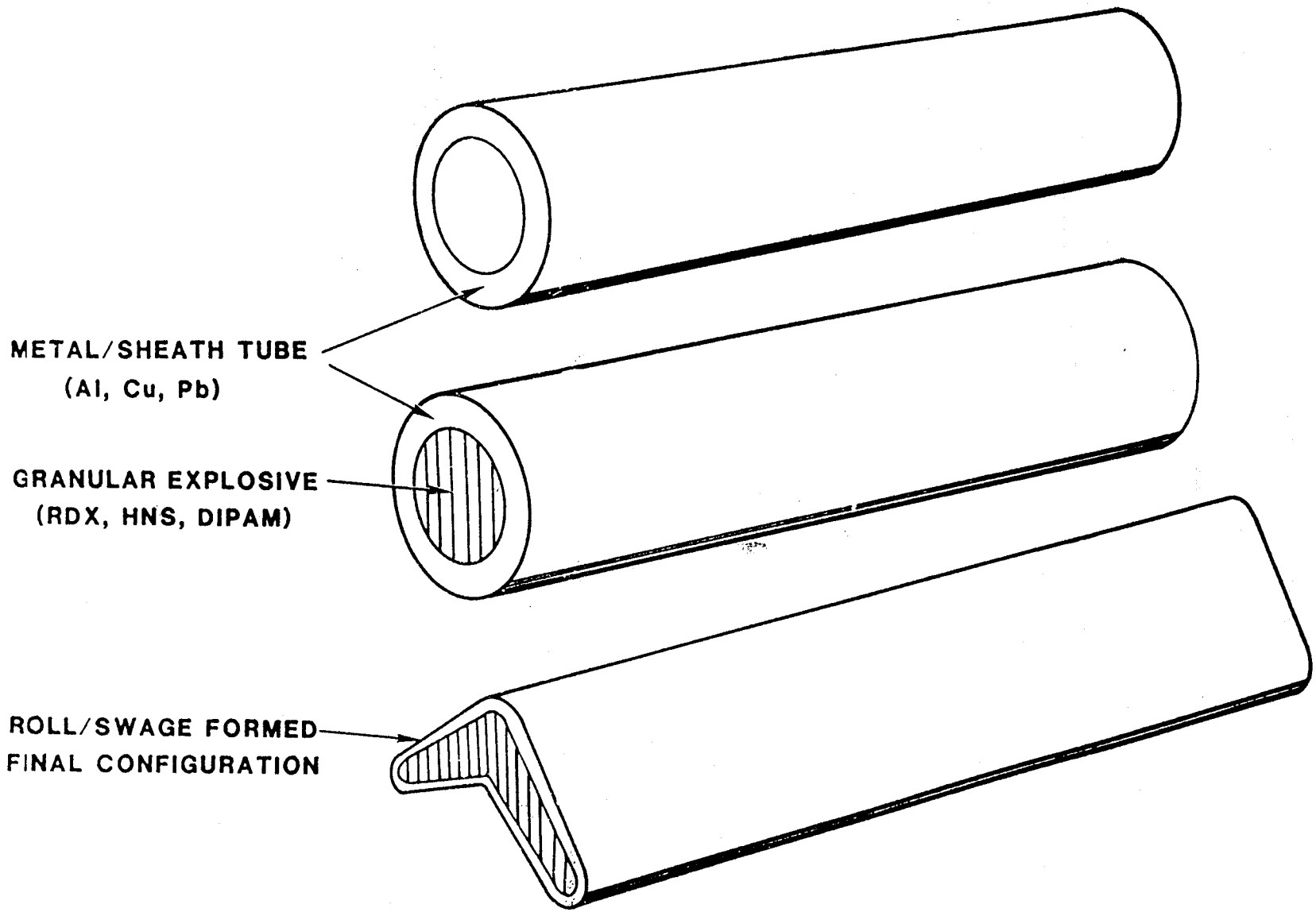

FIGURE 3. CONVENTIONAL LSC FABRICATION

MAGNIFICATION - 20X

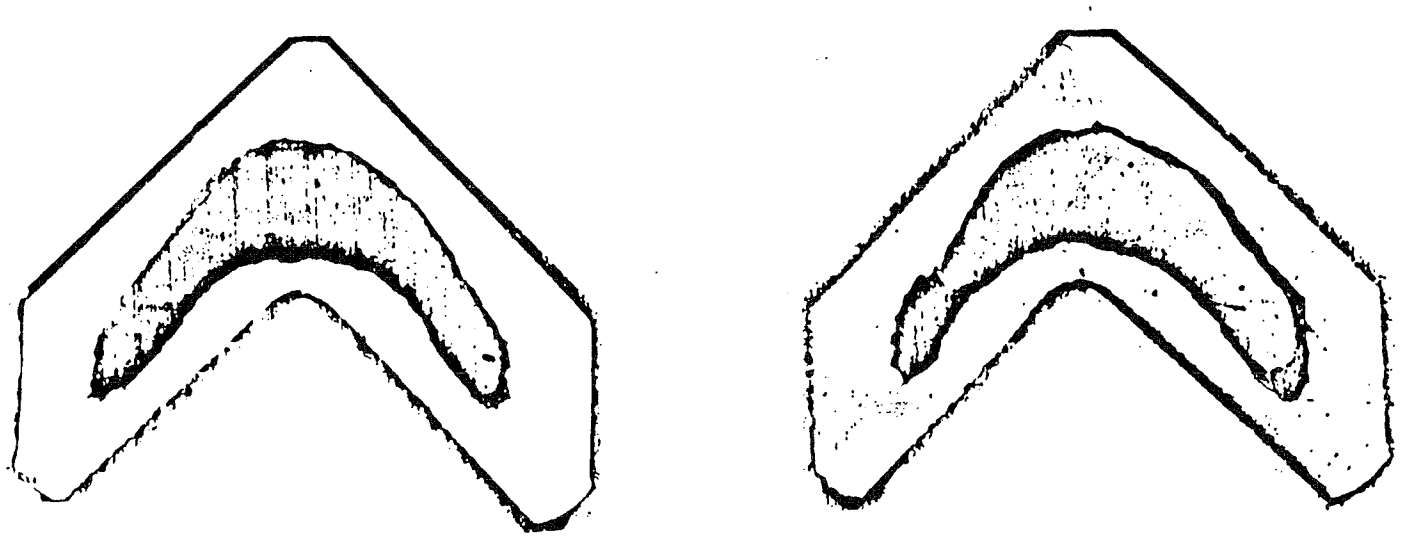

FIGURE 4. CONVENTIONAL 25 gr/ft, Al SHEATH, HNS EXPLOSIVE ACTUAL CROSS-SECTION

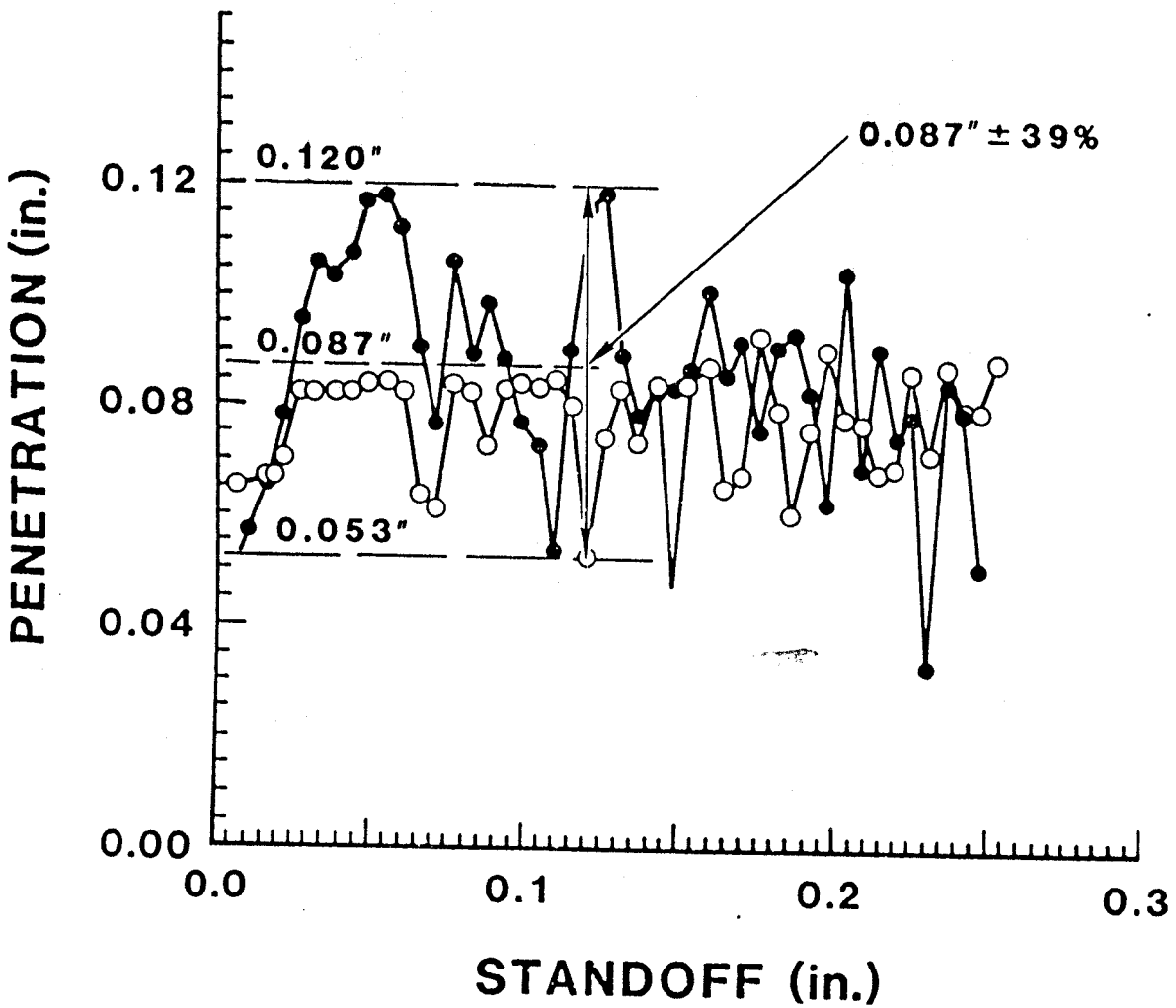

FIGURE 5. TEST TO TEST REPODUCIBILITY OF CONVENTIONAL LSC

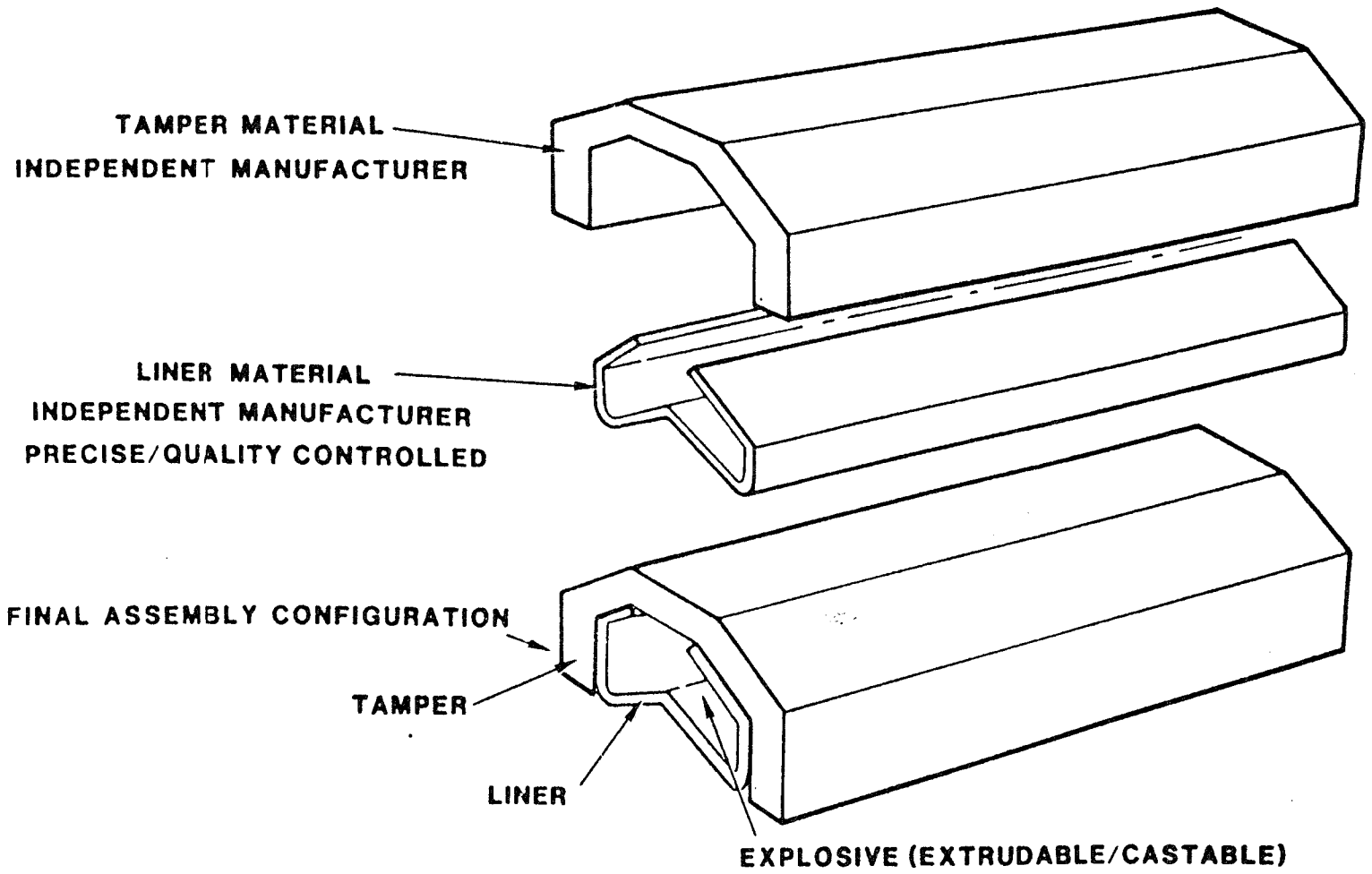

FIGURE 6. PLSC COMPONENTS

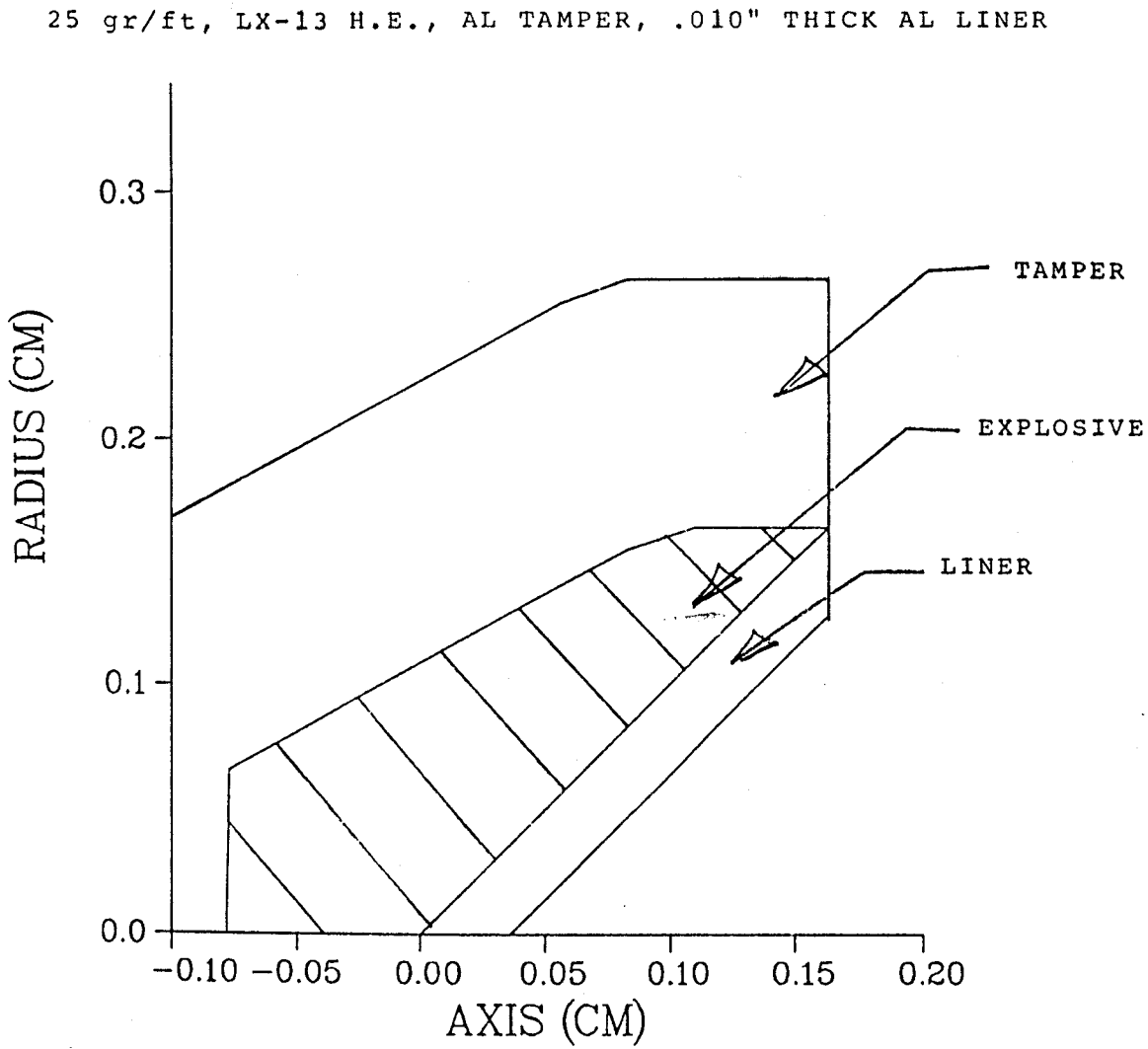

FIGURE 7. LESCA CODE MODEL OF LSC CROSS-SECTION

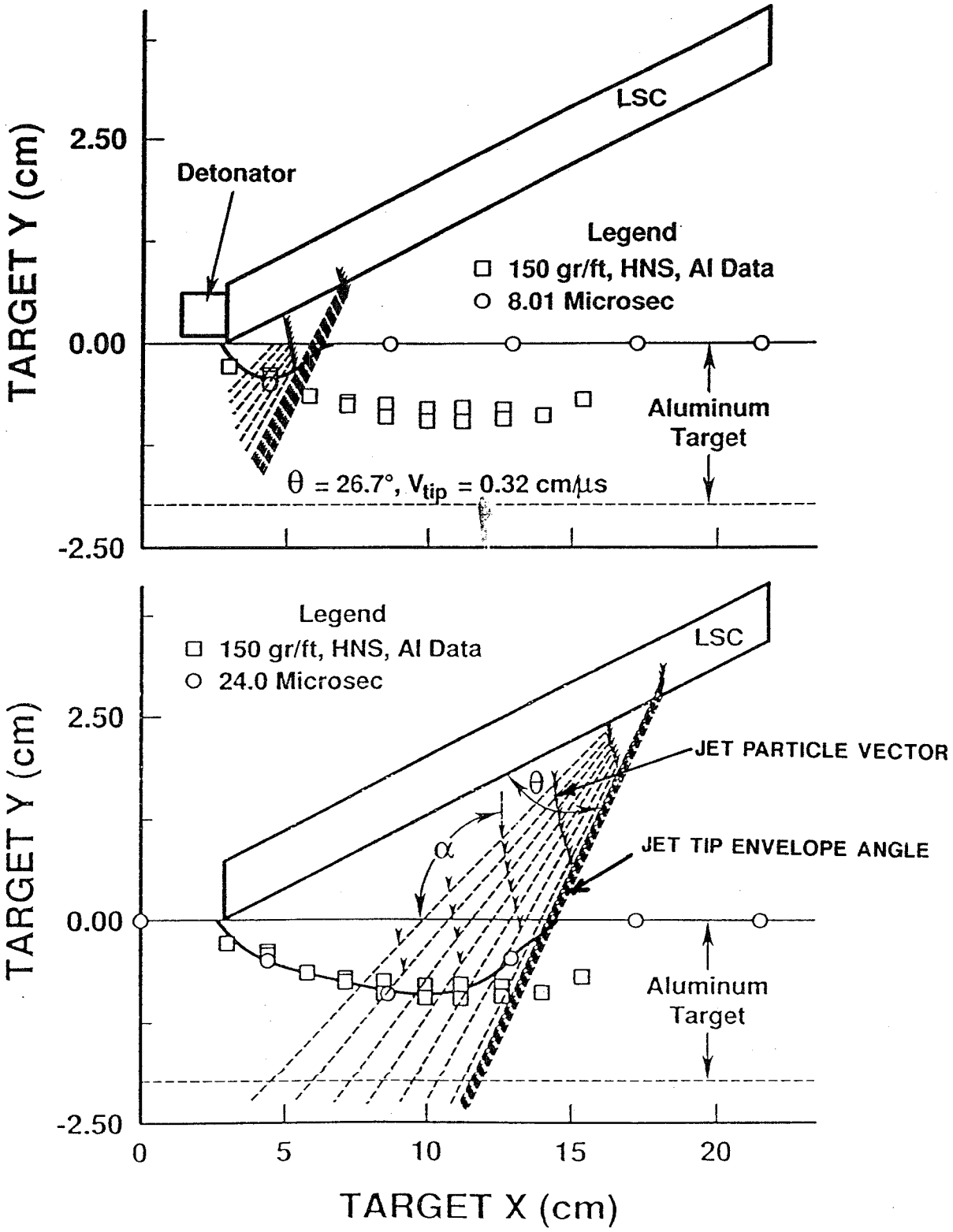

FIGURE 8. LESCA JET PENETRATION GRAPHICS

TA0117 01 08

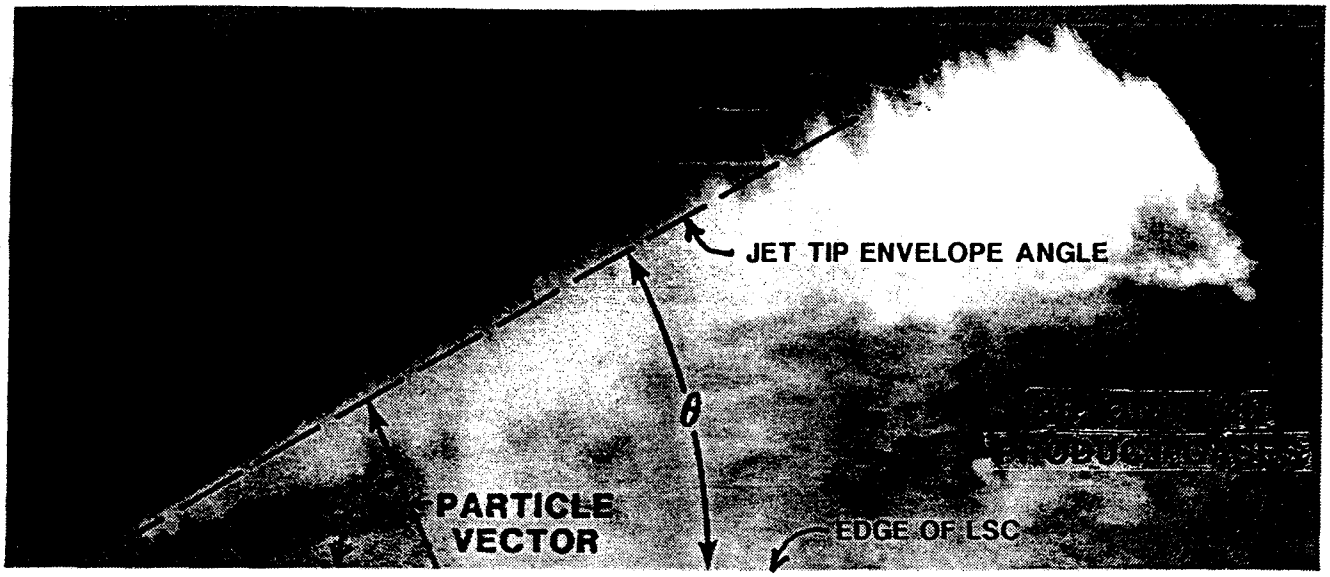

PHOTOGRAPH OF 150 gr/ft, RDX, Al SHEATH, LSC JET

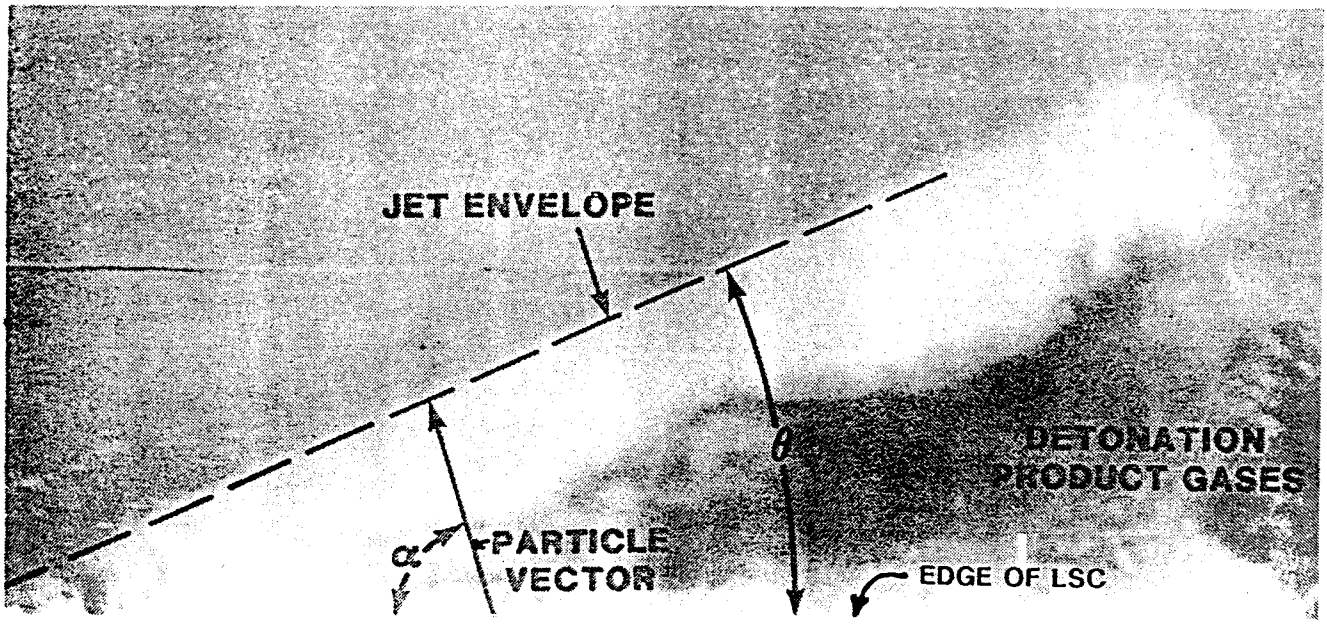

PHOTOGRAPH OF 220 gr/ft, RDX, Al SHEATH, LSC JET

FIGURE 9. PHOTOGRAPHS OF LSC JET TIP ENVELOPE ANGLE AND JET PARTICLE VELOCITY VECTOR

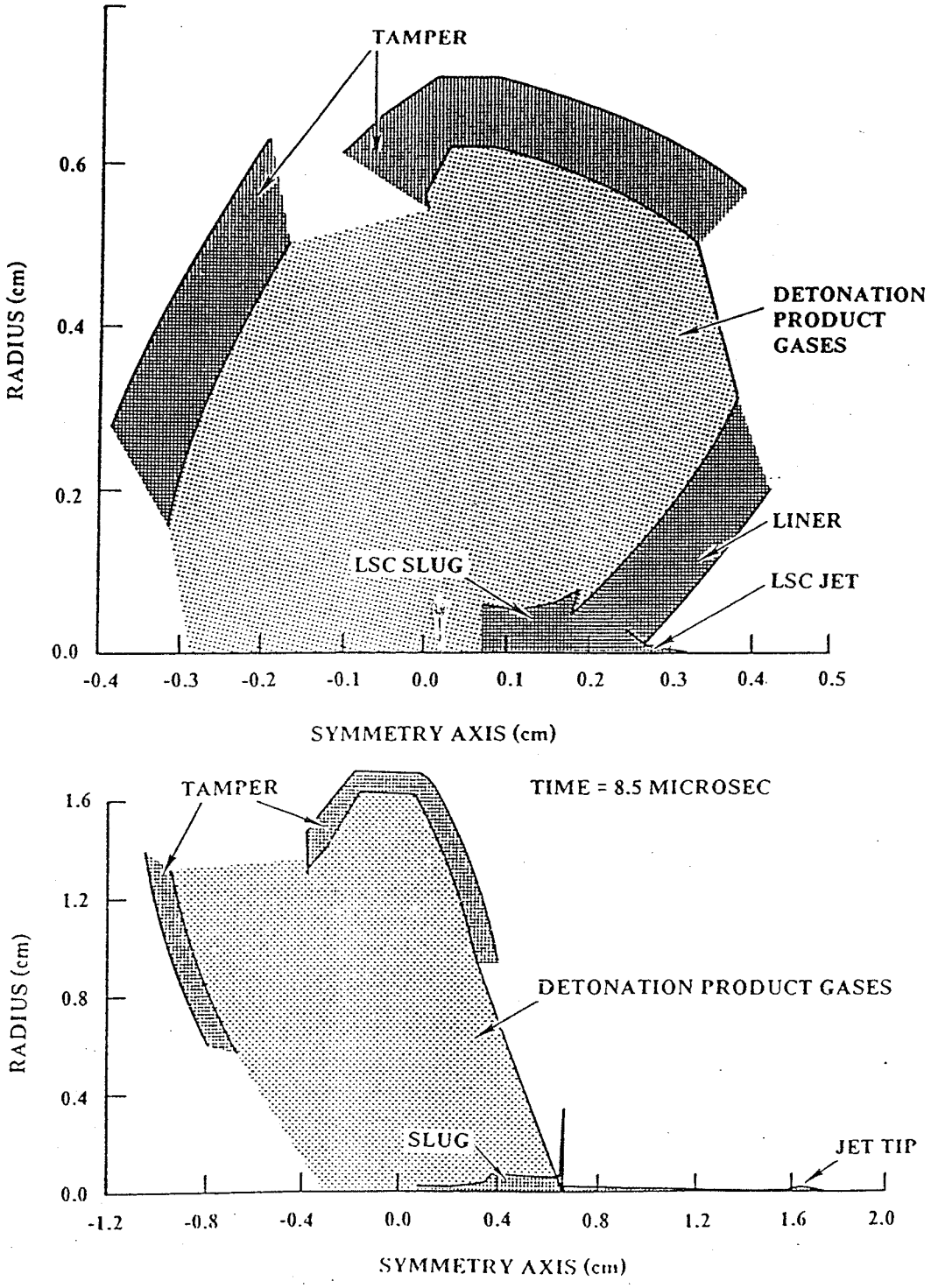

FIGURE 10. LESCA CODE GRAPHICAL REPRESENTATION OF HALF OF THE LSC LINER COLLAPSE PROCESS

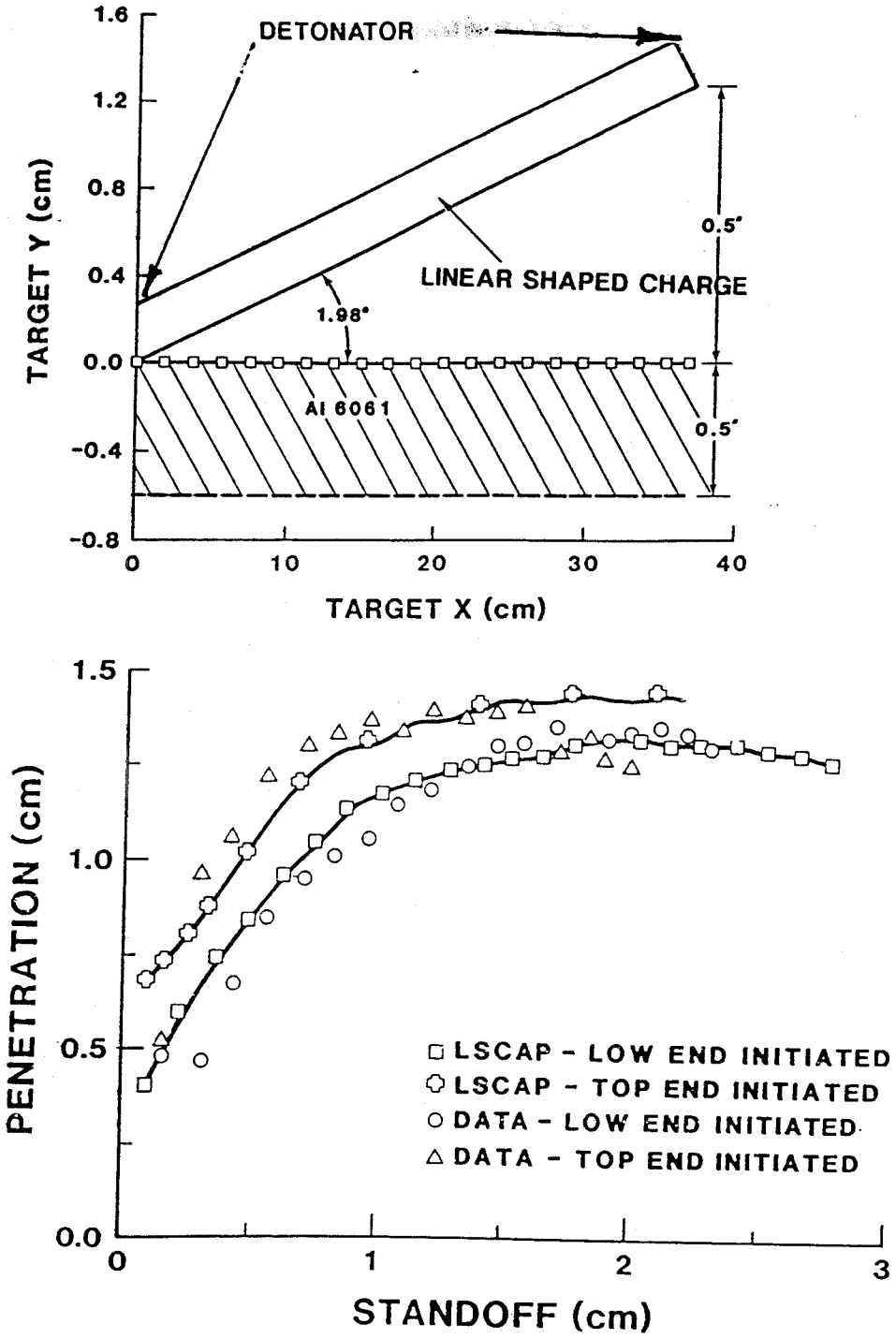

FIGURE 11. LESCA CODE LSC SIMULATION WITH DETONATOR AT MINIMUM VERSUS MAXIMUM STANDOFF

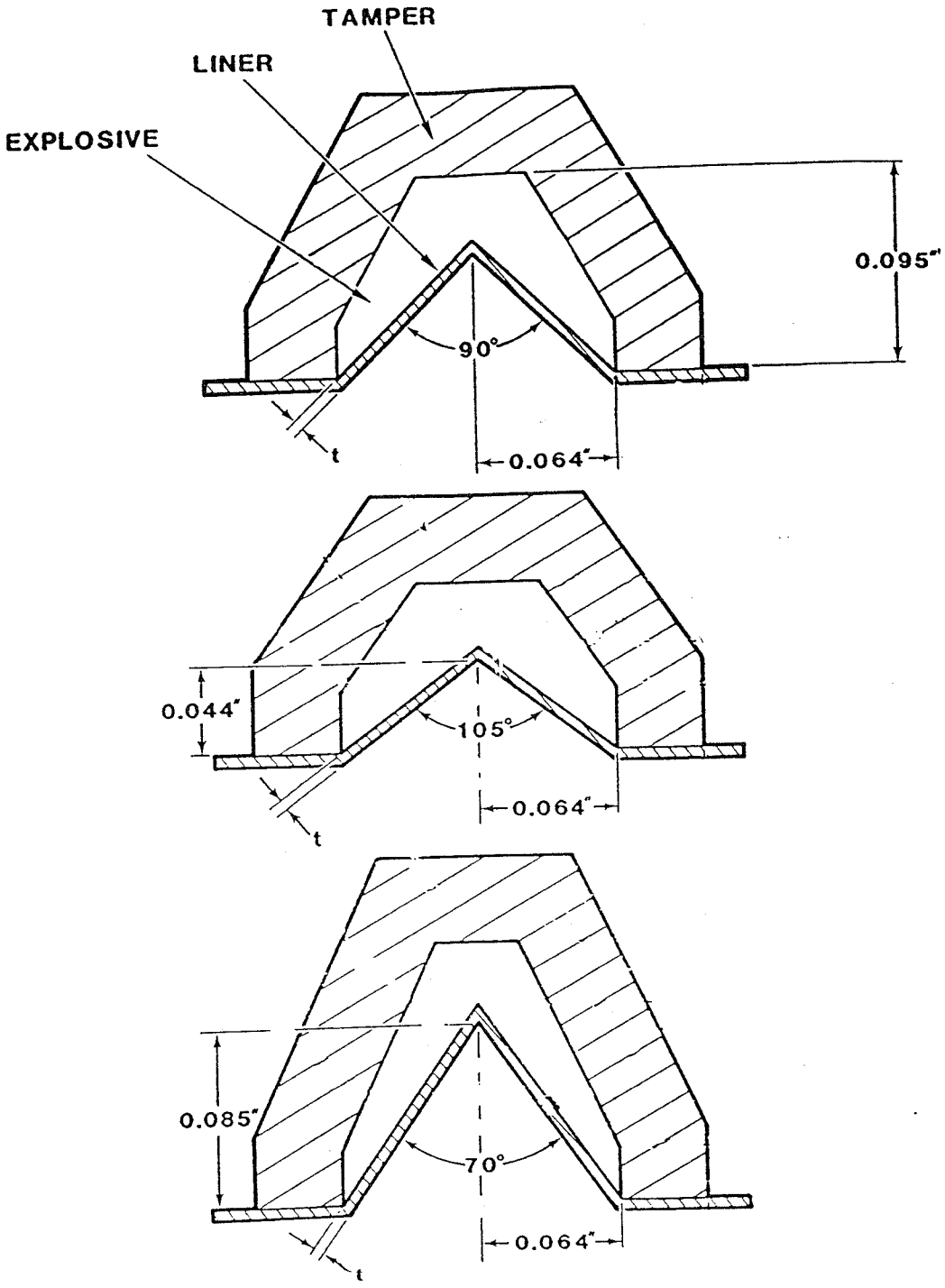

FIGURE 12. "FLANGE" TYPE 25 gr/ft PLSC

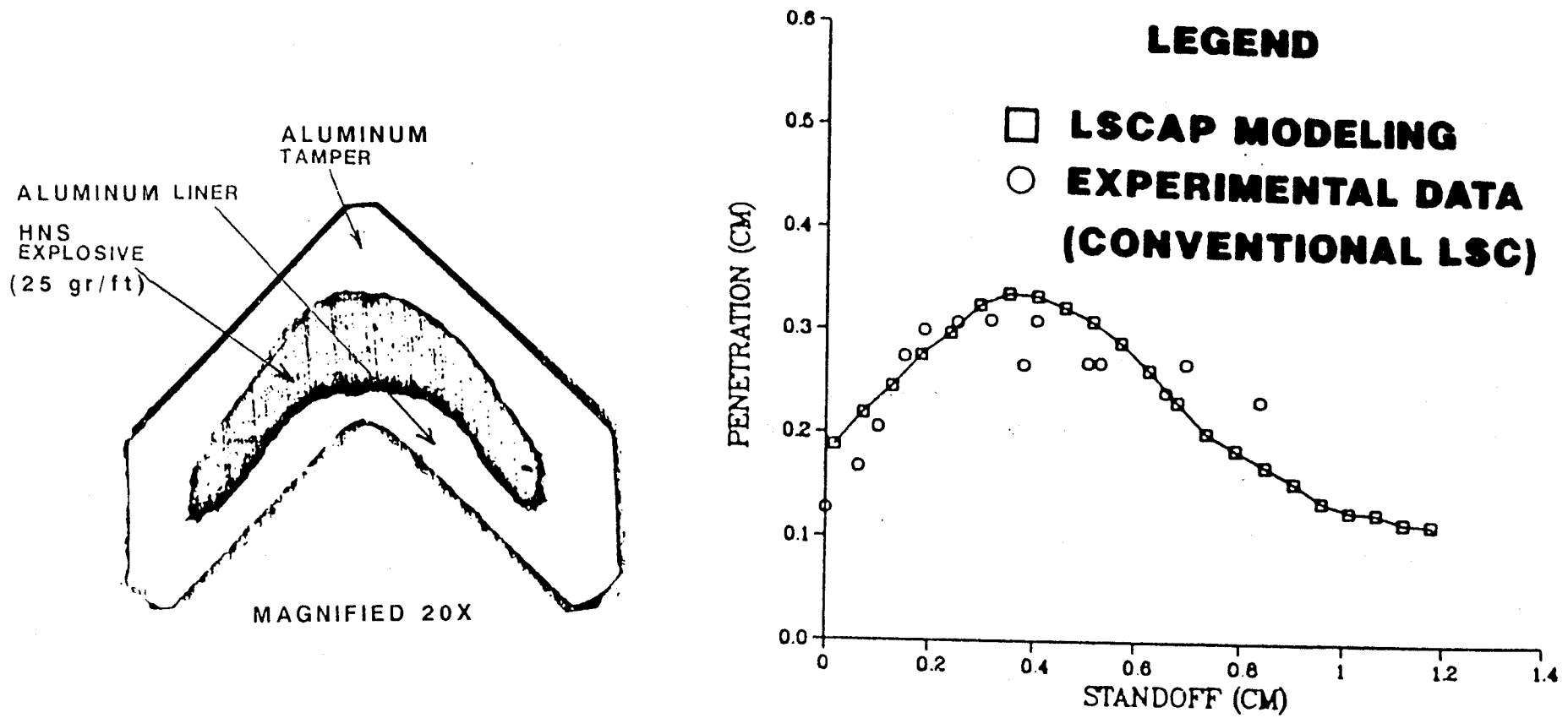

FIGURE 13. CONVENTIONAL LSC PREDICTED JET PENETRATION VERSUS STANDOFF COMPARED TO EXPERIMENTAL DATA

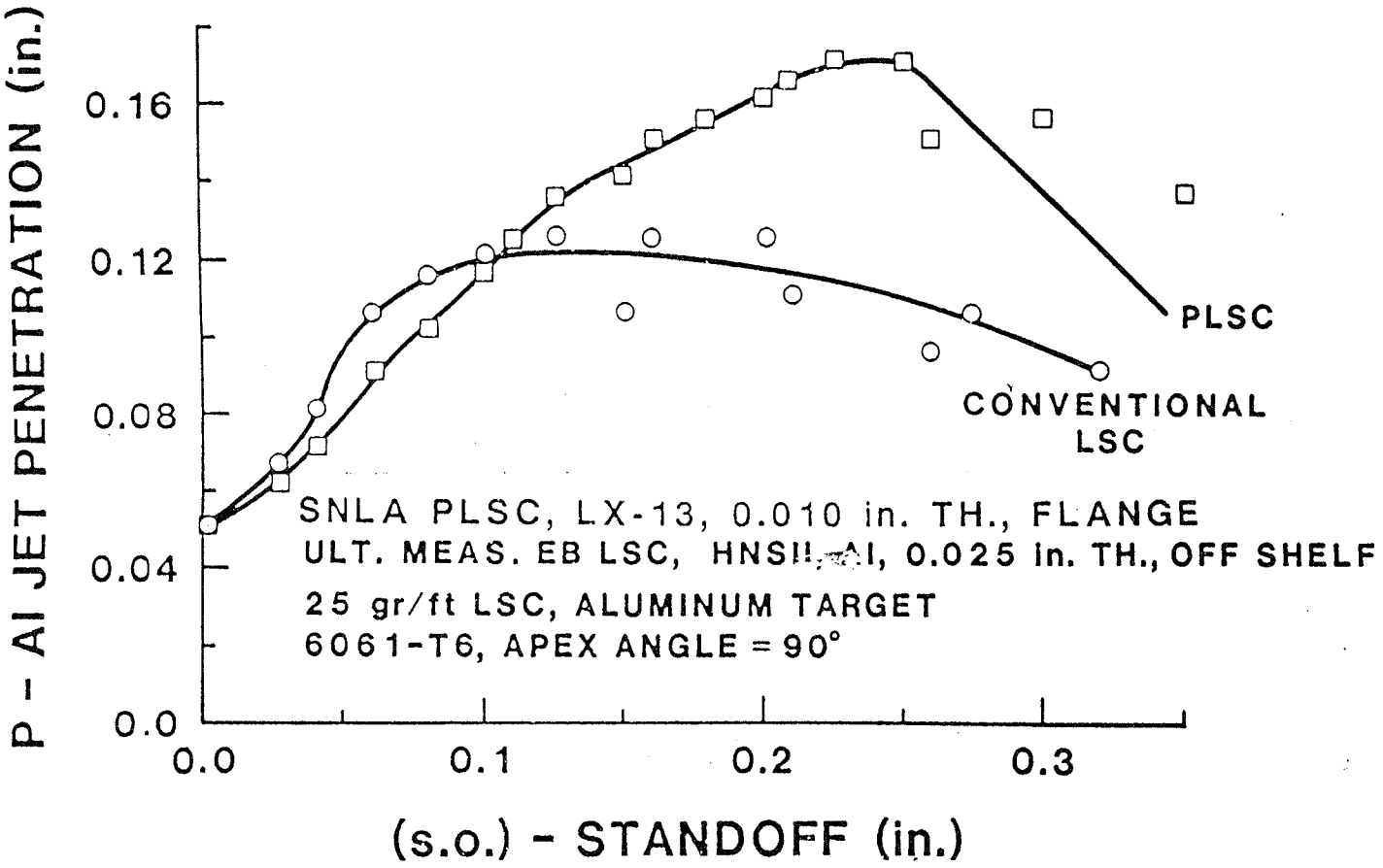

FIGURE 14. JET PENETRATION IN ALUMINUM VERSUS STANDOFF FOR PLSC VERSUS CONVENTIONAL LSC (Al LINER, 90 degree apex, Al TAMPER)

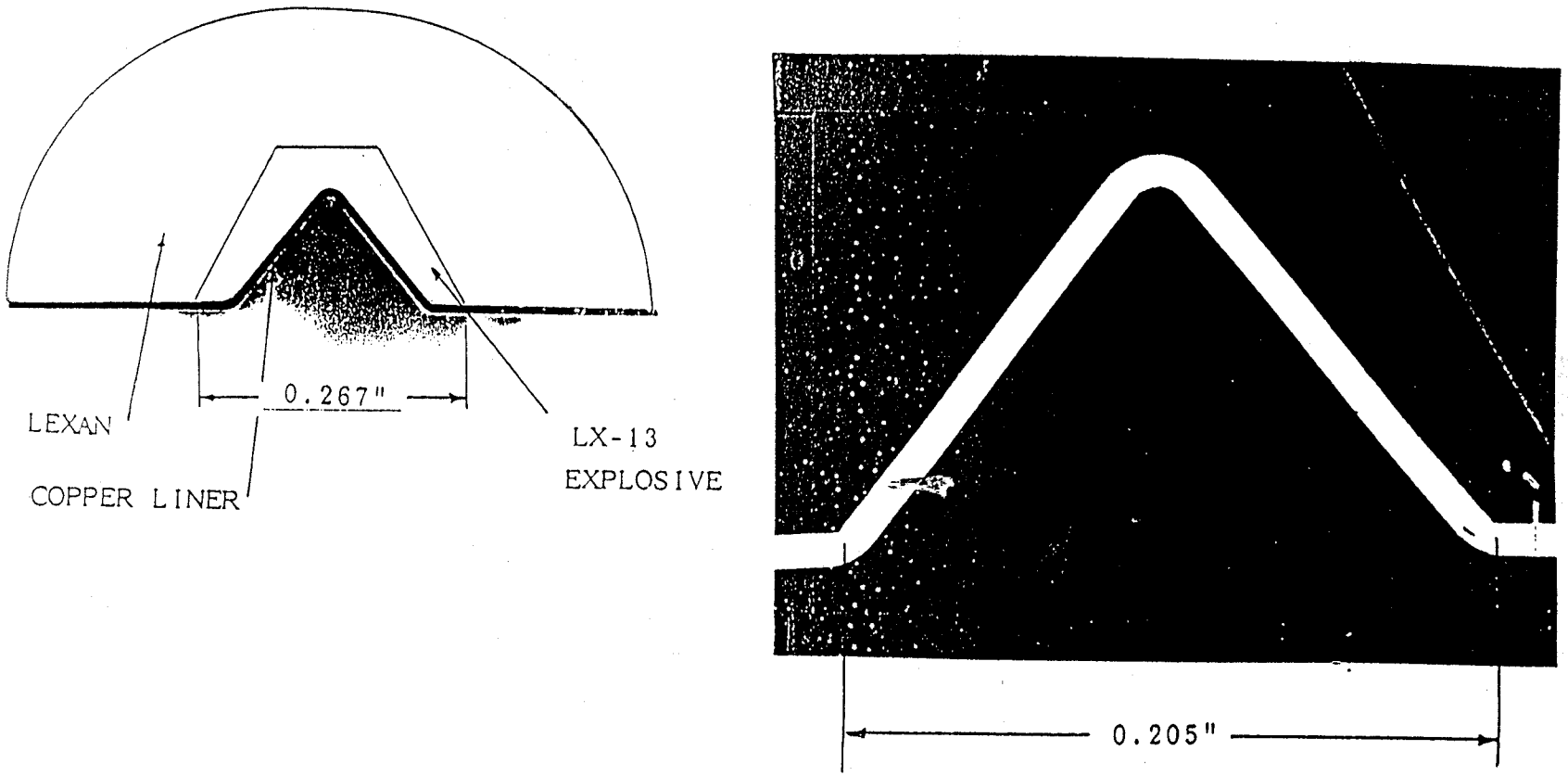

FIGURE 15. 65 gr/ft, PLSC7 ACTUAL CROSS-SECTION

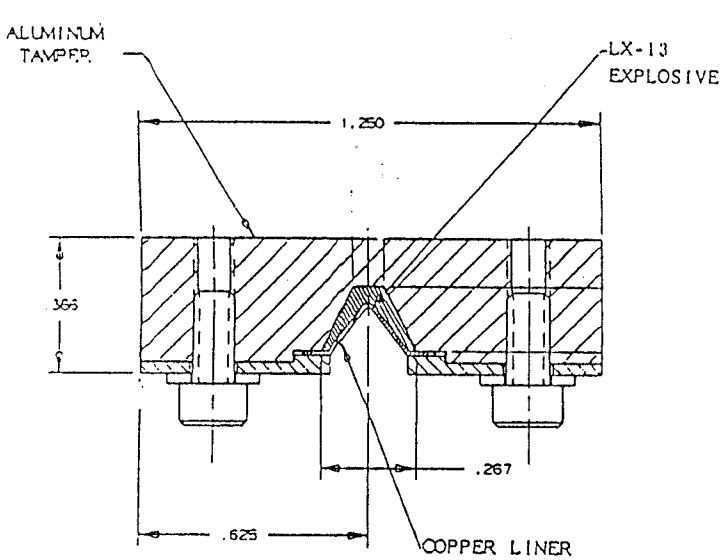

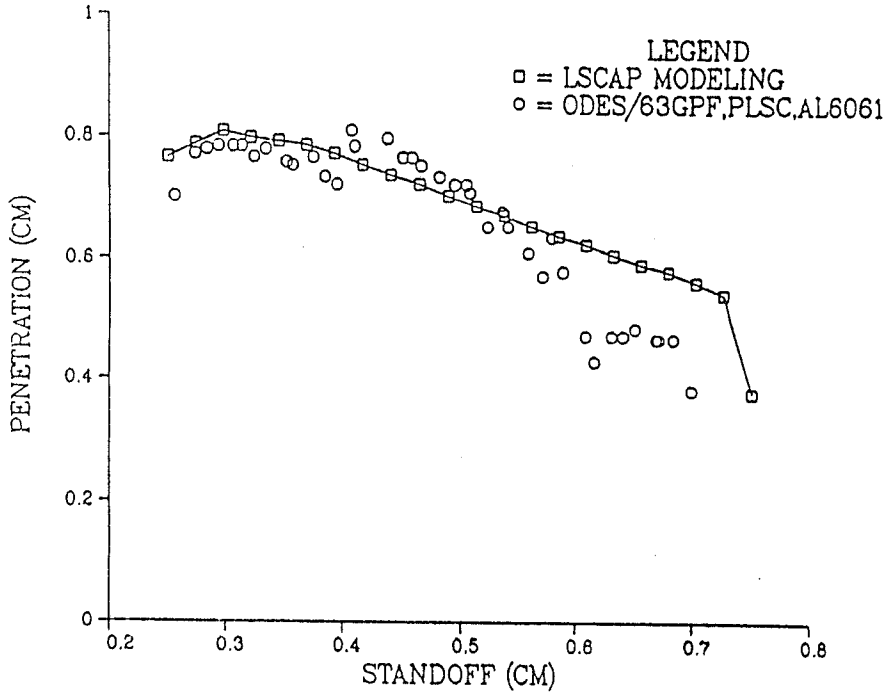

FIGURE 16. 65 gr/ft PLSC 7 CROSS-SECTION AND JET PENETRATION INTO ALUMINUM 6061-T6 VERSUS STANDOFF(LESCA VERSUS MEASURED DATA)

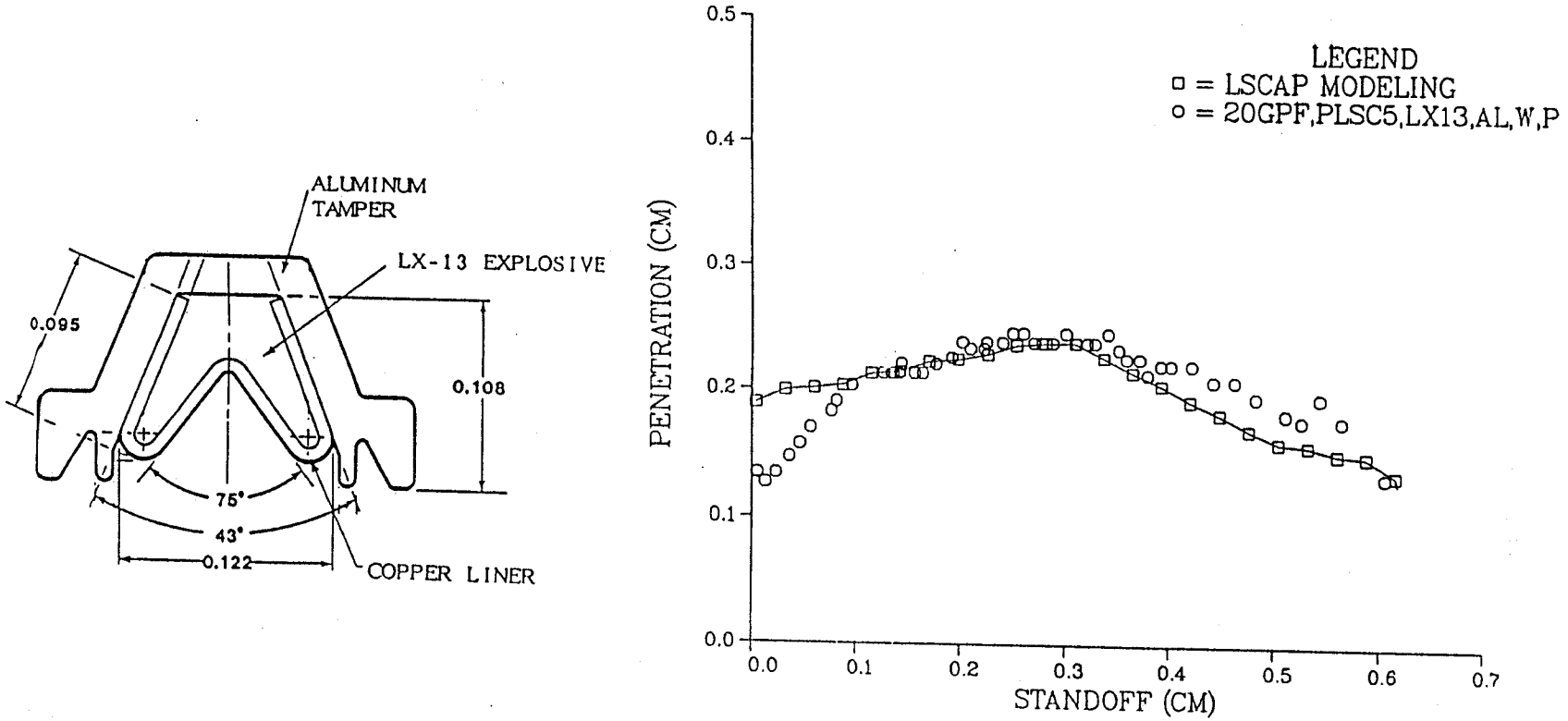

FIGURE 17. 20 gr/ft PLSC JET PENETRATION IN 6061-T6 ALUMINUM VERSUS STANDOFF(LESCA VERSUS MEASURED DATA)

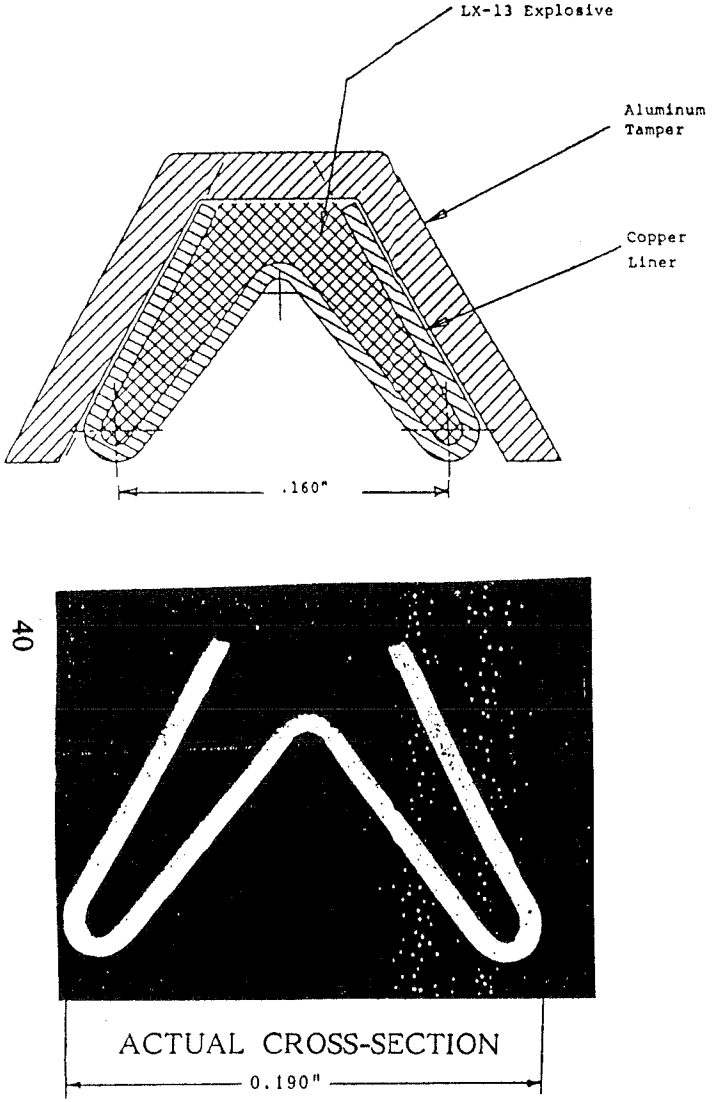

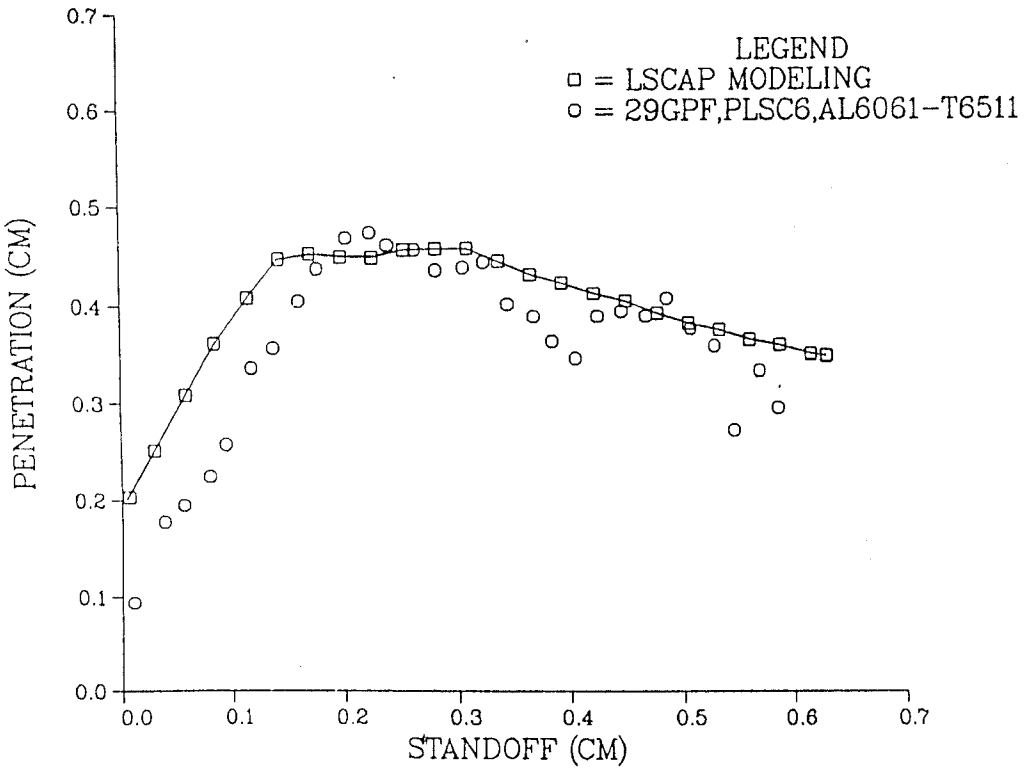

FIGURE 18. 30 gr/ft PLSC6 JET PENETRATION VERSUS STANDOFF (LESCA CODE VERSUS MEASURED DATA)

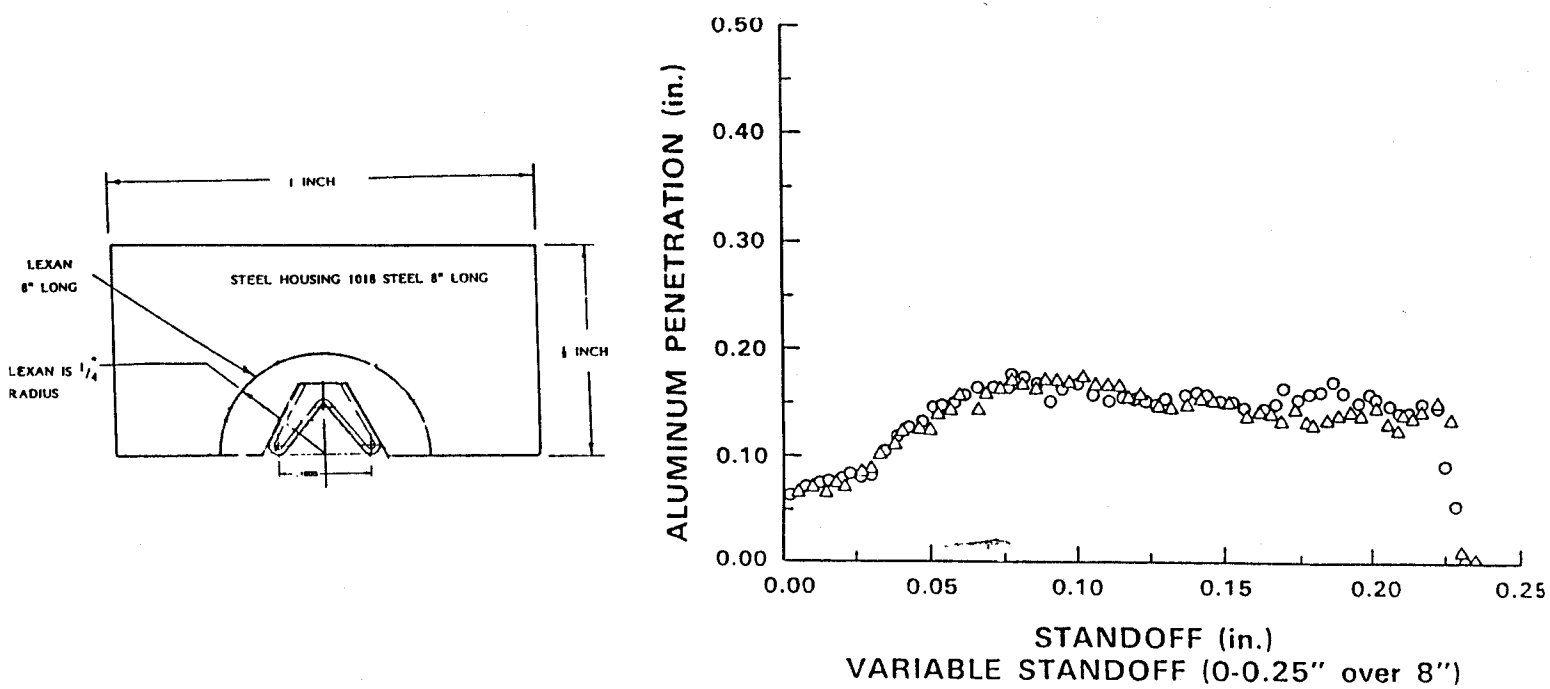

FIGURE 19. REPRODUCIBILITY OF MEASURED 30 gr/ft PLSC6 JET PENETRATION VERSUS STANDOFF DATA(TWO TESTS)

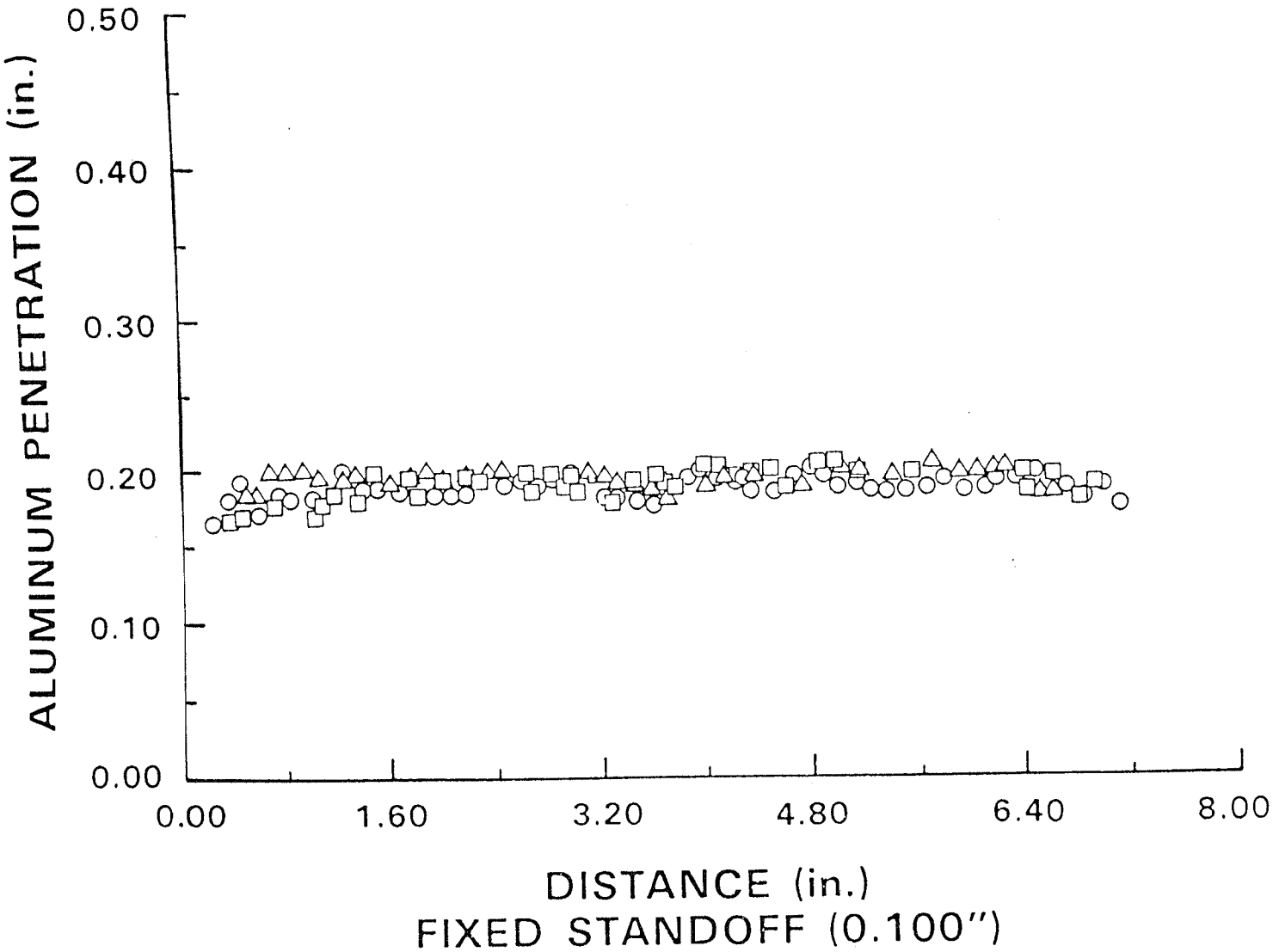

FIGURE 20. REPRODUCIBILITY OF 30 gr/ft PLSC6 JET PENETRATION VERSUS DISTANCE ALONG TARGET(CONSTANT STANDOFF, FOAM TAMPER)

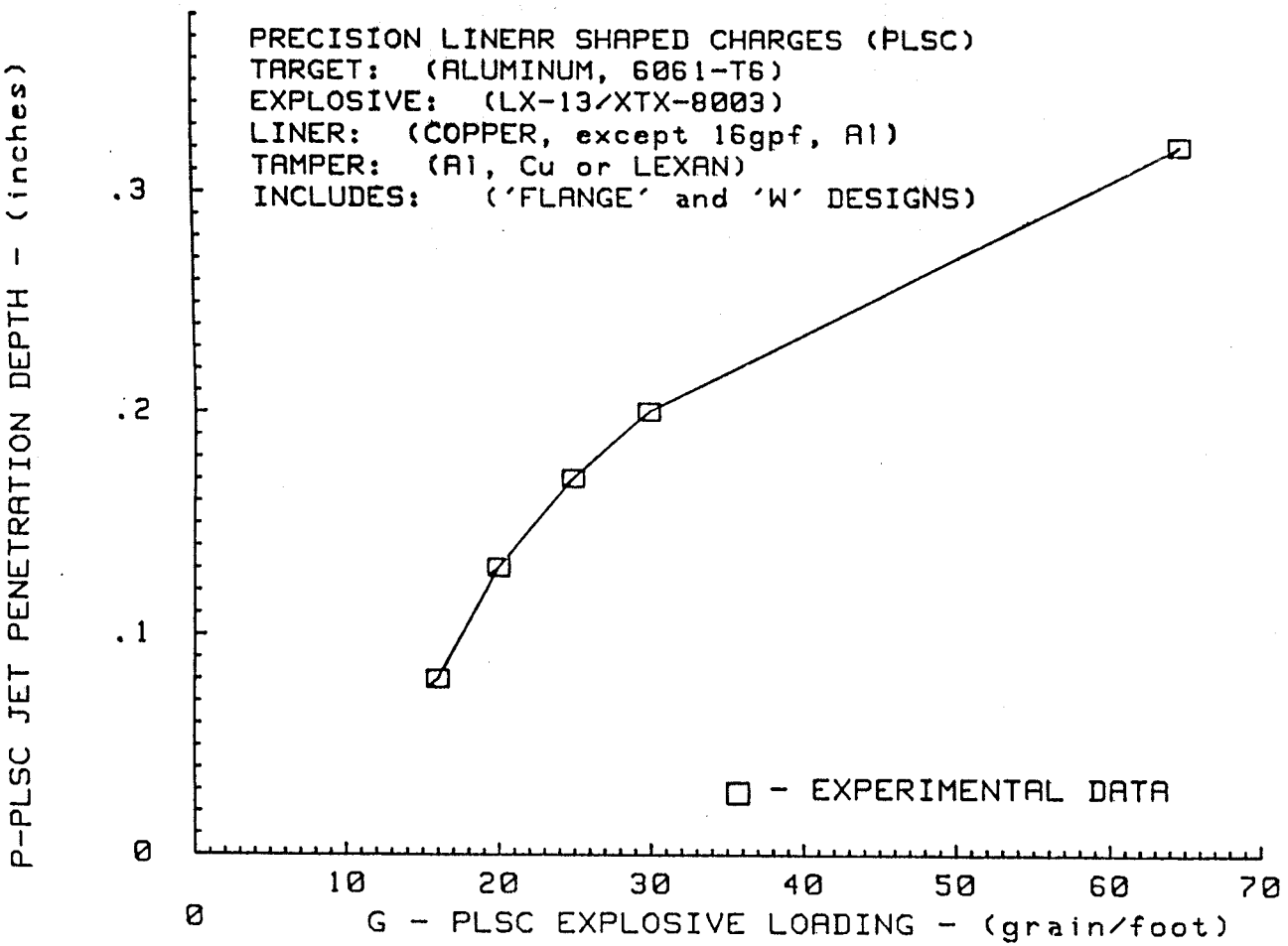

FIGURE 21. PLSC JET PENETRATION DEPTH (P) VERSUS PLSC EXPLOSIVE LOADING (G) FOR ALUMINUM TARGETS

Intentionally Left Blank

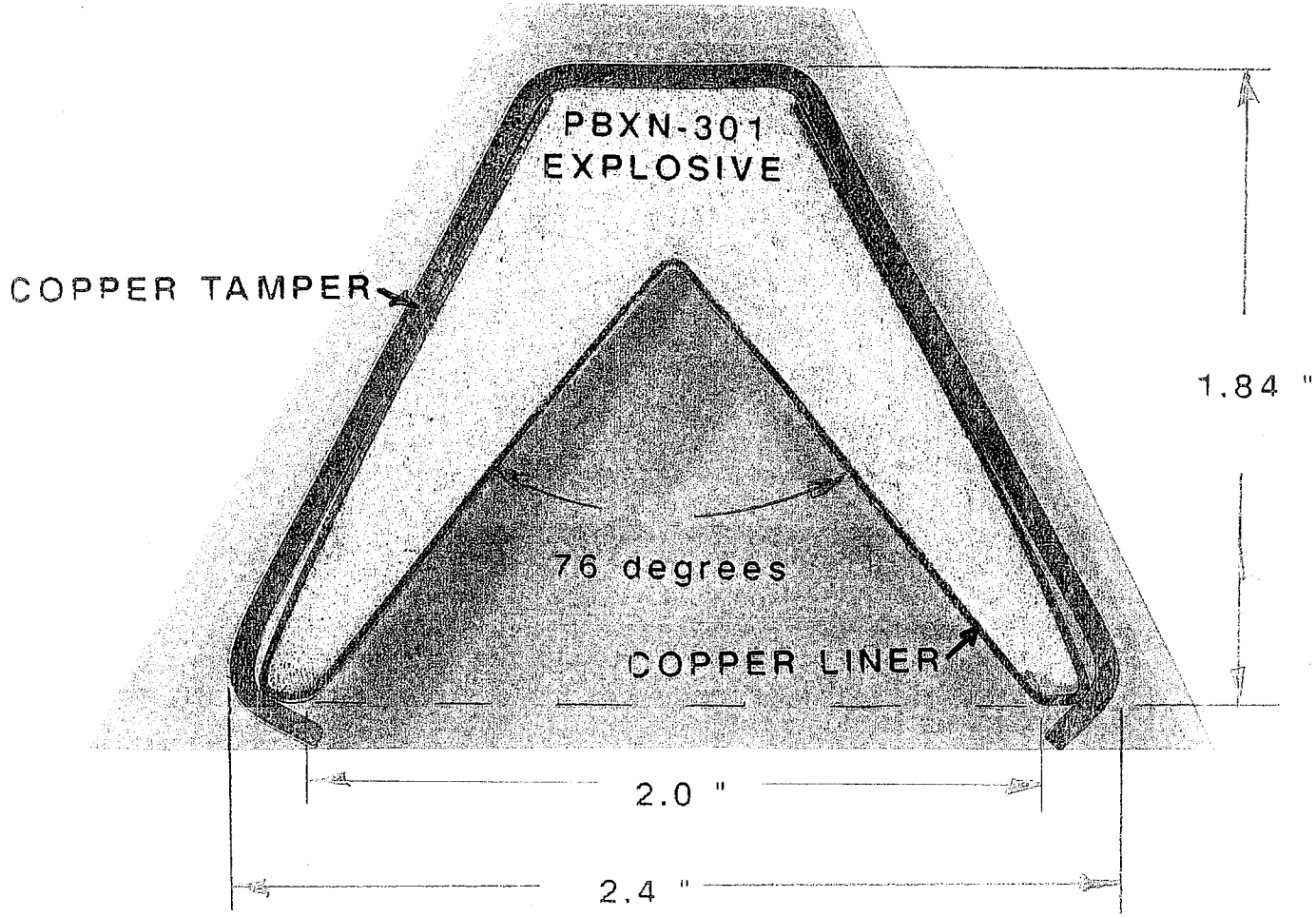

FIGURE 21A. 5000 gr/ft PLSC CONFIGURATION

Intentionally Left Blank

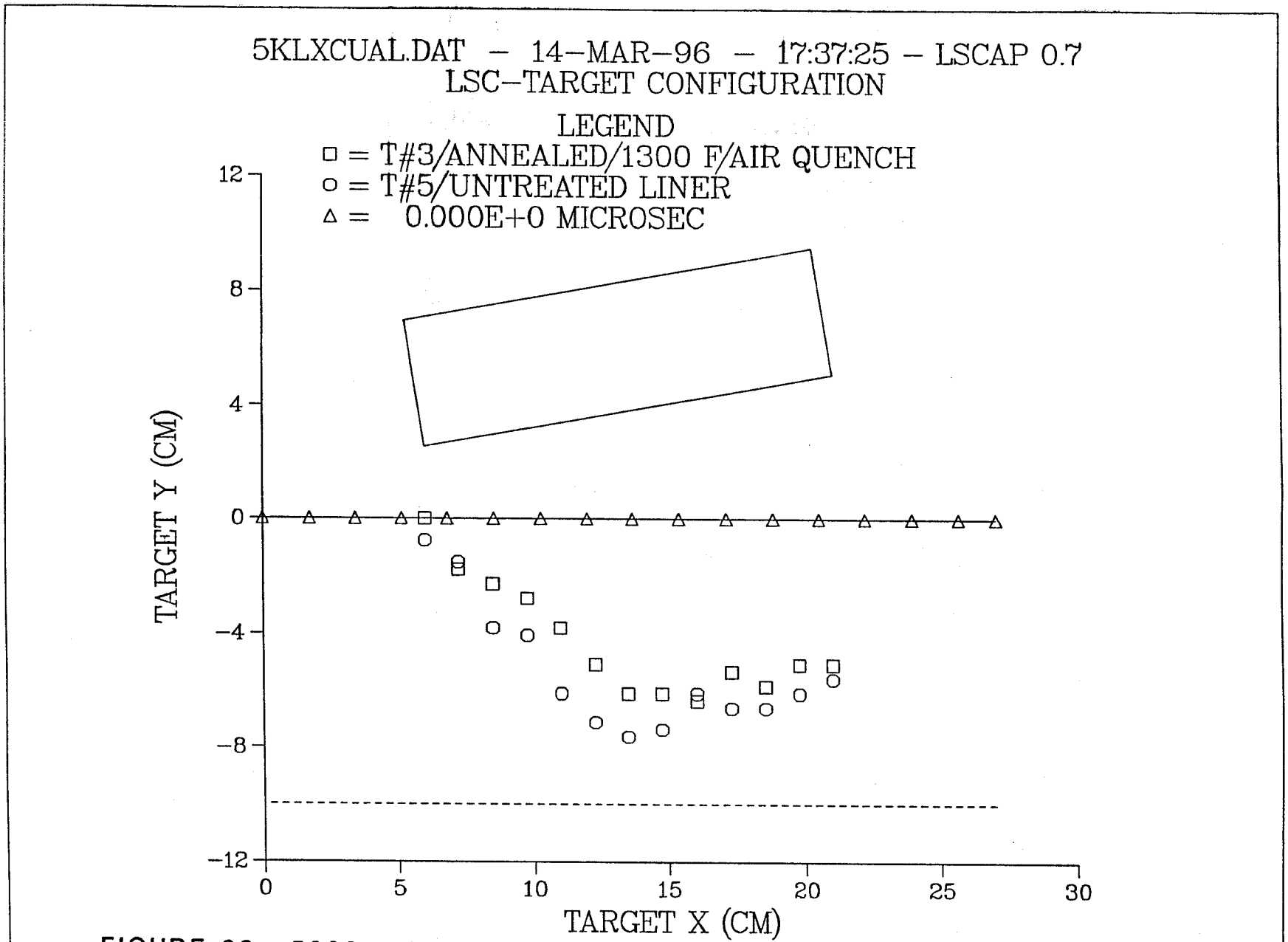

FIGURE 22. 5000 gr/ft PLSC - ALUMINUM TARGET CONFIGURATION

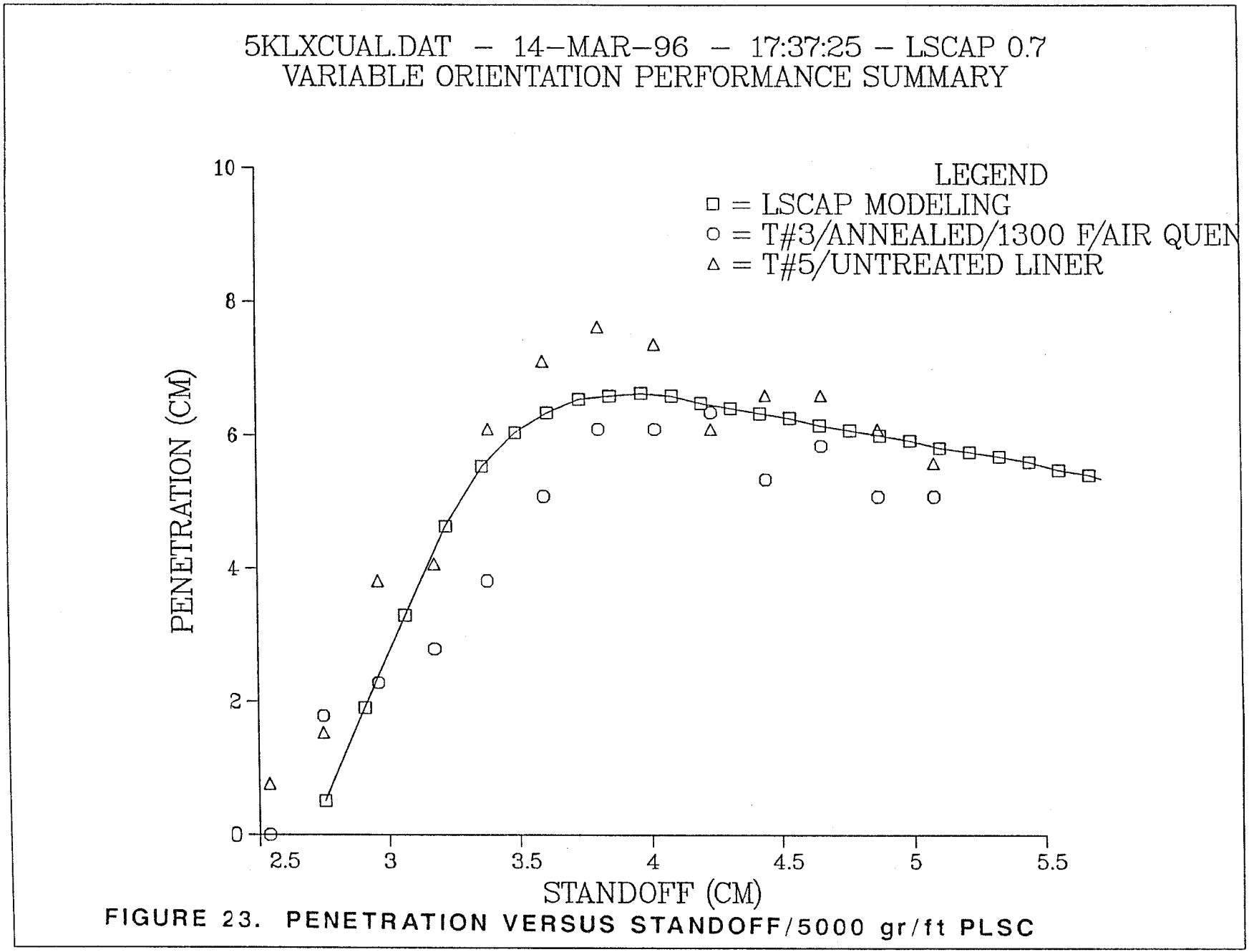

FIGURE 23. PENETRATION VERSUS STANDOFF/5000 gr/ft PLSC

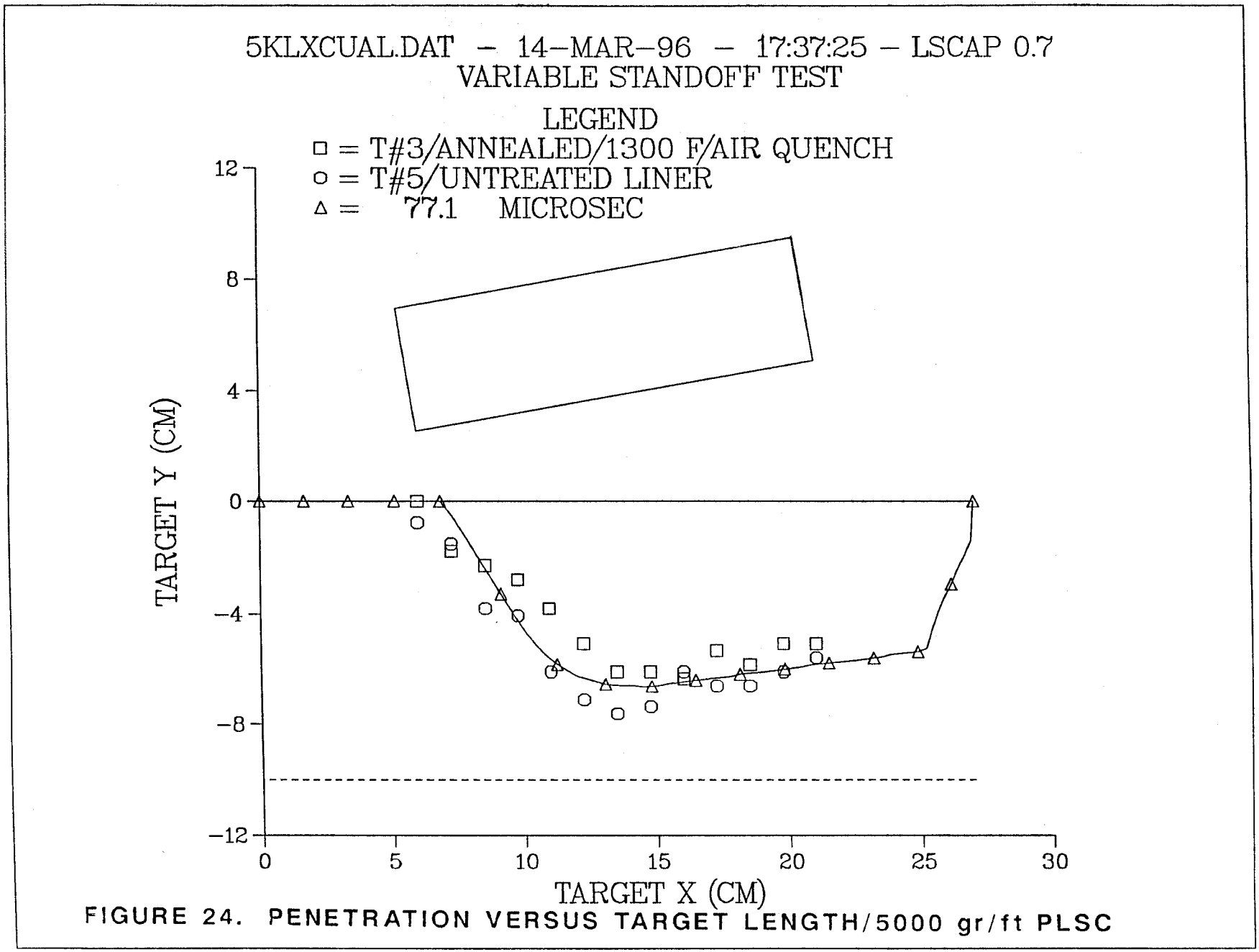

FIGURE 24. PENETRATION VERSUS TARGET LENGTH/5000 gr/ft PLSC

Intentionally Left Blank

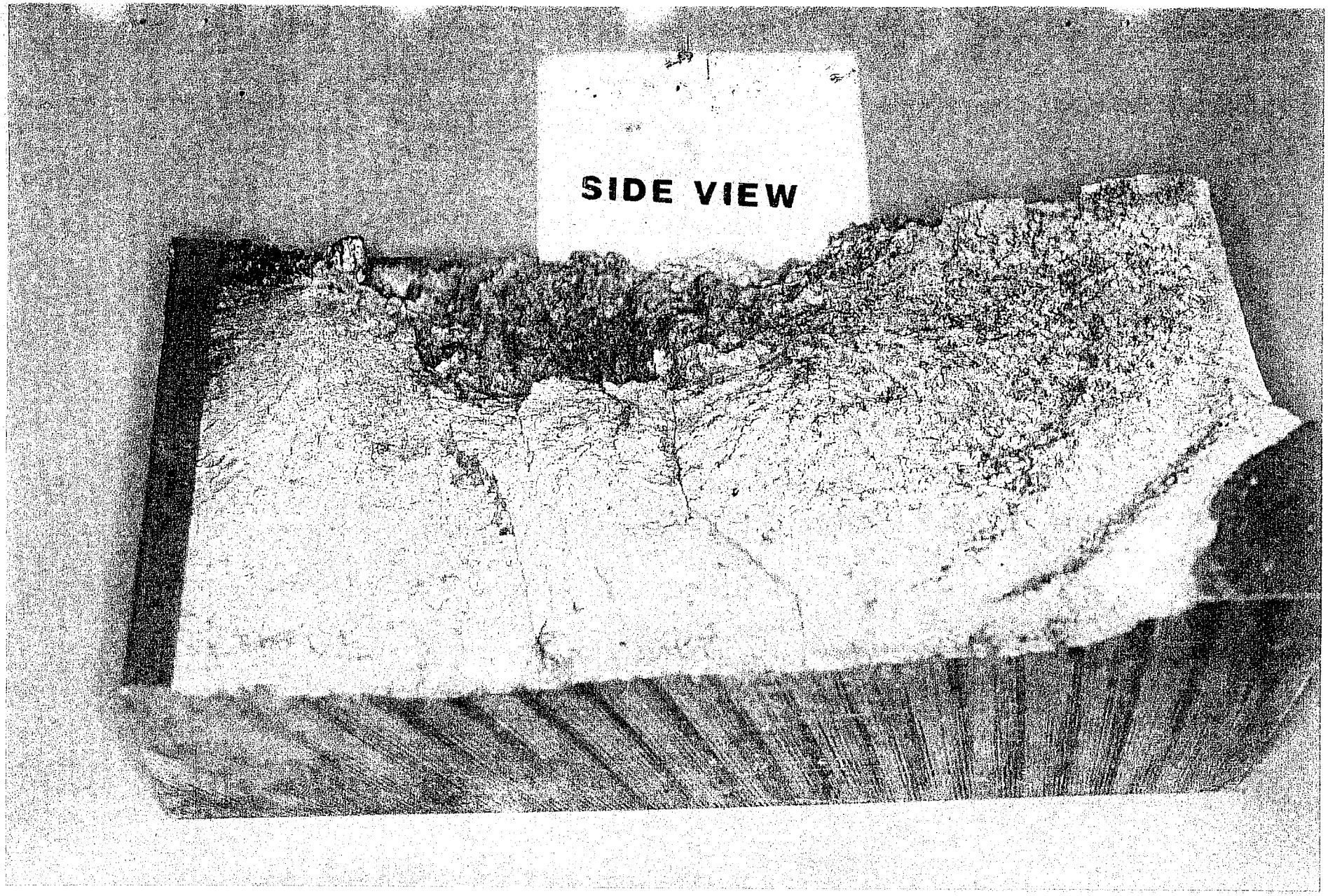

FIGURE 25. PENETRATION & FRACTURE OF ALUMINUM TARGET/5000 gr/ft PLSC

Intentionally Left Blank

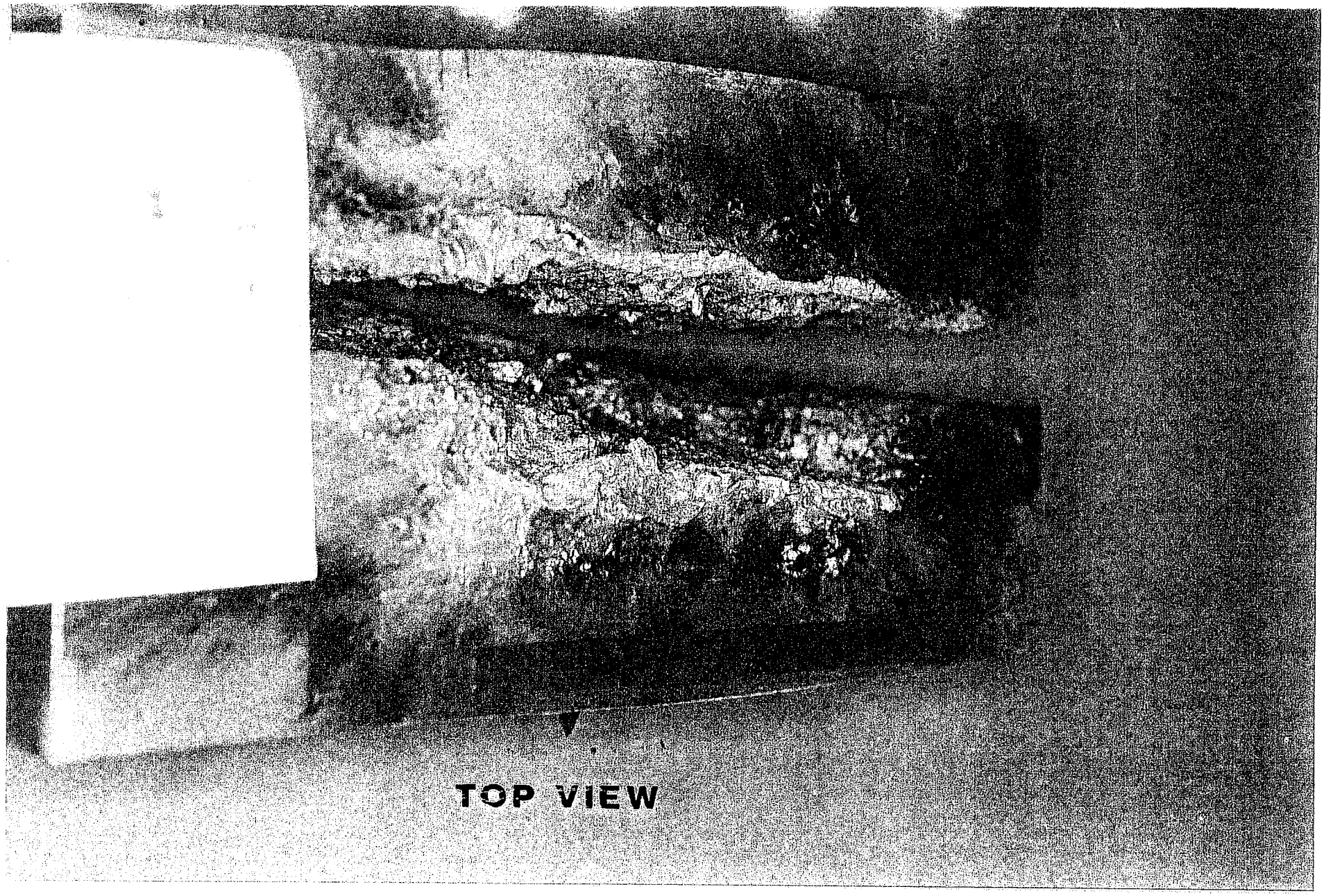

FIGURE 26. PENETRATION & FRACTURE OF ALUMINUM TARGET/5000 gr/ft PLSC

Intentionally Left Blank

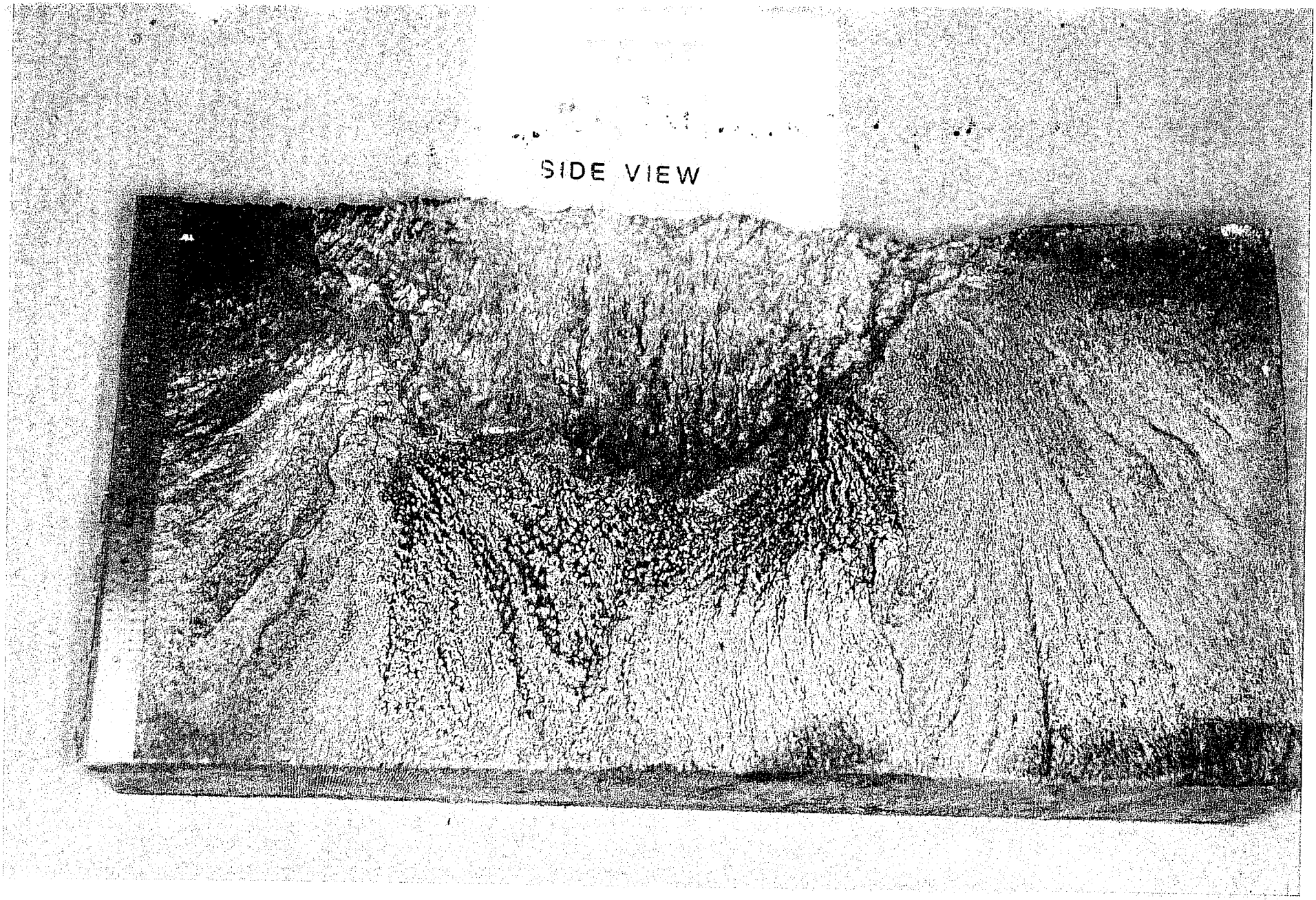

FIGURE 27. PENETRATION & FRACTURE OF ALUMINUM TARGET/5000 gr/ft PLSC

Intentionally Left Blank

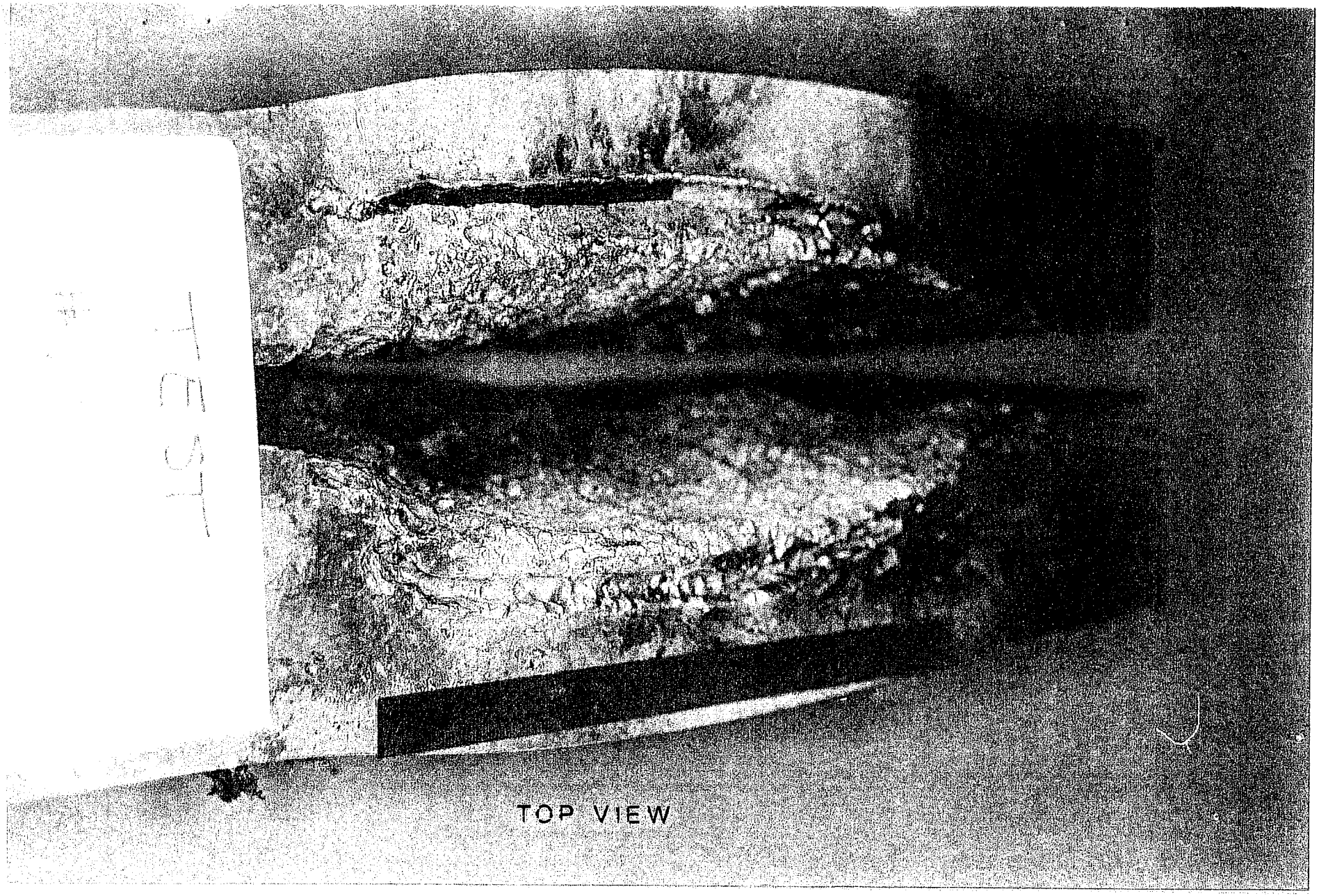

FIGURE 28. PENETRATION & FRACTURE OF ALUMINUM TARGET/5000 gr/ft PLSC

Intentionally Left Blank

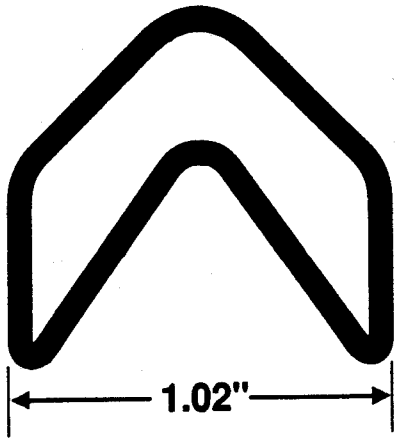

FIGURE 29. 600 gr/ft Cu SHEATH, RDX EXPLOSIVE LSC

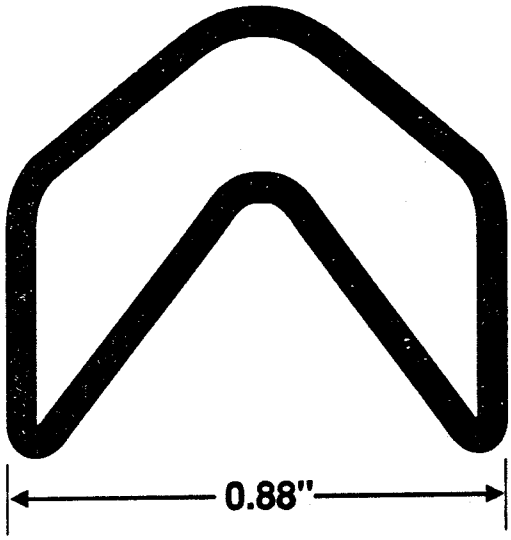

FIGURE 30. 1440 gr/ft Cu SHEATH, RDX EXPLOSIVE LSC

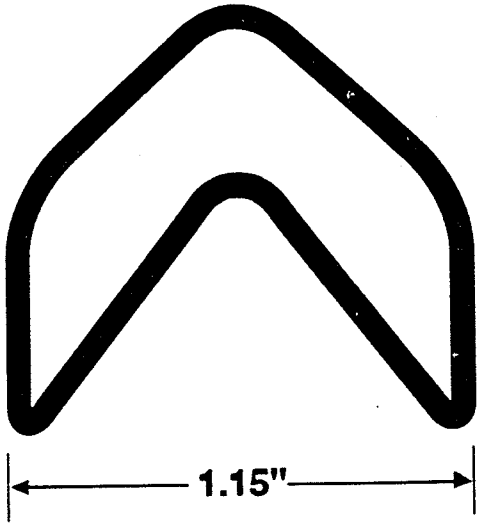

FIGURE 31. 2000 gr/ft Cu SHEATH, RDX EXPLOSIVE LSC

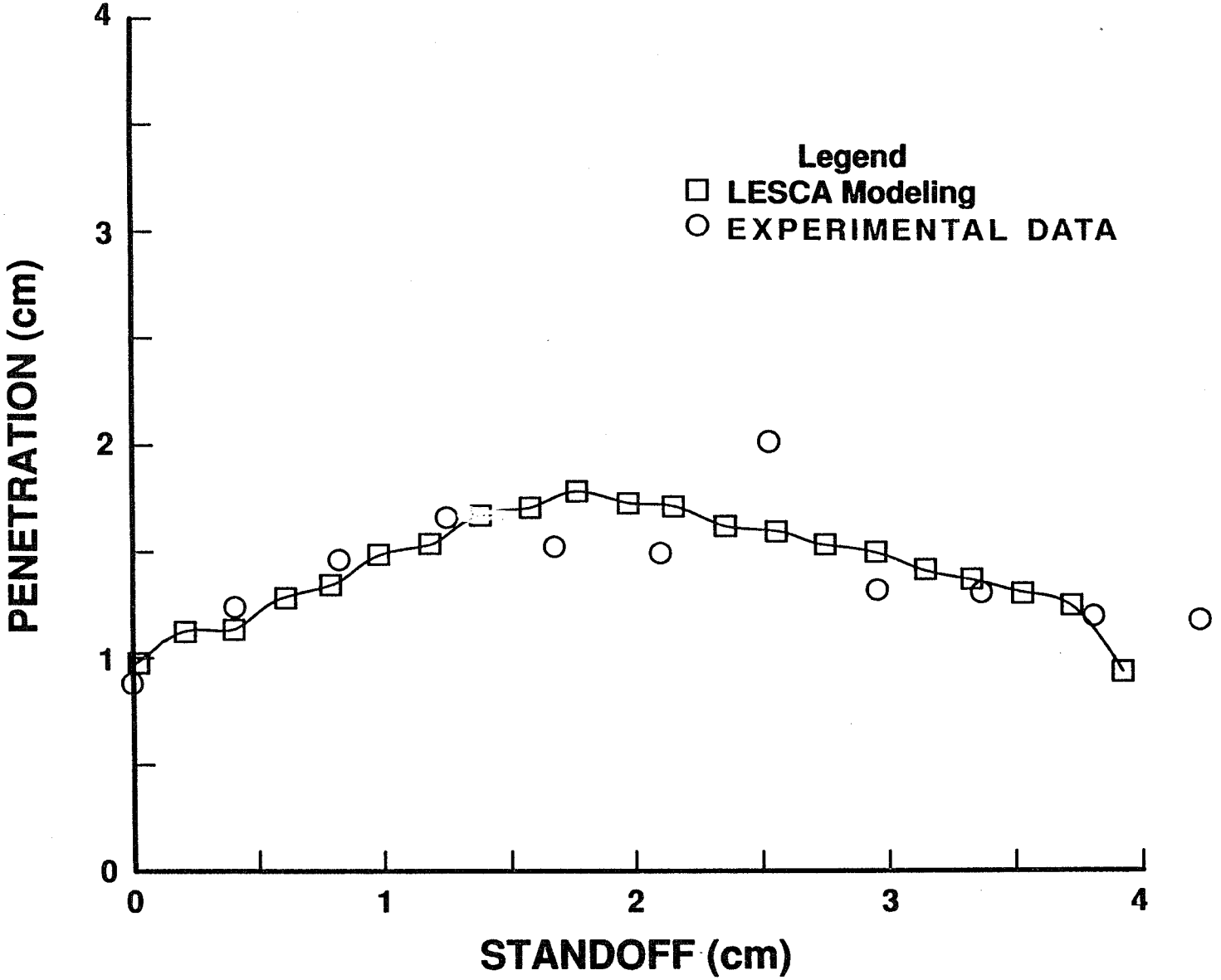

FIGURE 32. PENETRATION VS. STANDOFF/600 gr/ft LSC

TA0119.01.18

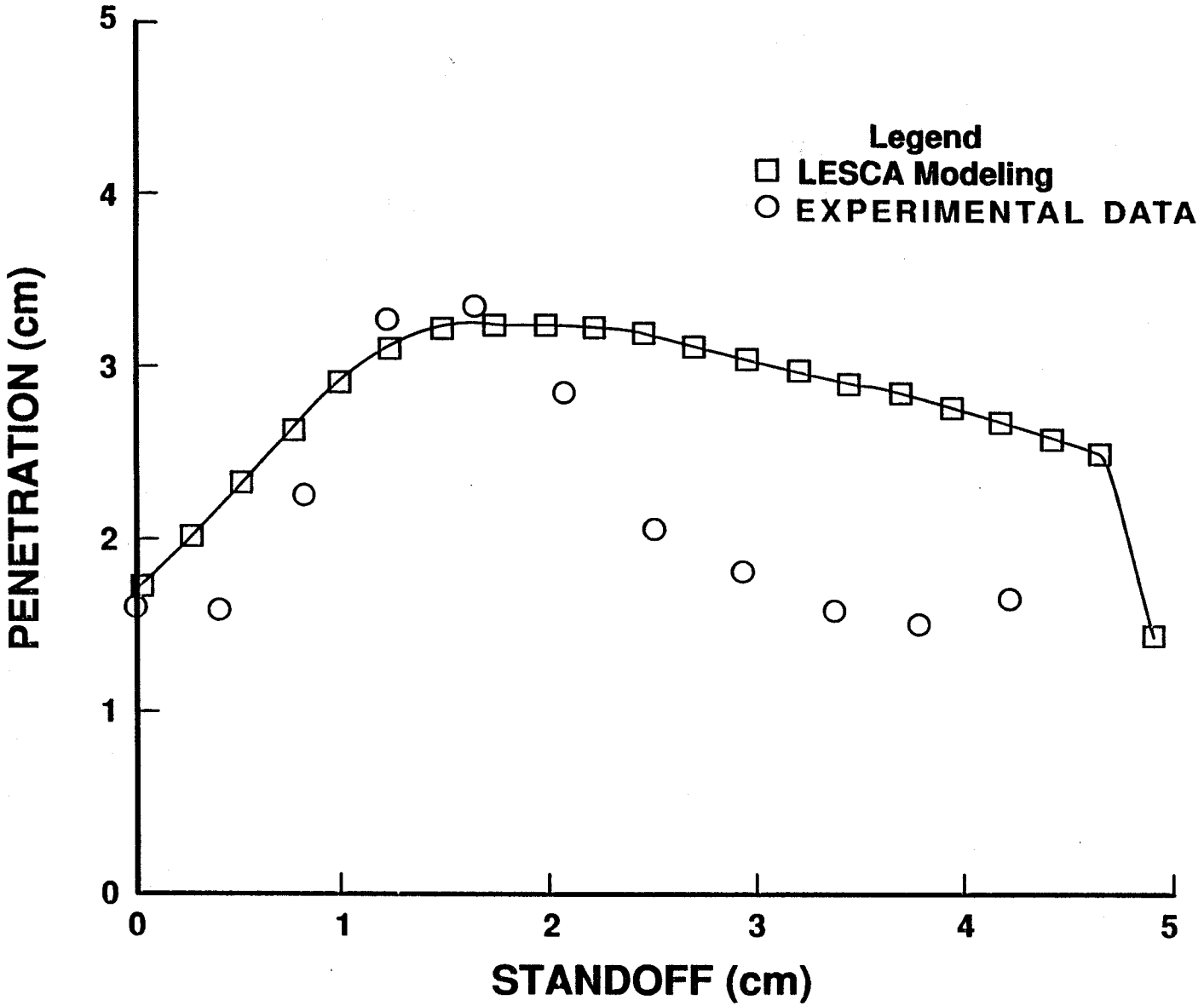

FIGURE 33. PENETRATION VS. STANDOFF/1440 gr/ft LSC

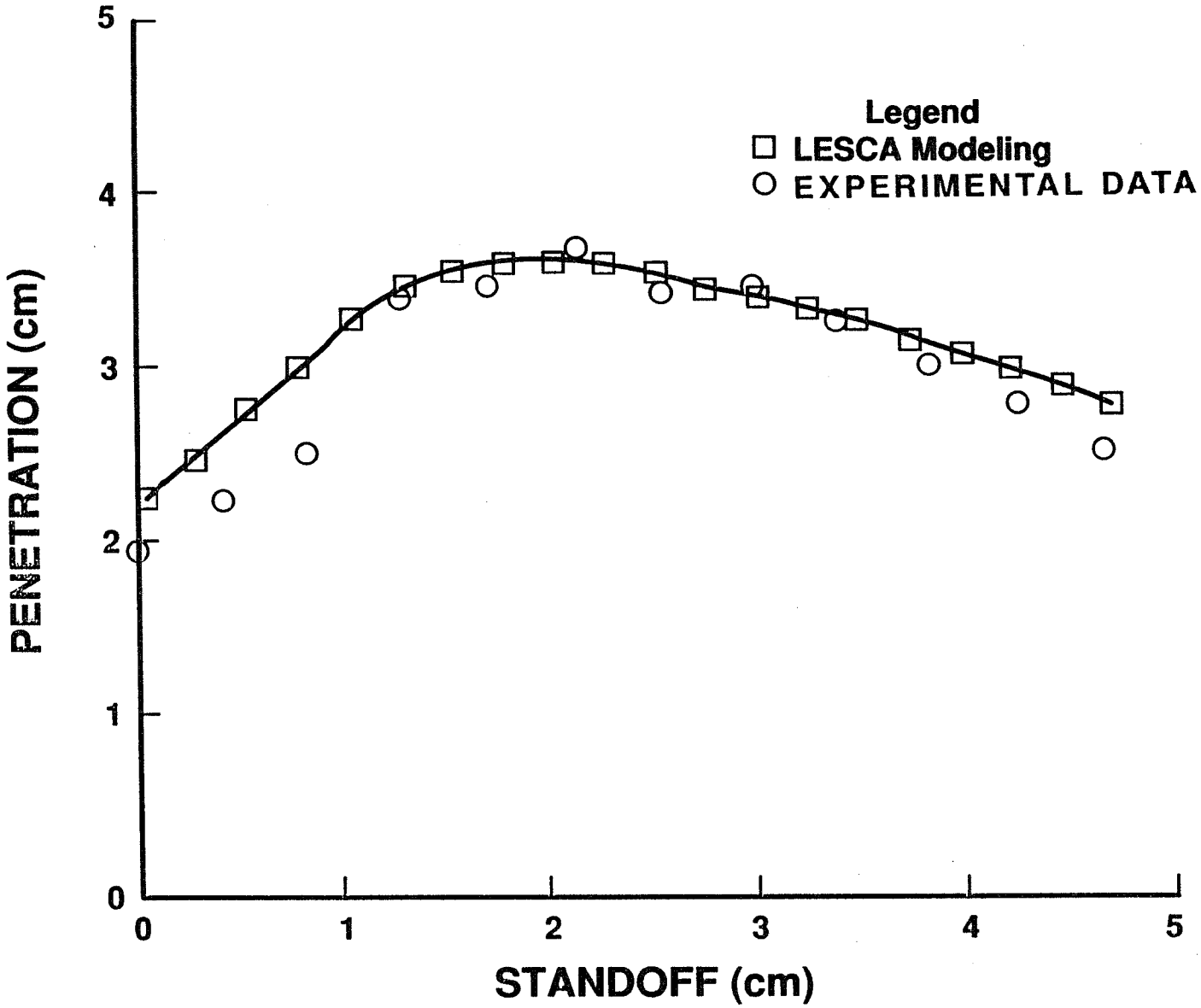

FIGURE 34. PENETRATION VS. STANDOFF/2000 gr/ft LSC

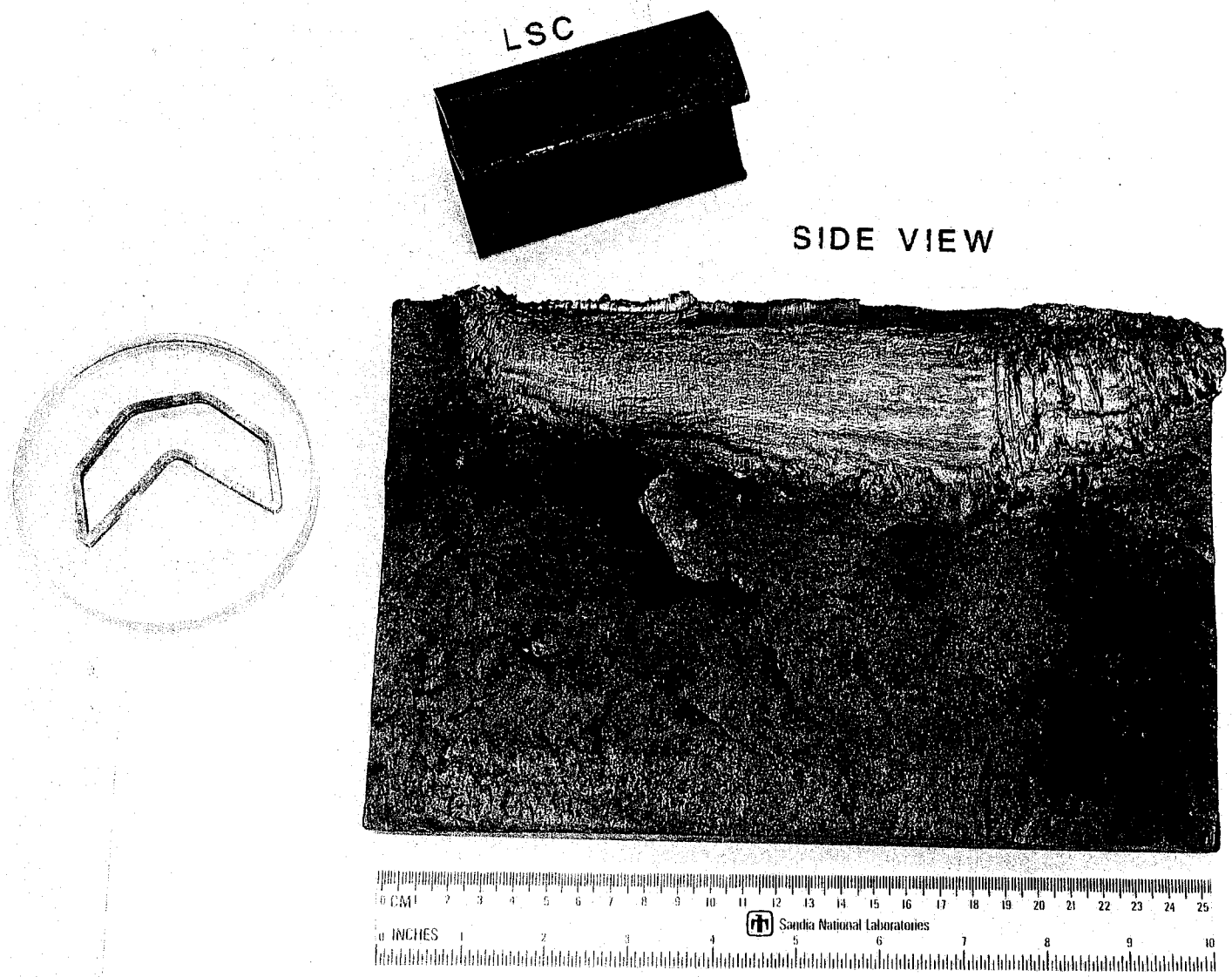

FIGURE 35. JET PENETRATION & FRACTURE OF 1018 STEEL TARGET

Intentionally Left Blank

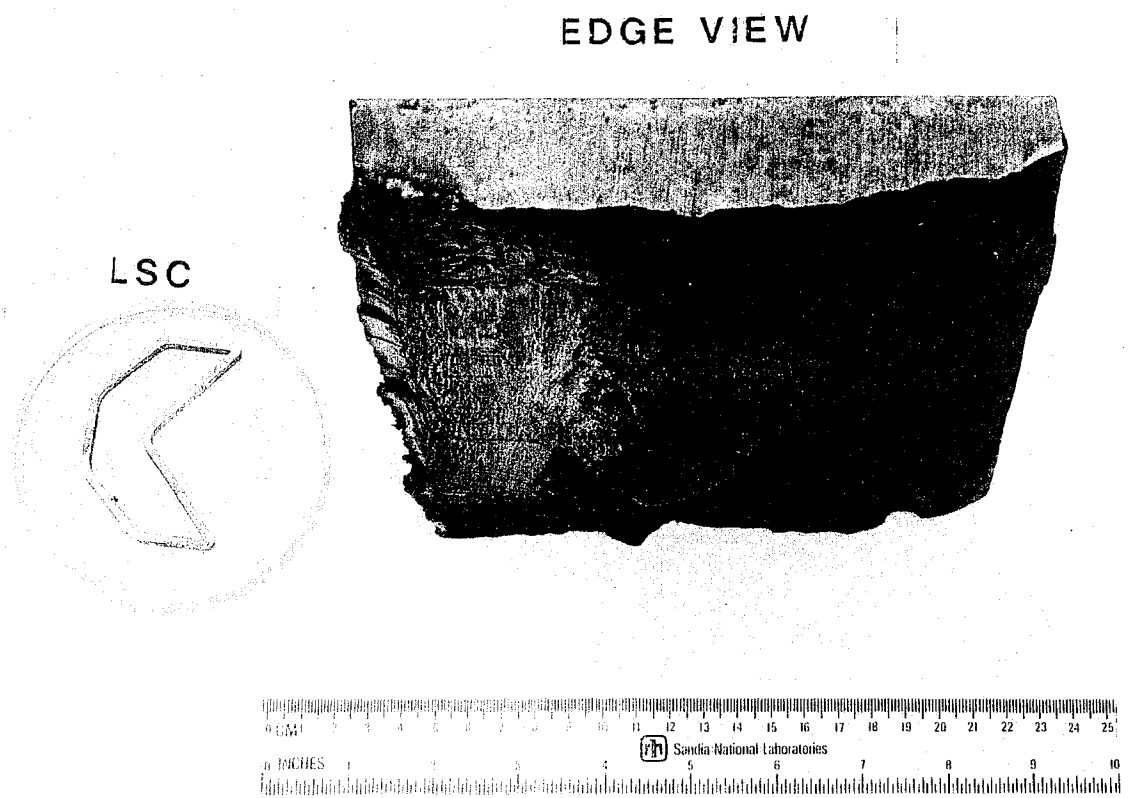

FIGURE 36. JET PENETRATION & FRACTURE OF 1018 STEEL TARGET

Intentionally Left Blank

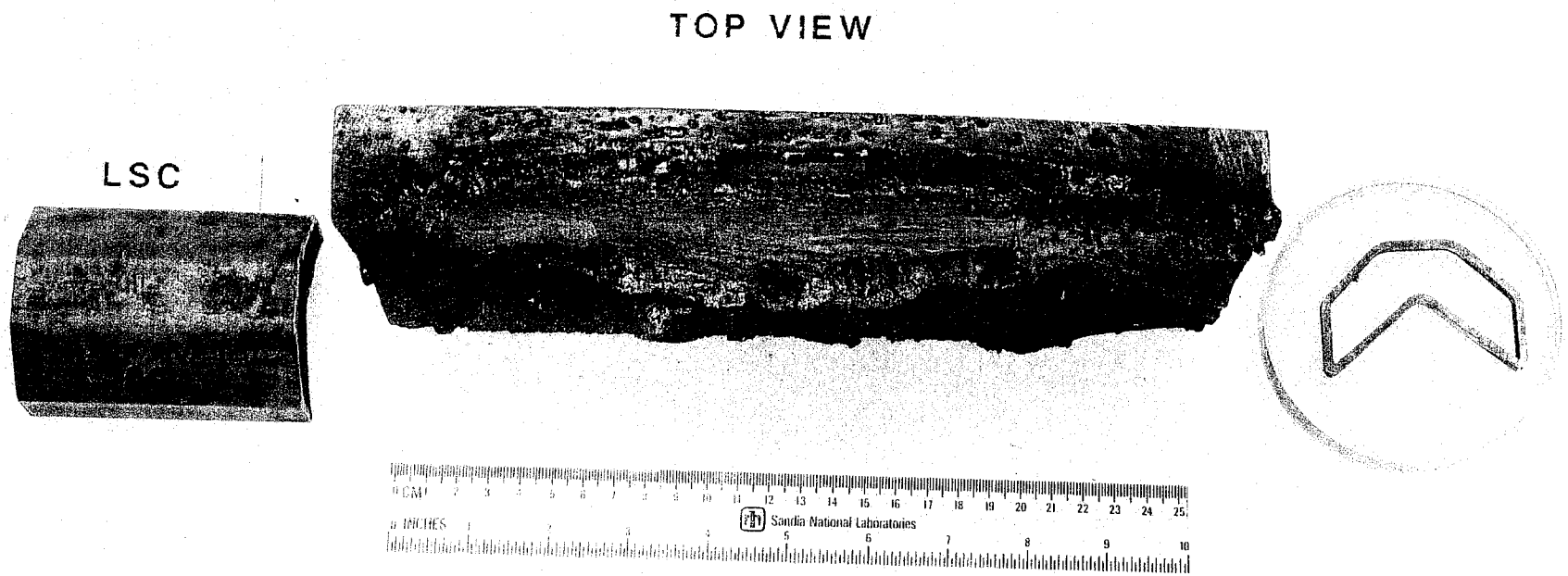

FIGURE 37. JET PENETRATION & FRACTURE OF 1018 STEEL TARGET

Intentionally Left Blank

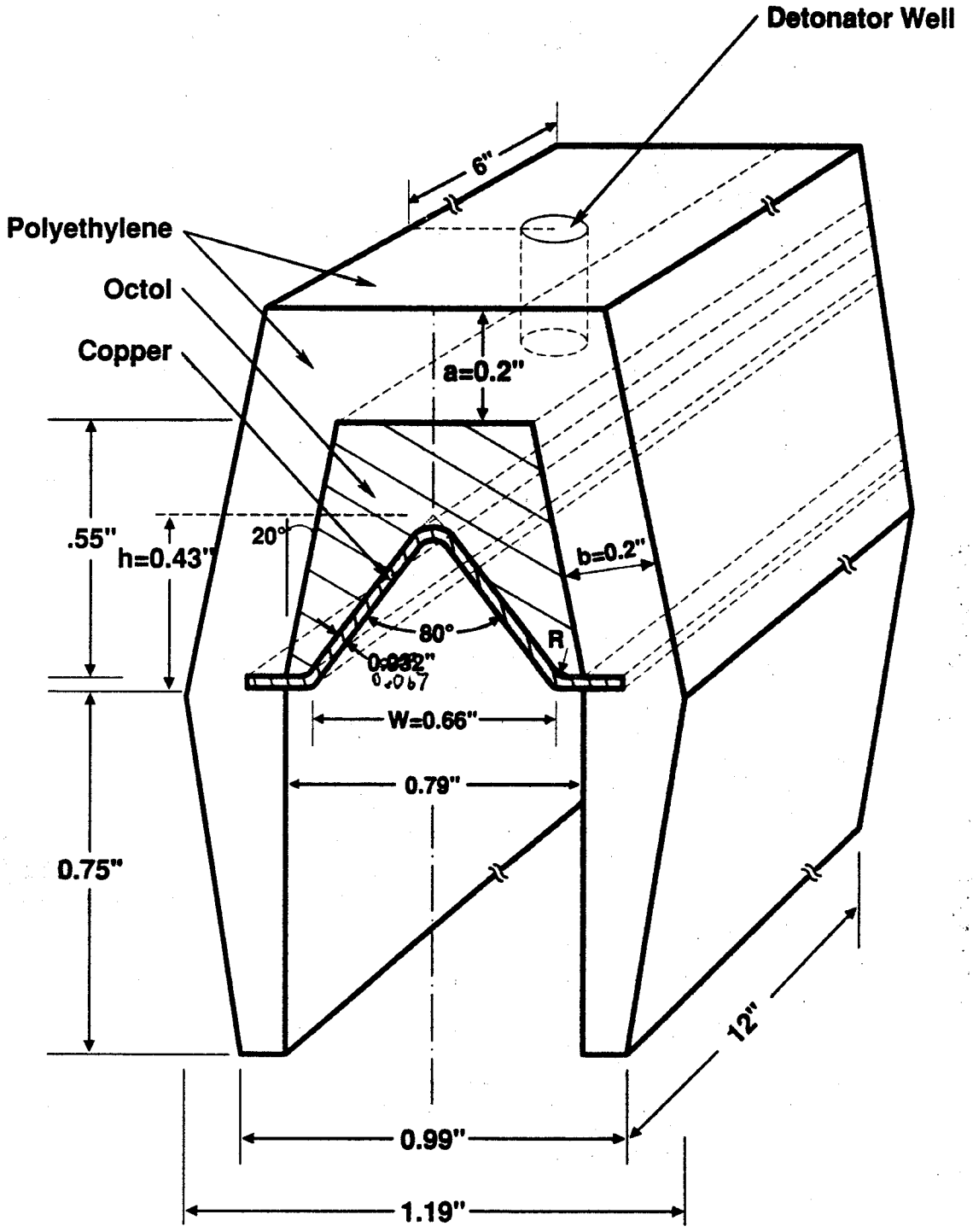

FIGURE 38. 850 gr/ft PLSC CONFIGURATION

Not to Scale

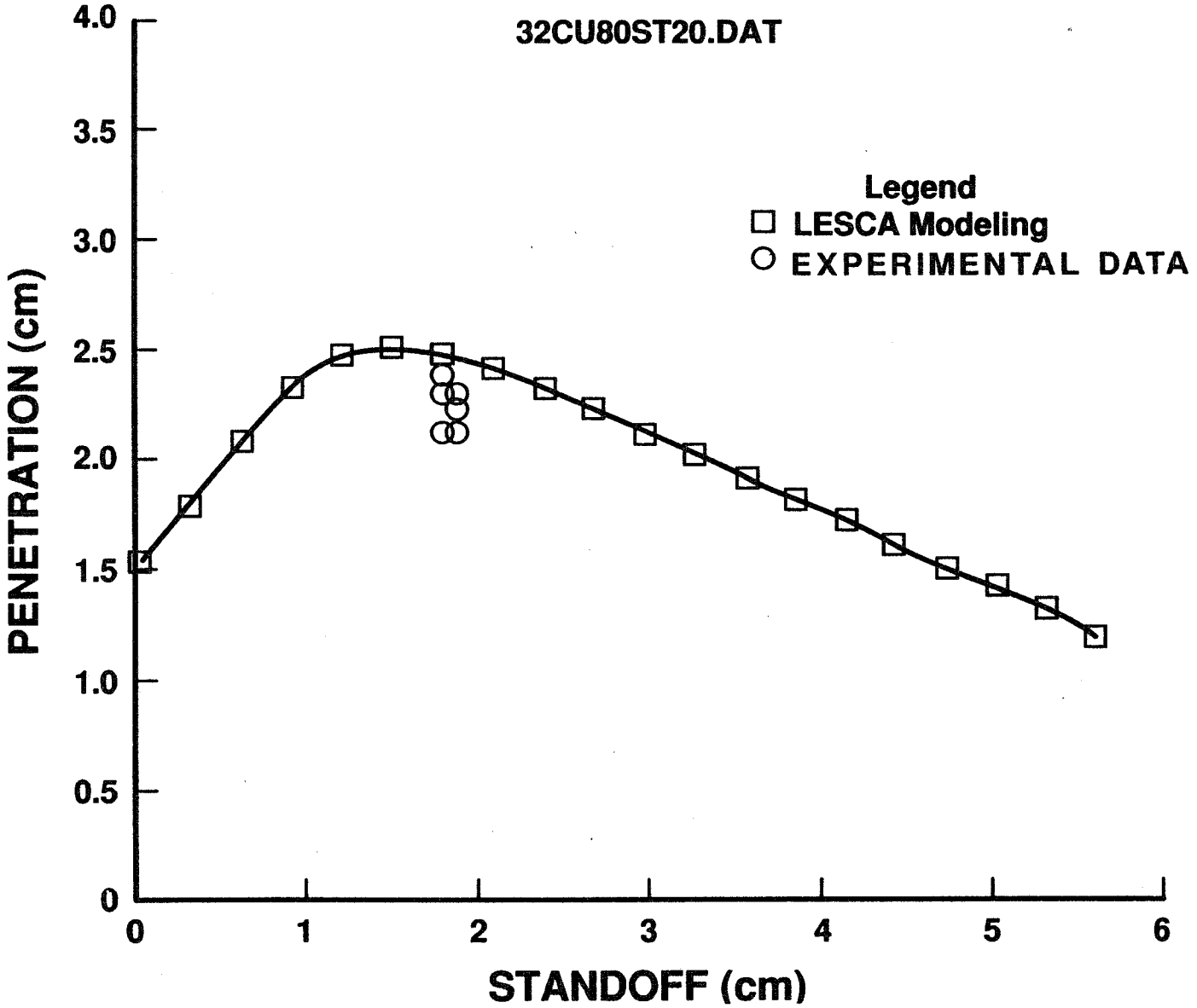

FIGURE 39. PENETRATION VS. STANDOFF/850 gr/ft PLSC

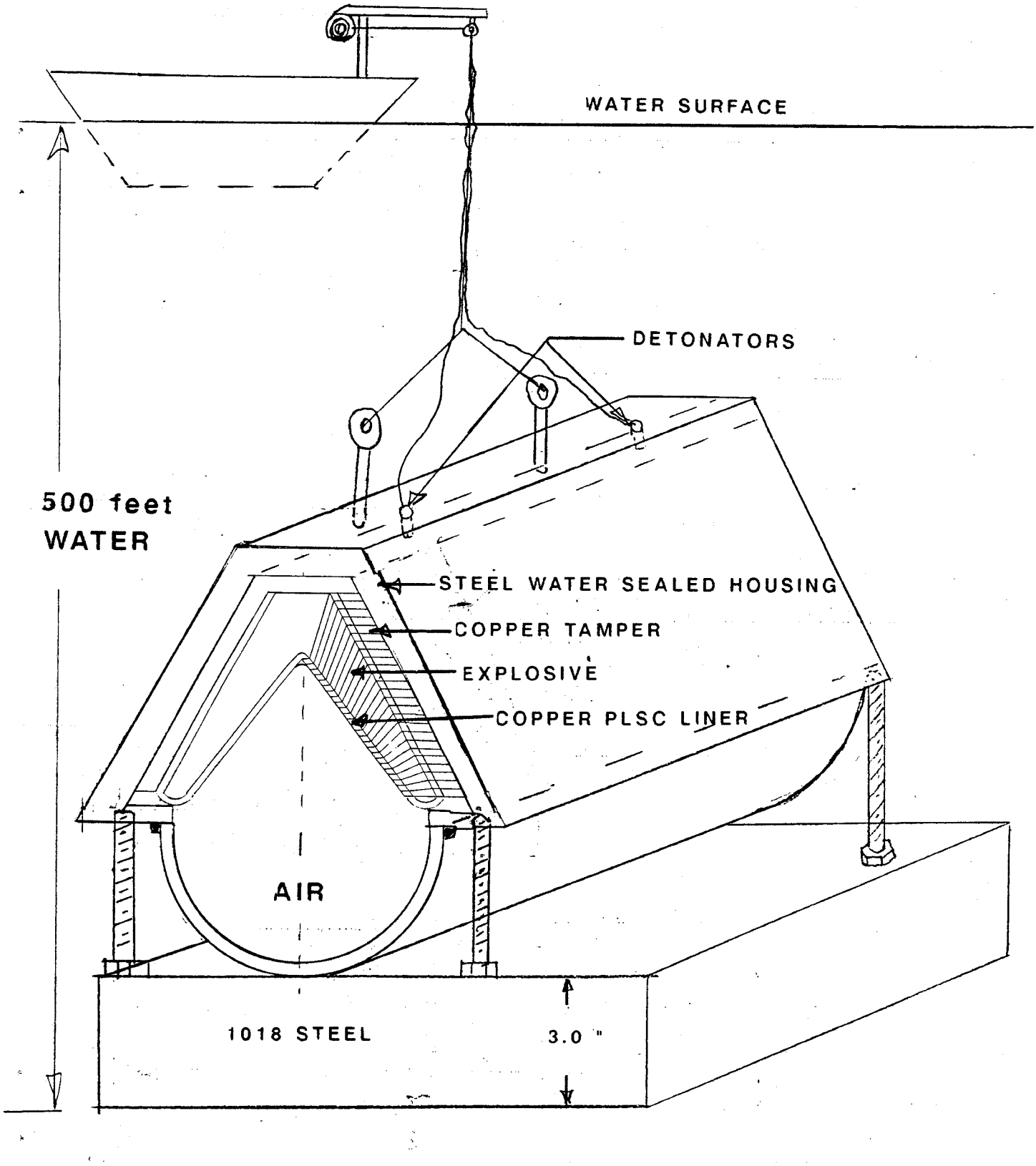

FIGURE 40. EXAMPLE PROBLEM CONFIGURATION

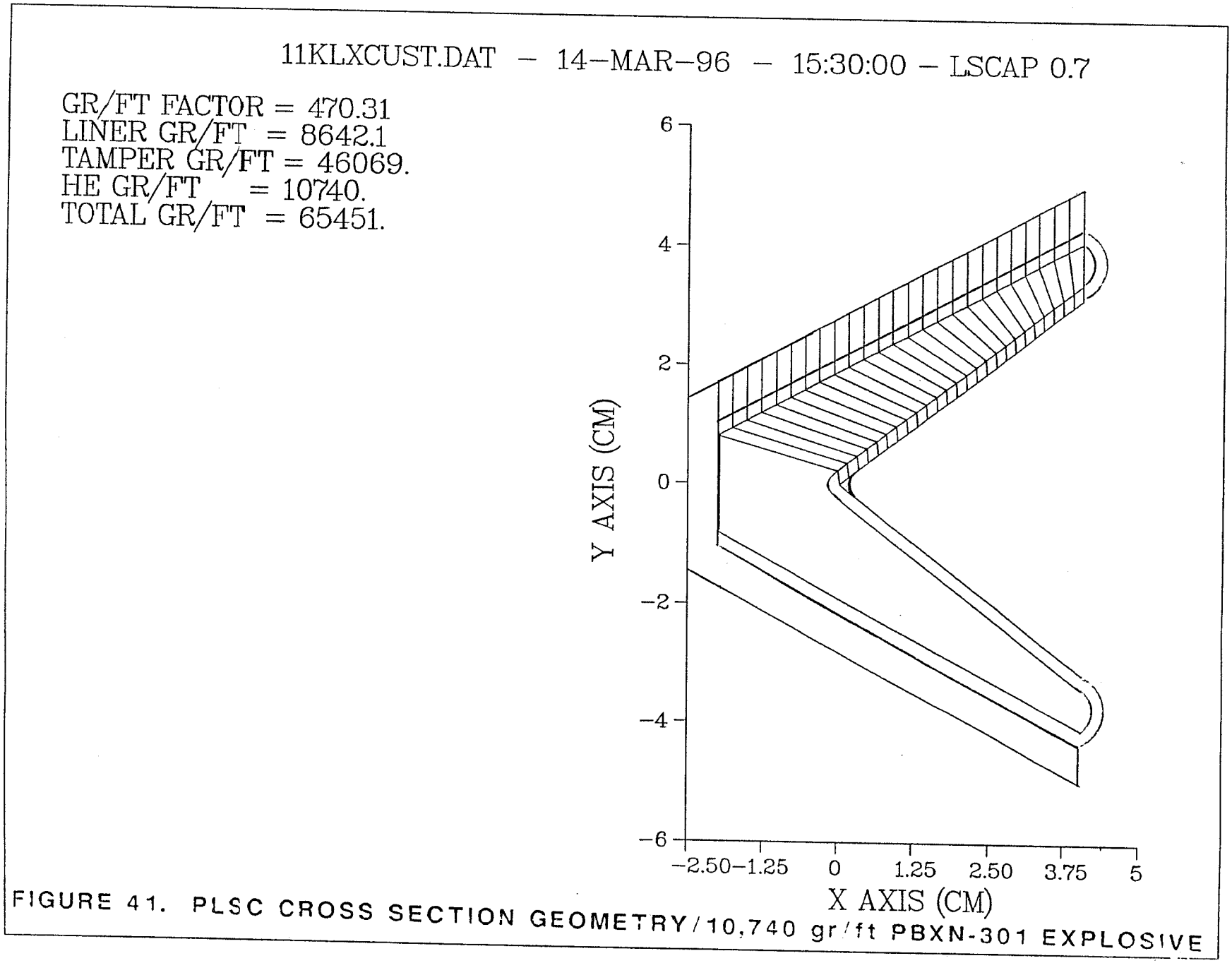

FIGURE 41. PLSC CROSS SECTION GEOMETRY/10,740 gr/ft PBXN-301 EXPLOSIVE

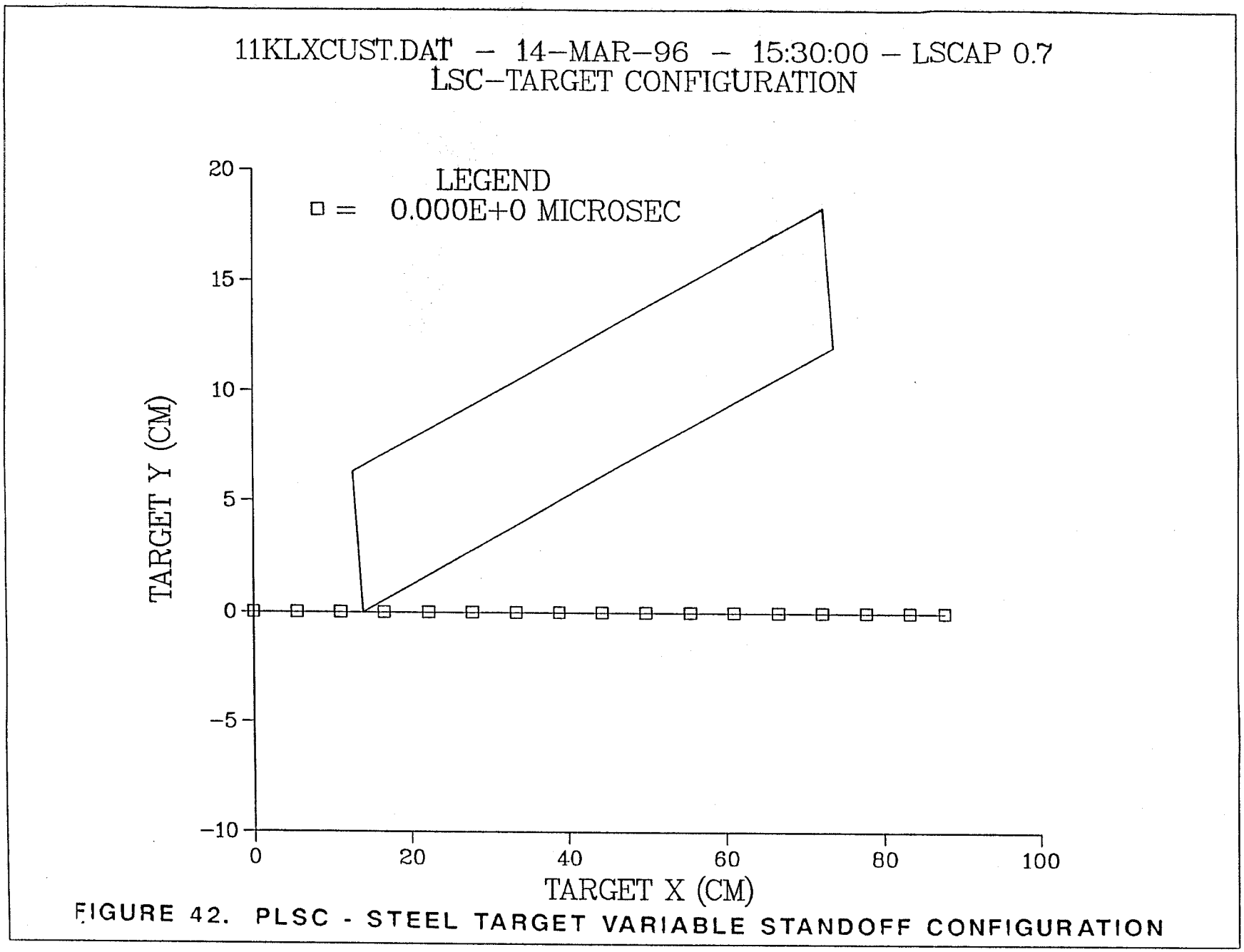

FIGURE 42. PLSC - STEEL TARGET VARIABLE STANDOFF CONFIGURATION

LINEAR SHAPED CHARGE (LSC) - TARGET PROFILE CONFIGURATION

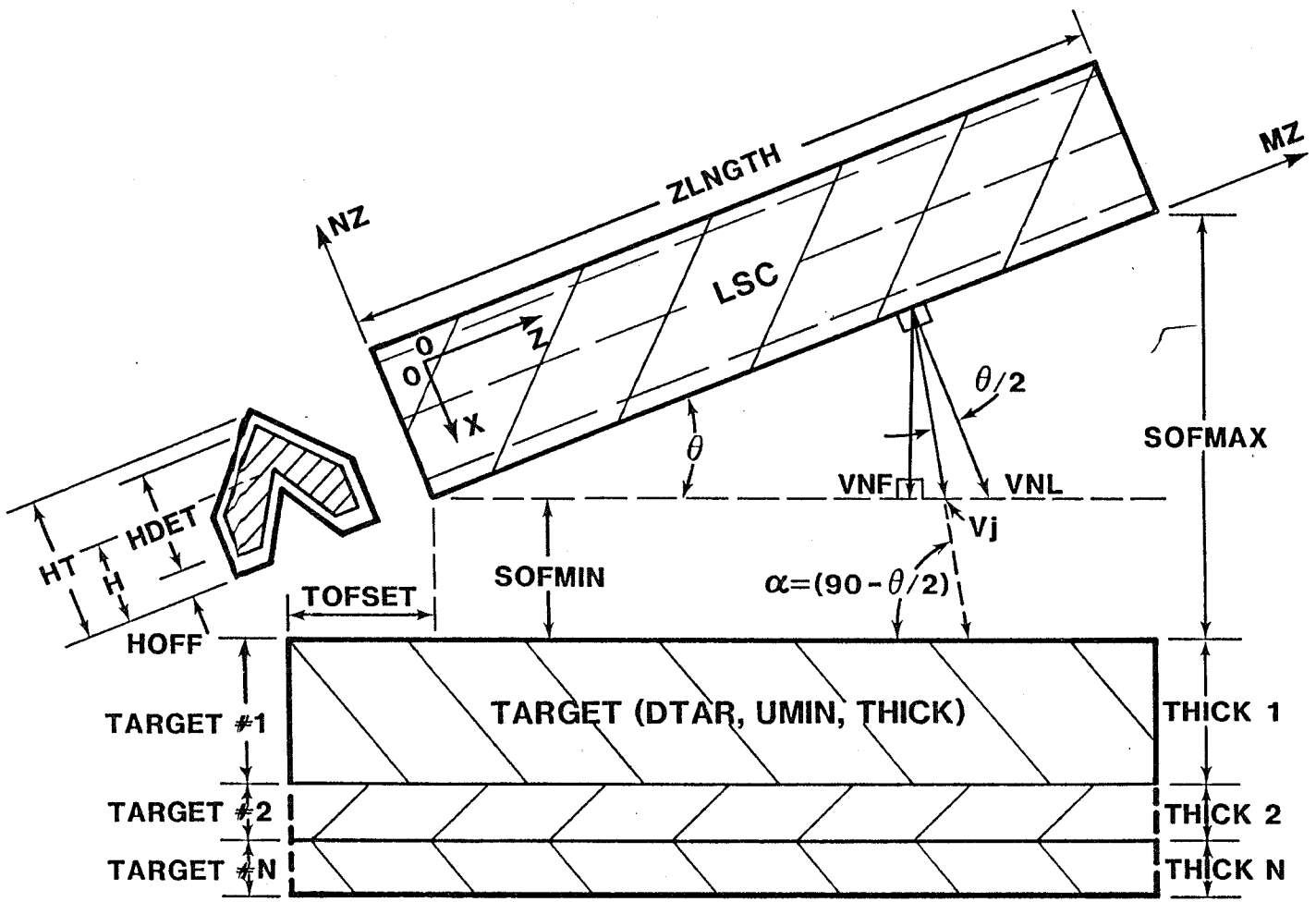

FIGURE 43. LSC - STEEL TARGET VARIABLE STANDOFF CONFIGURATION

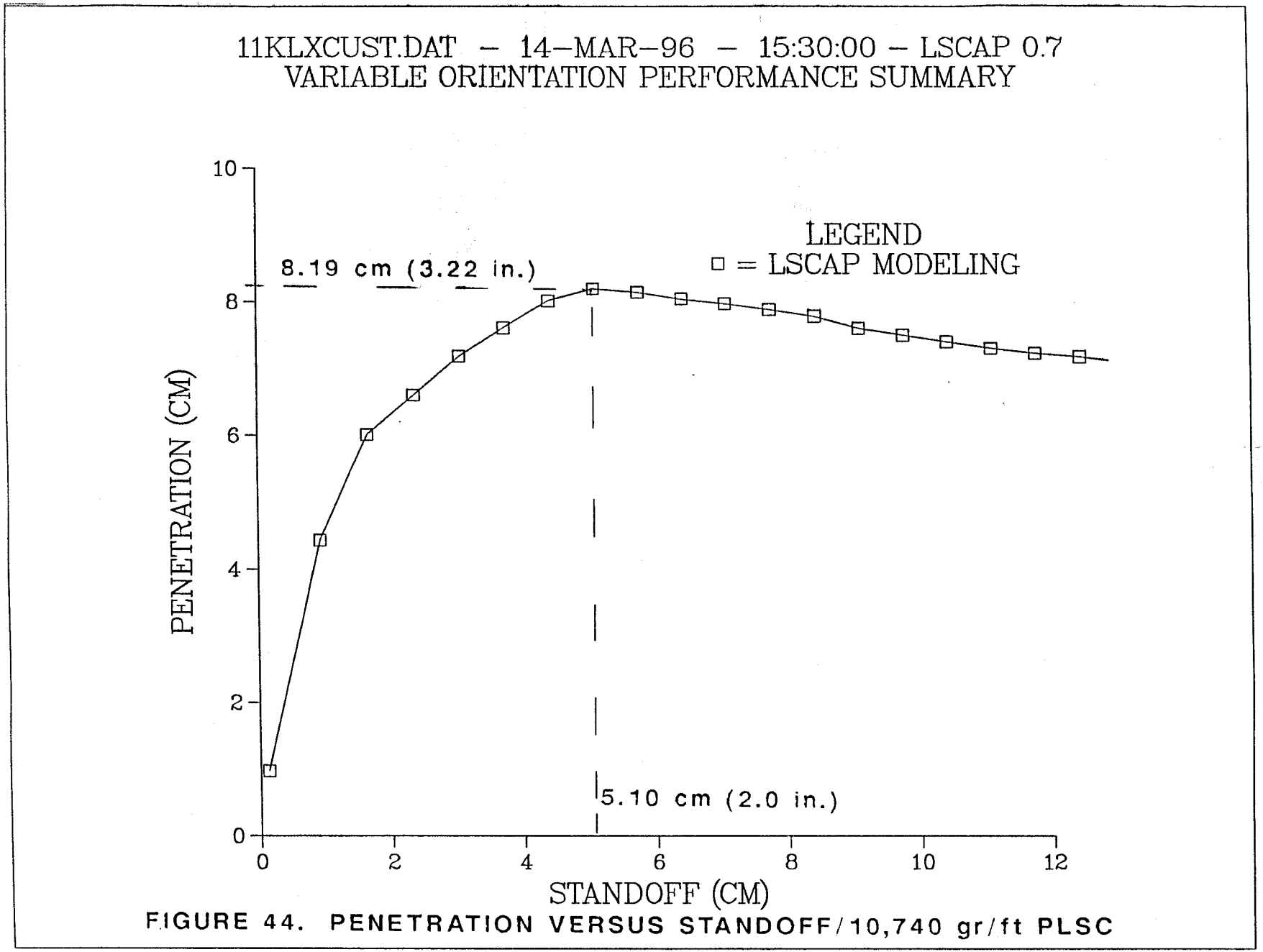

FIGURE 44. PENETRATION VERSUS STANDOFF/10,740 gr/ft PLSC

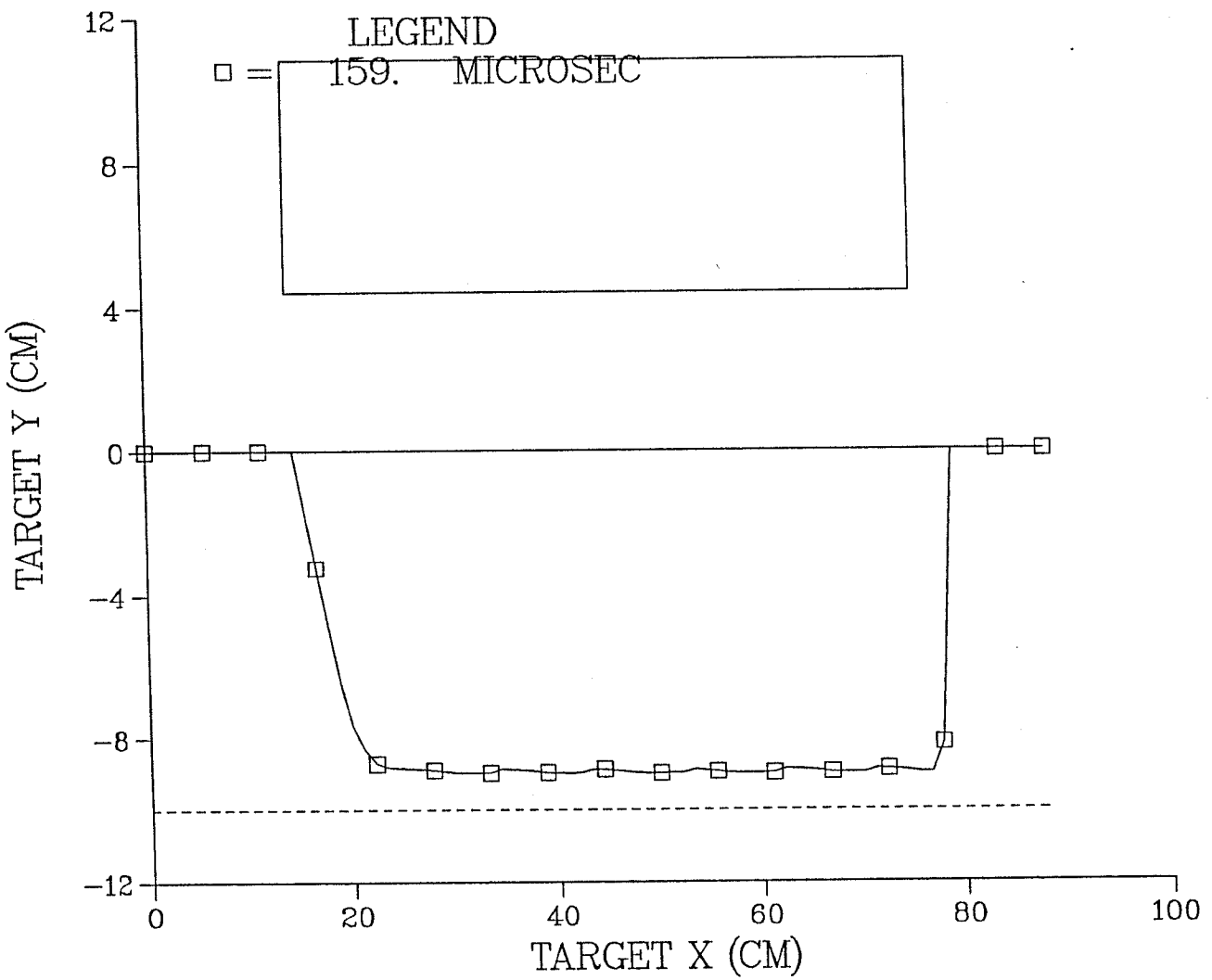

FIGURE 45. PLSC - STEEL TARGET CONSTANT STANDOFF CONFIGURATION

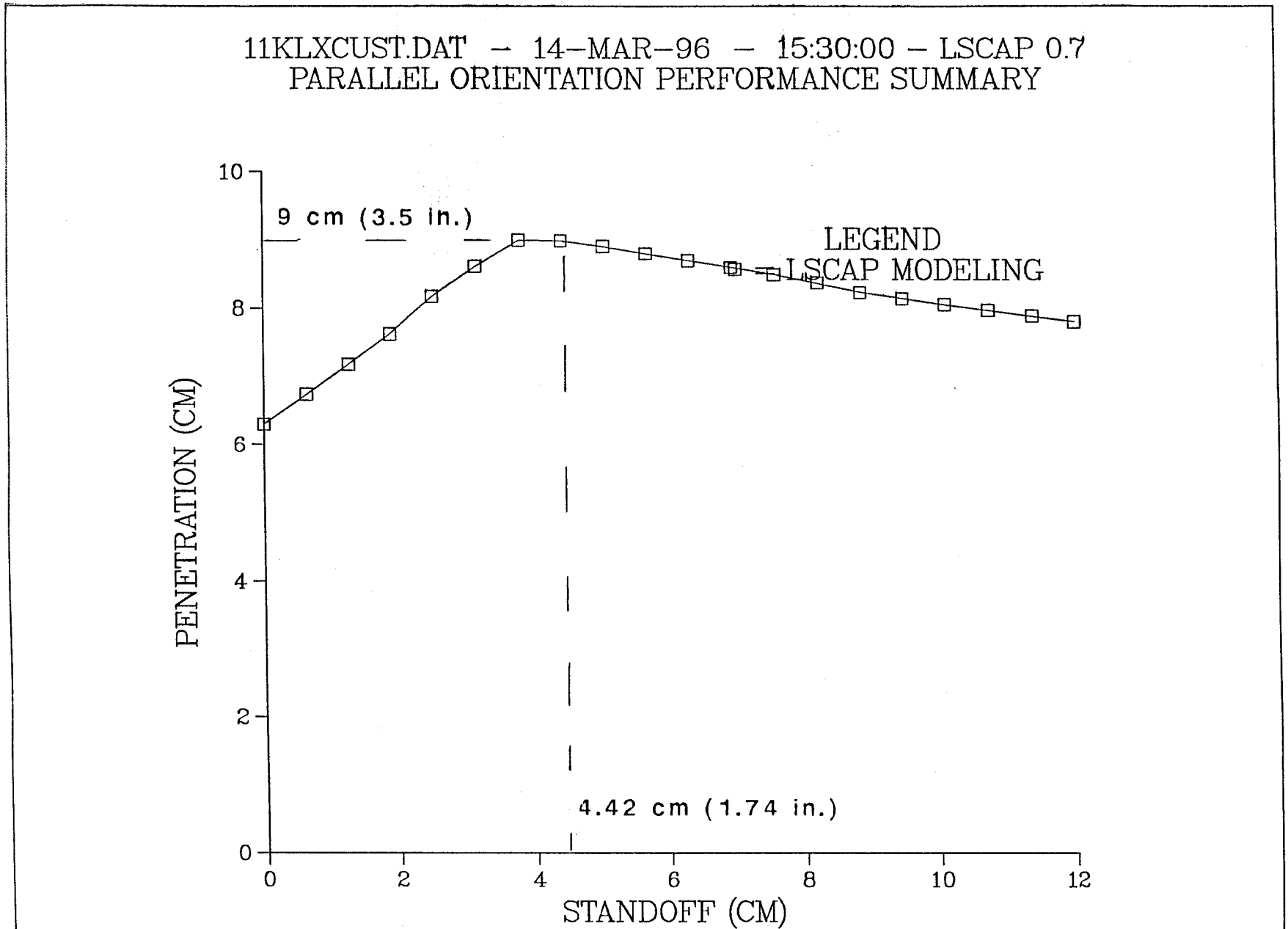

FIGURE 46. PENETRATION VERSUS PARALLEL STANDOFF

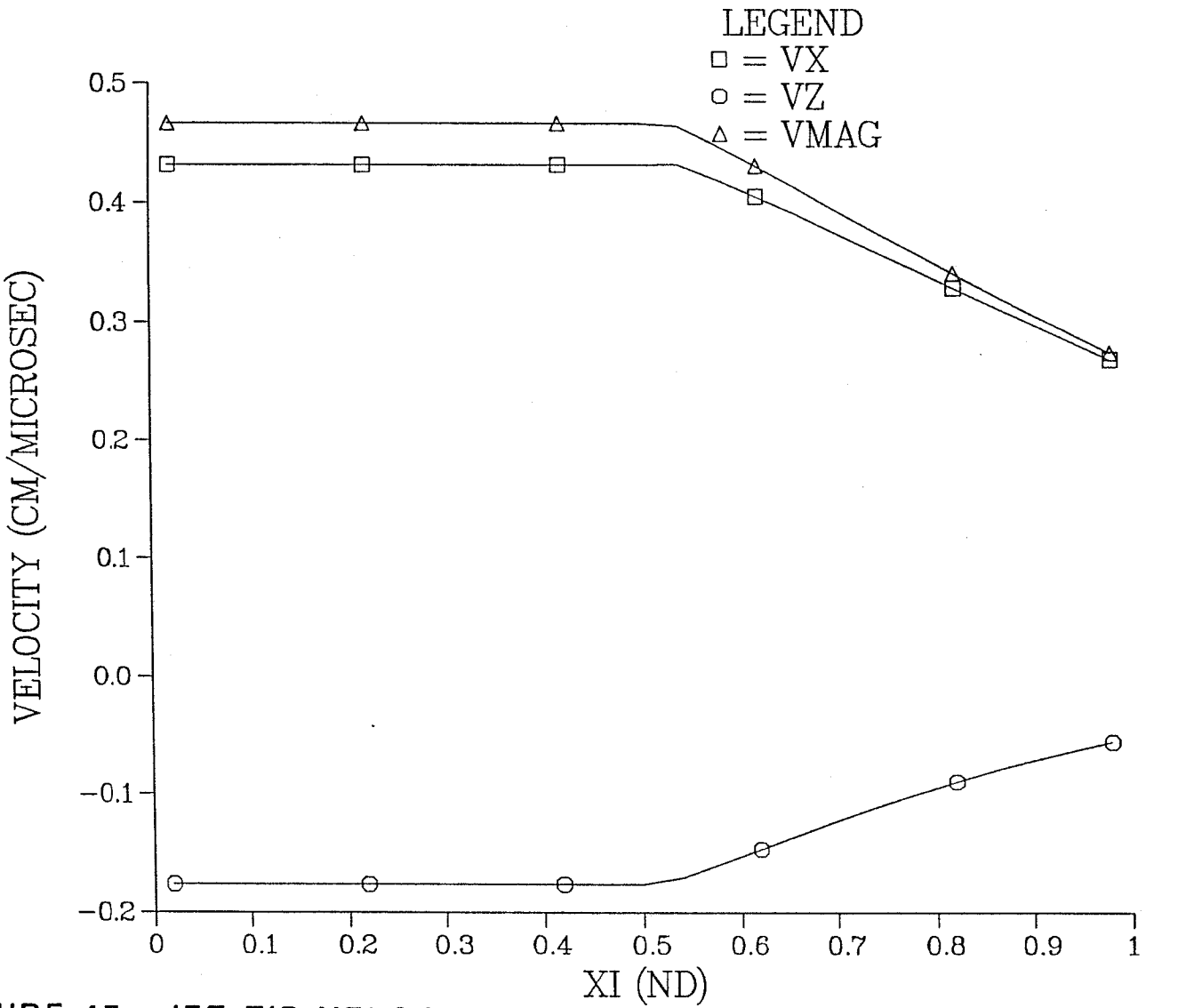

FIGURE 47. JET TIP VELOCITES VERSUS DISTANCE ALONG THE LINER

APPENDIX A

VARIABLE STANDOFF CONFIGURATION

10,740 gr/ft PLSC Jet Penetration Versus Target Distance Data

Page

A1 Jet Penetration/10.5 μs 81

A2 Jet Penetration/20.3 μs 82

A3 Jet Penetration/40.5 μs 83

A4 Jet Penetration/60/8 μs 84

A5 Jet Penetration/80.2 μs 85

A6 Jet Penetration/100 μs 86

A7 Jet Penetration/121 μs 87

A8 Jet Penetration/140 μs 88

A9 Jet Penetration/160 μs 89

Intentionally Left Blank

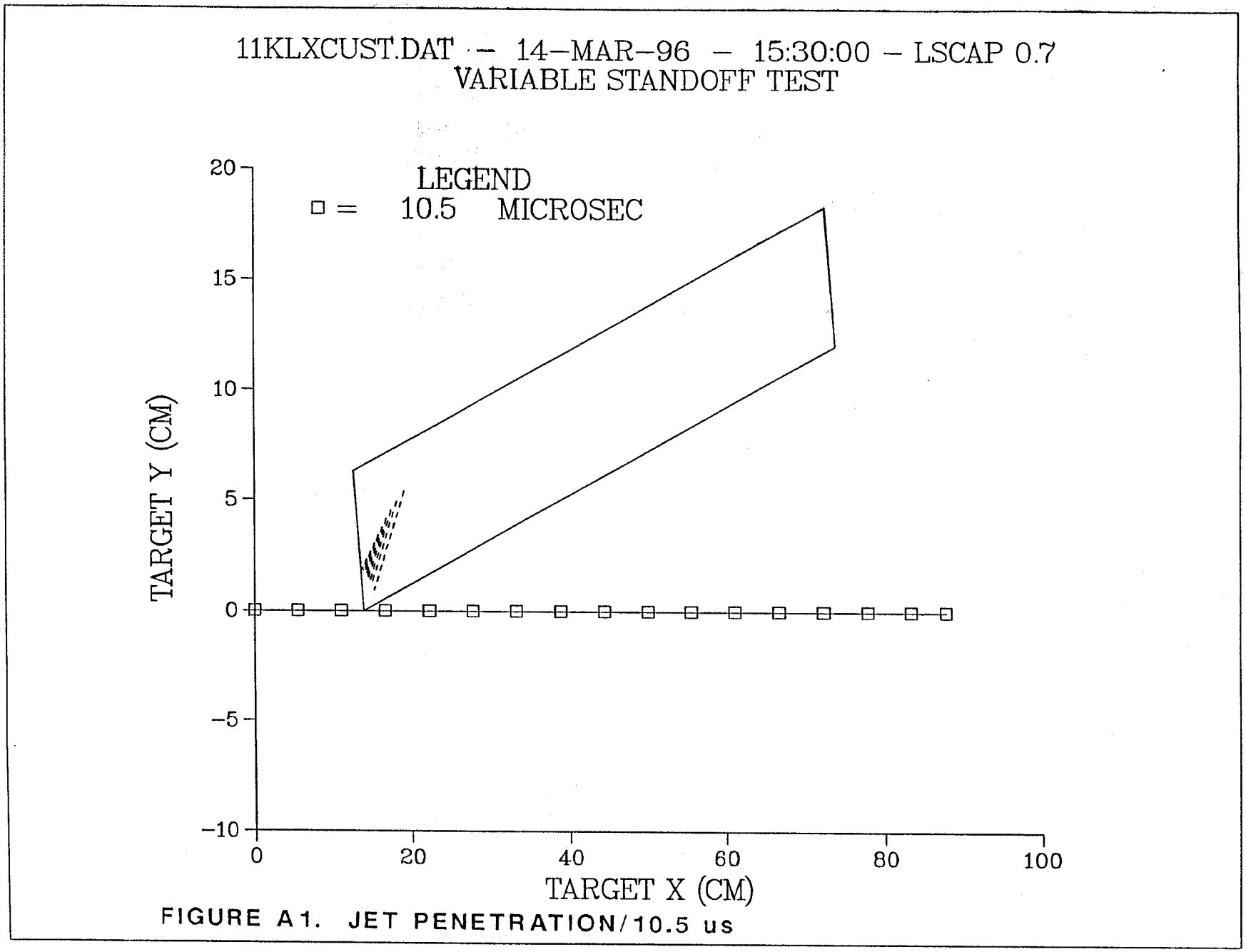

FIGURE A1. JET PENETRATION/10.5 us

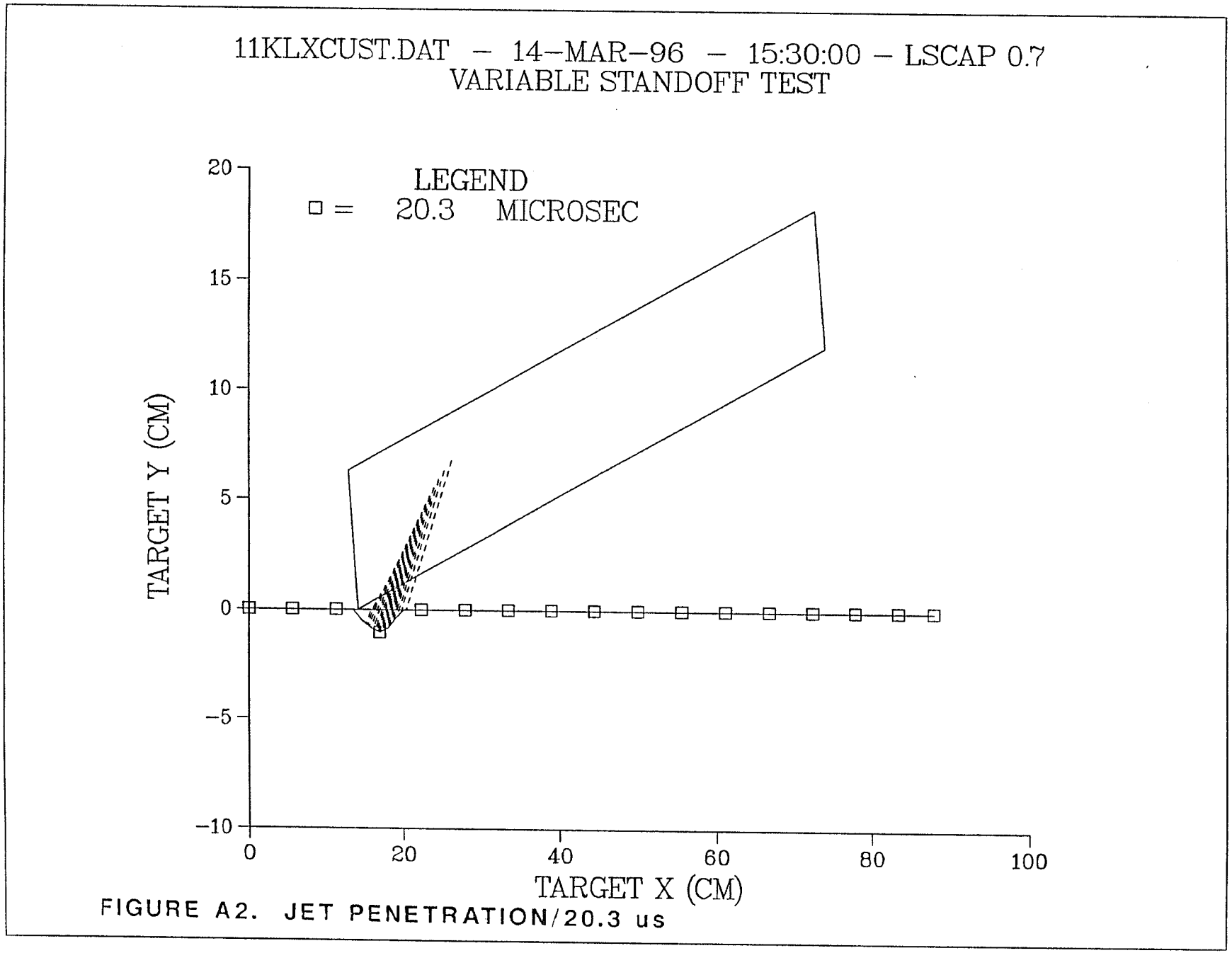

FIGURE A2. JET PENETRATION/20.3 us

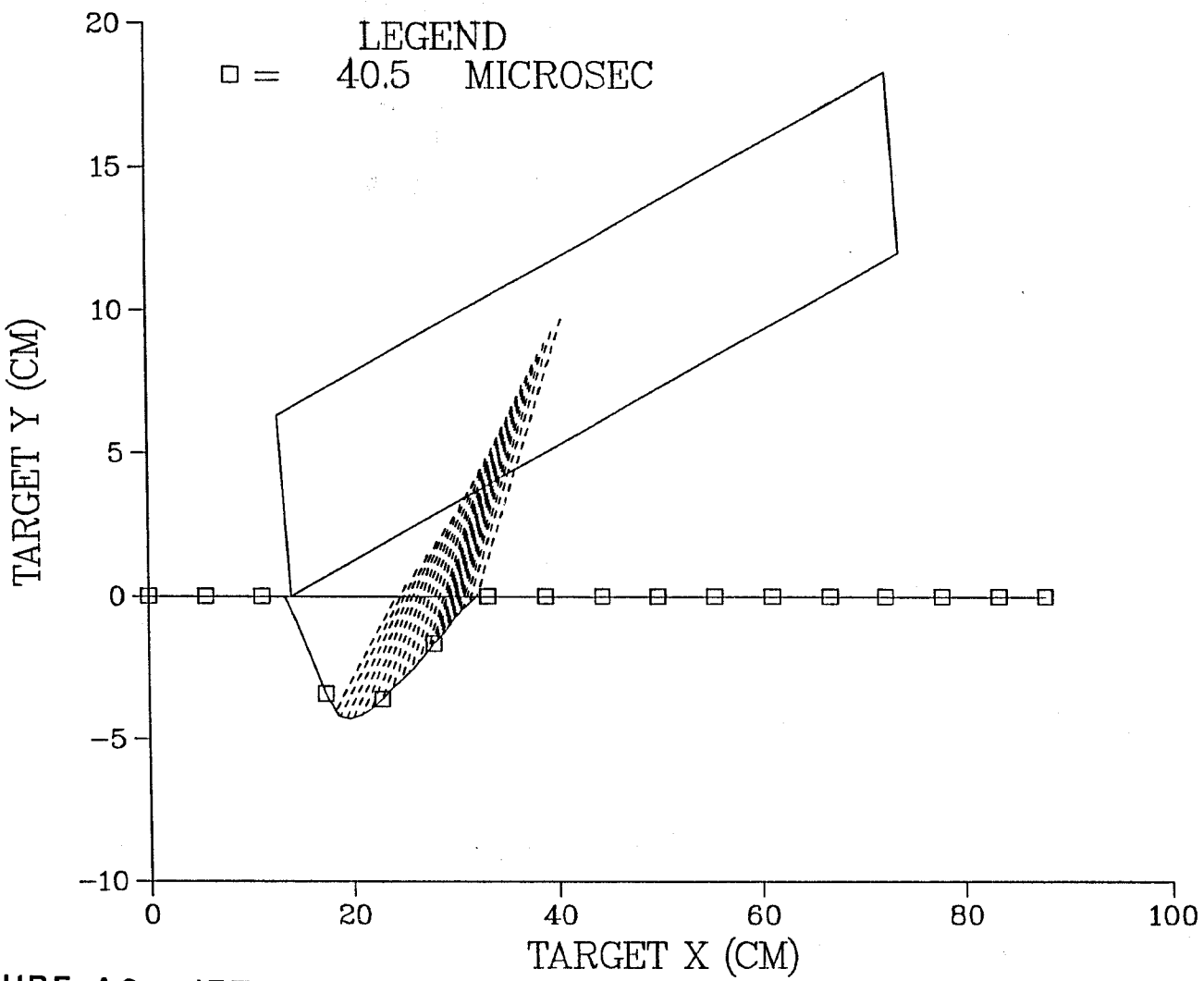

FIGURE A3. JET PENETRATION/40.5 us

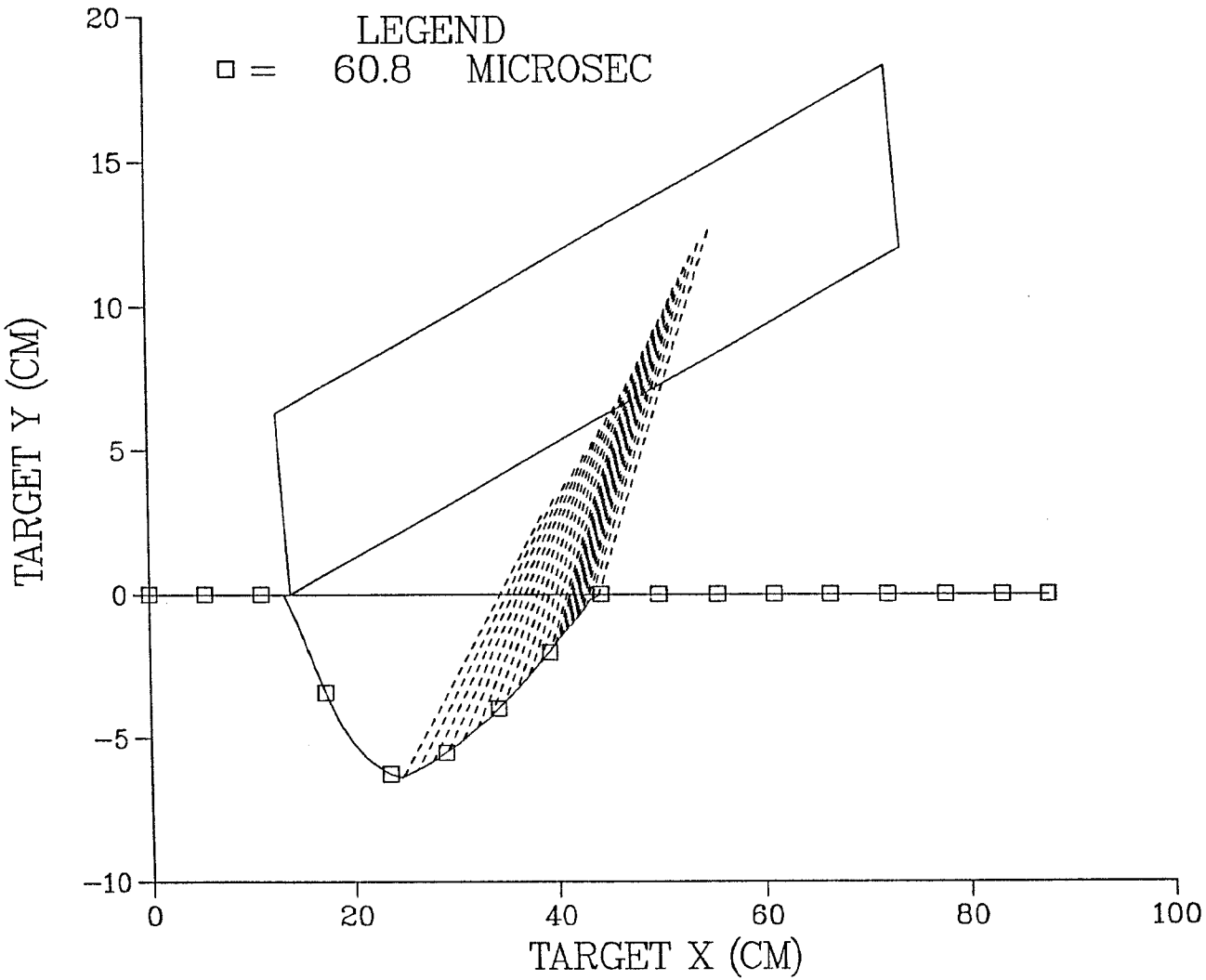

FIGURE A4. JET PENETRATION/60.8 us

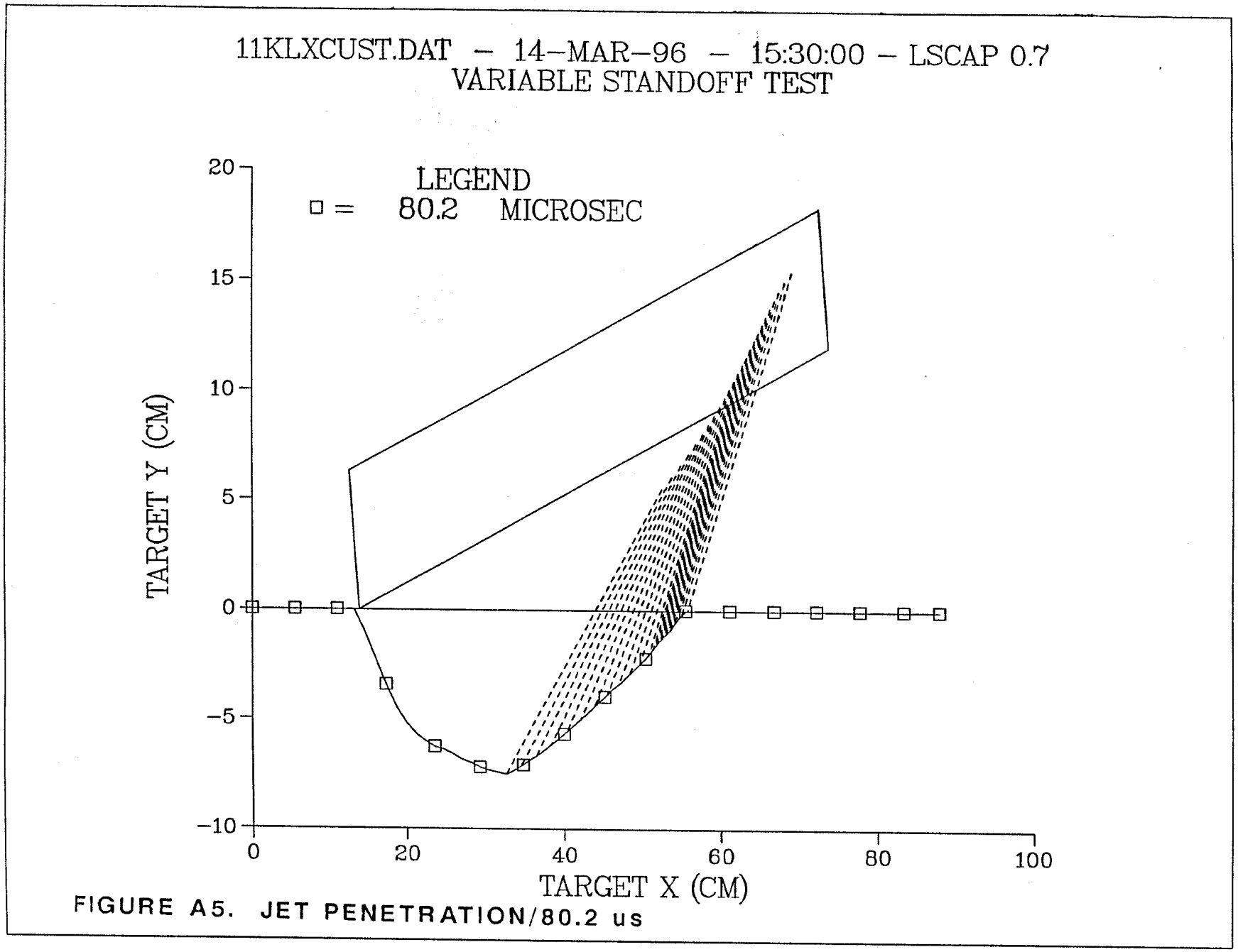

FIGURE A5. JET PENETRATION/80.2 us

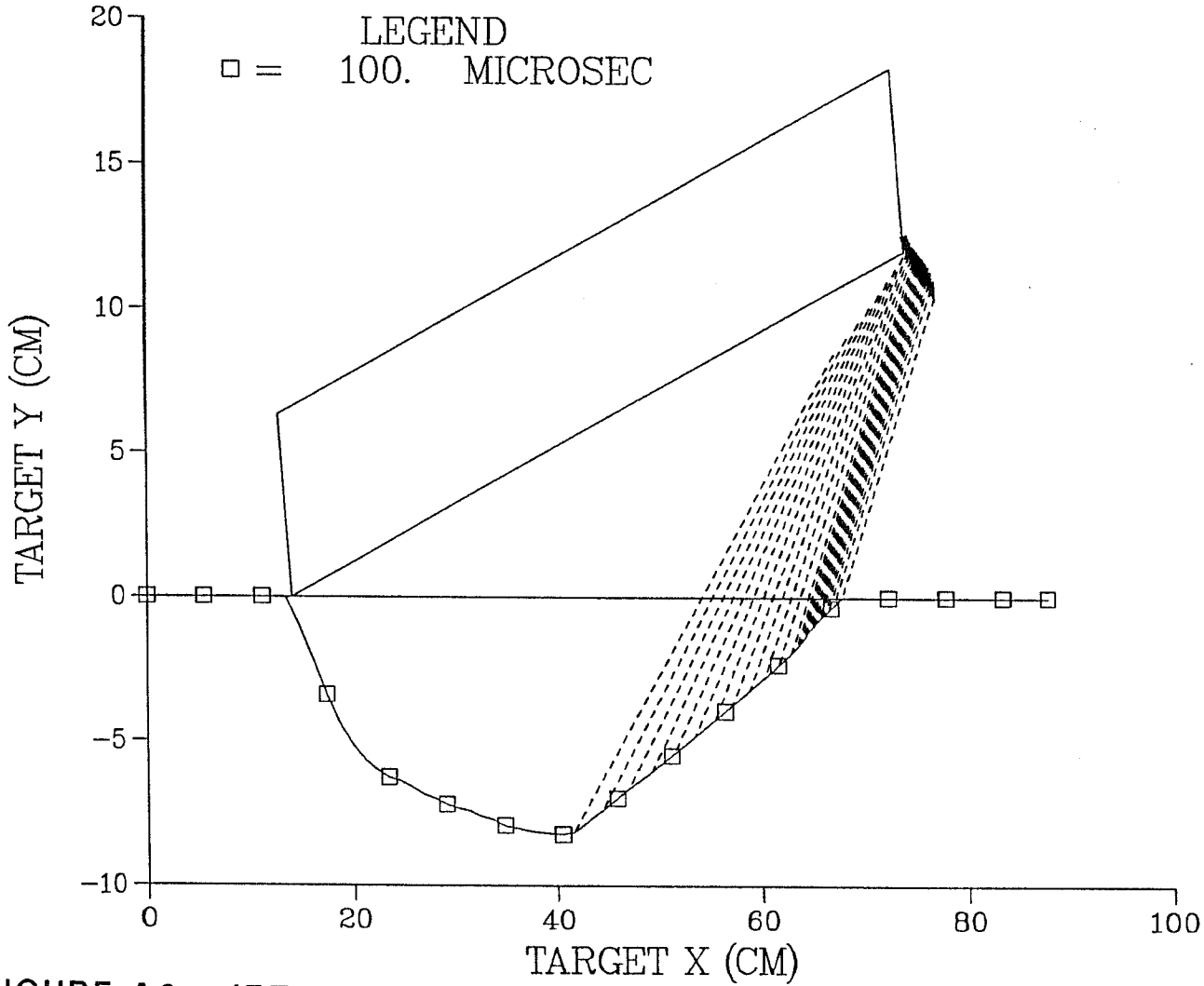

FIGURE A6. JET PENETRATION/100 us

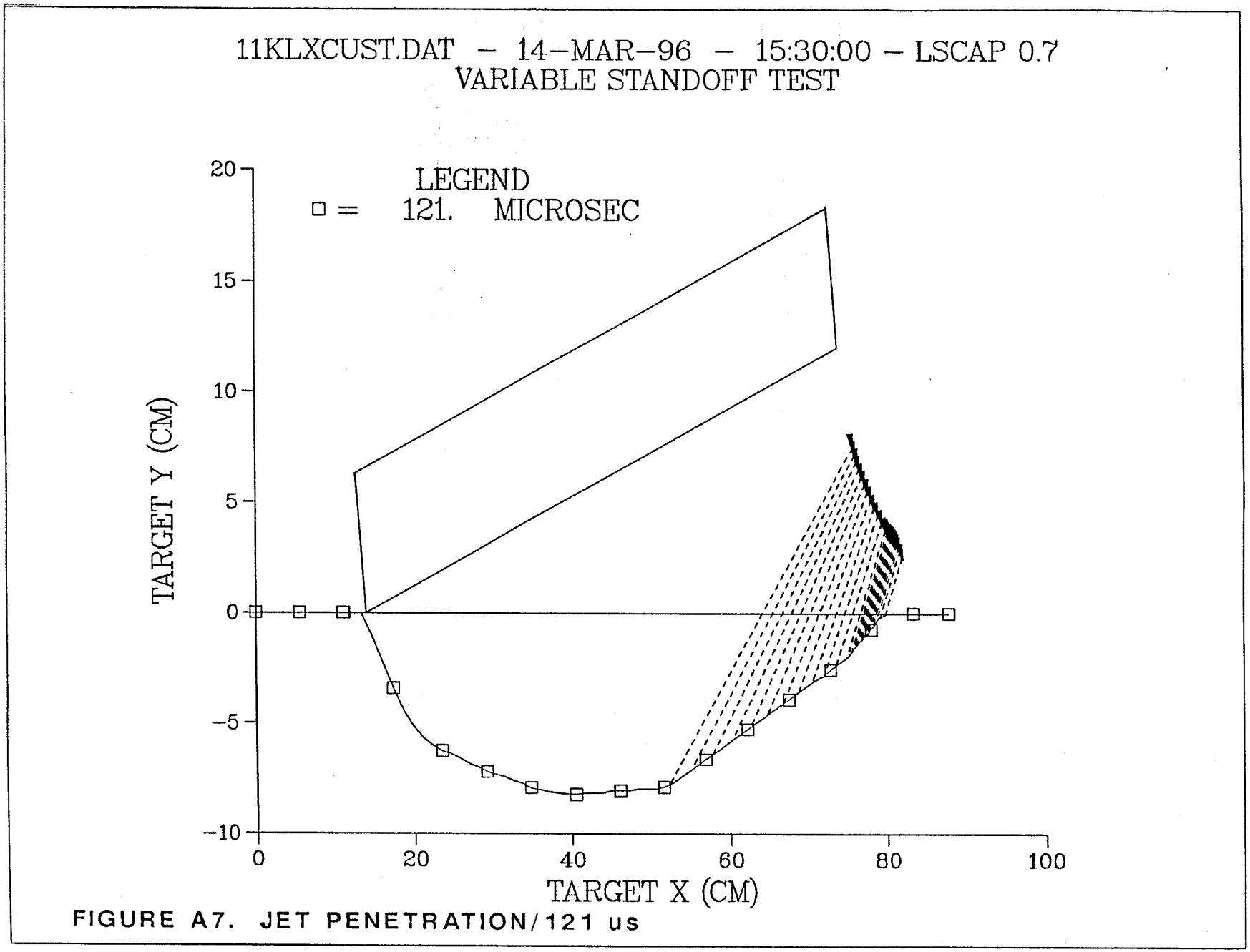

FIGURE A7. JET PENETRATION/121 us

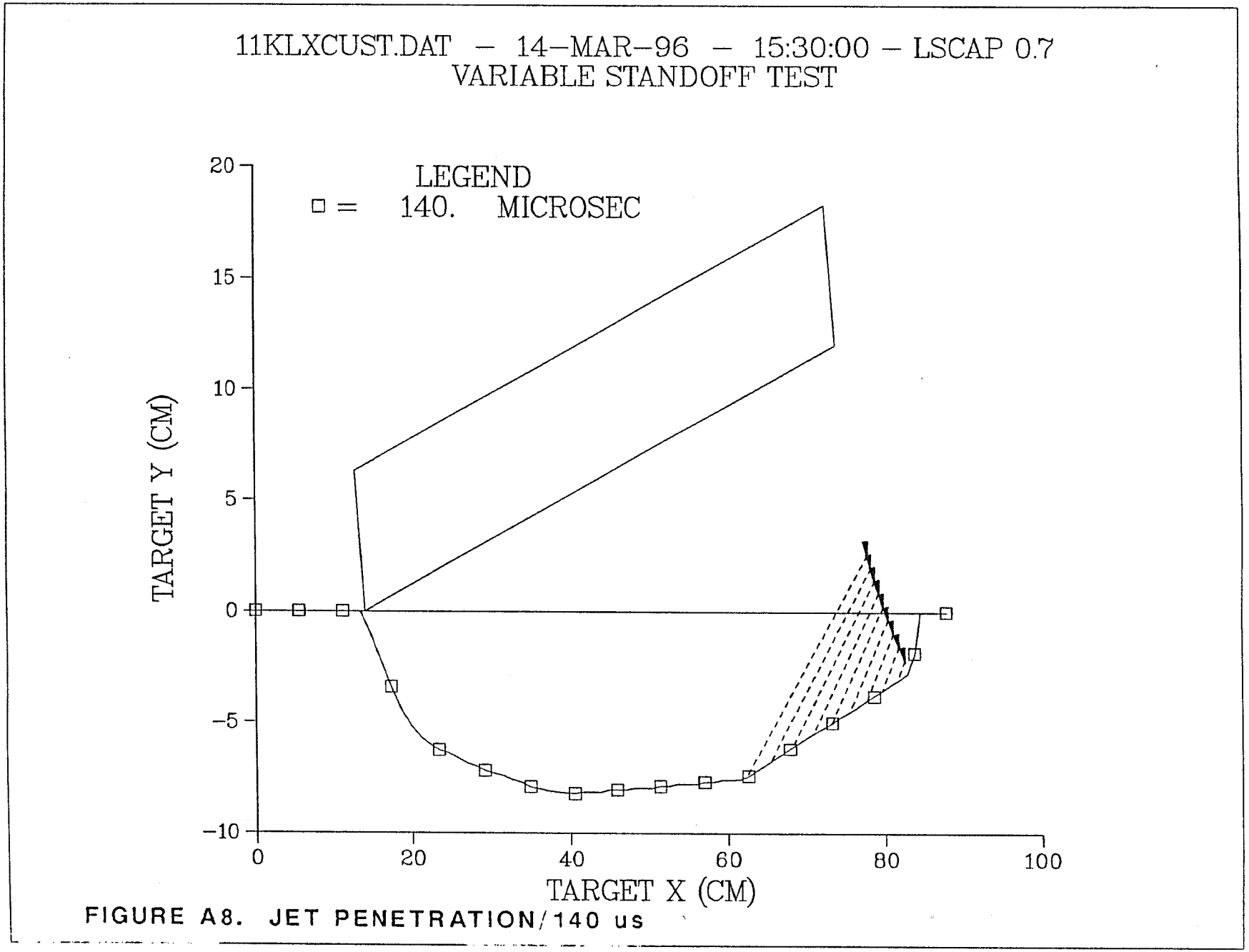

FIGURE A8. JET PENETRATION/140 us

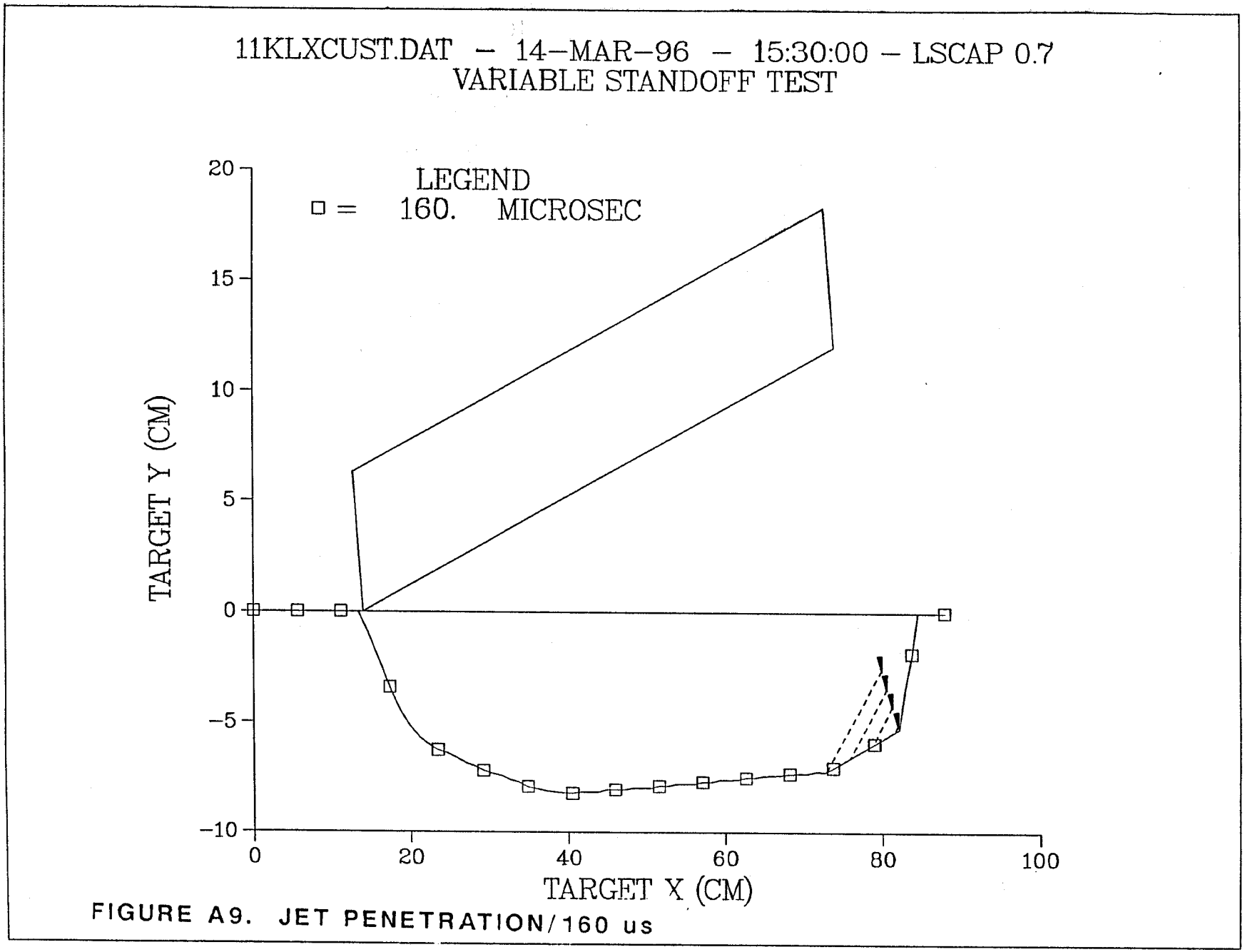

FIGURE A9. JET PENETRATION/160 us

Intentionally Left Blank

APPENDIX B

CONSTANT STANDOFF CONFIGURATION

10,740 gr/ft PLSC Jet Penetration Versus Target Distance Data

Page

B1 Jet Penetration/132 μs 93

B2 Jet Penetration/142 μs 94

B3 Jet Penetration/149 μs 95

B4 Jet Penetration/156 μs 96

B5 Jet Penetration/164 μs 97

B6 Jet Penetration/168 μs 98

B7 Jet Penetration/171 μs 99

B8 Jet Penetration/175 μs 100

B9 Jet Penetration/178 μs 101

Intentionally Left Blank

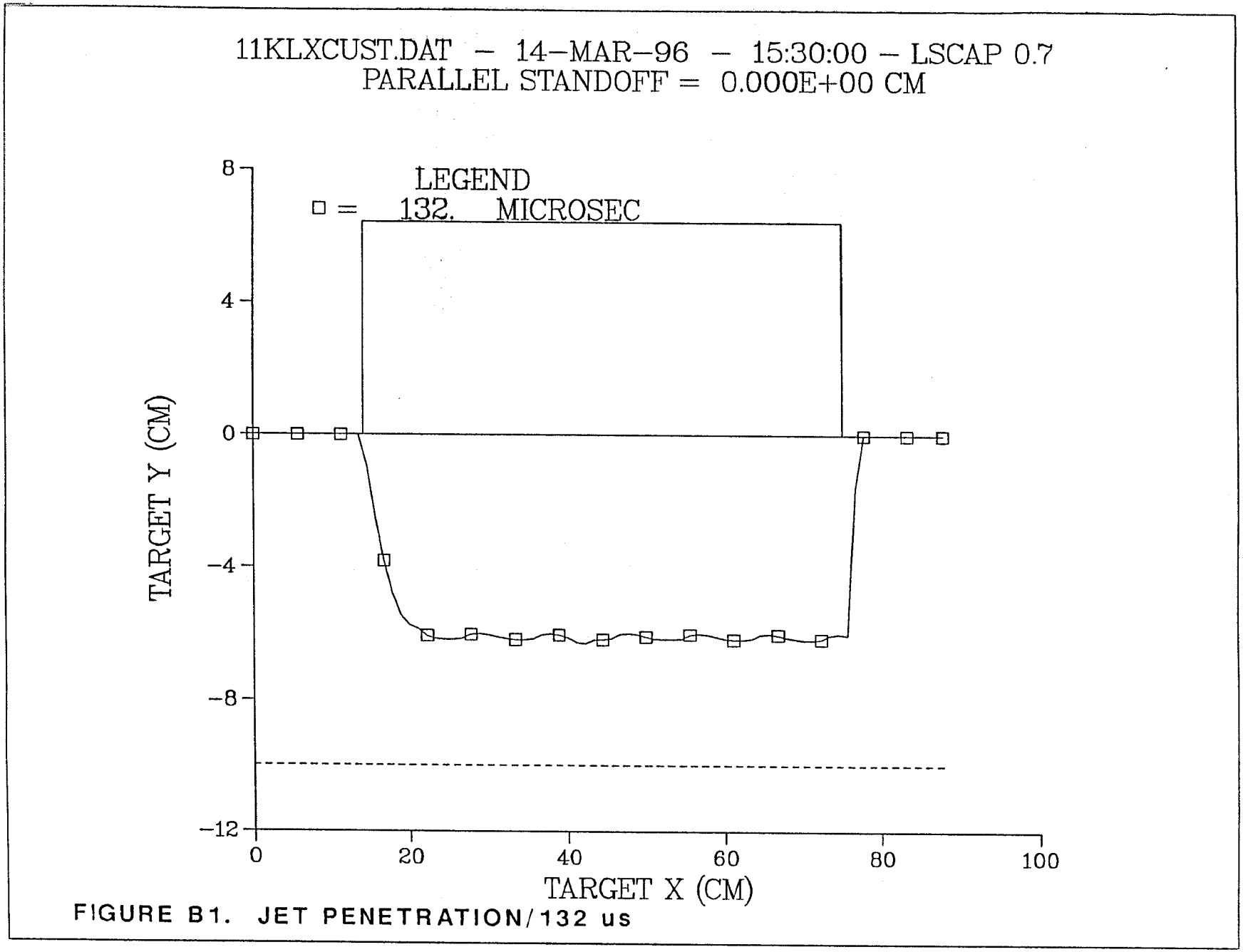

FIGURE B1. JET PENETRATION/132 us

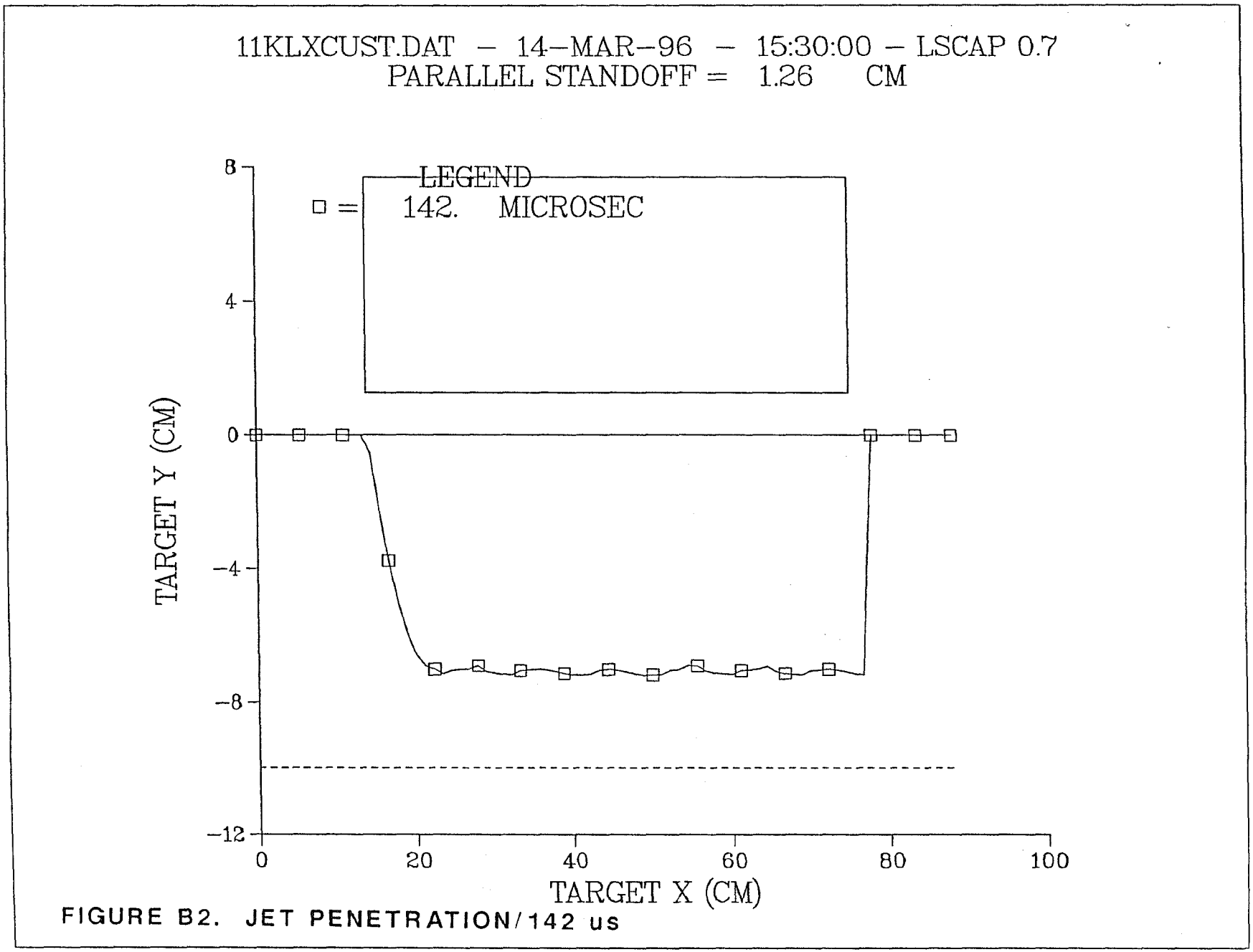

FIGURE B2. JET PENETRATION/142 us

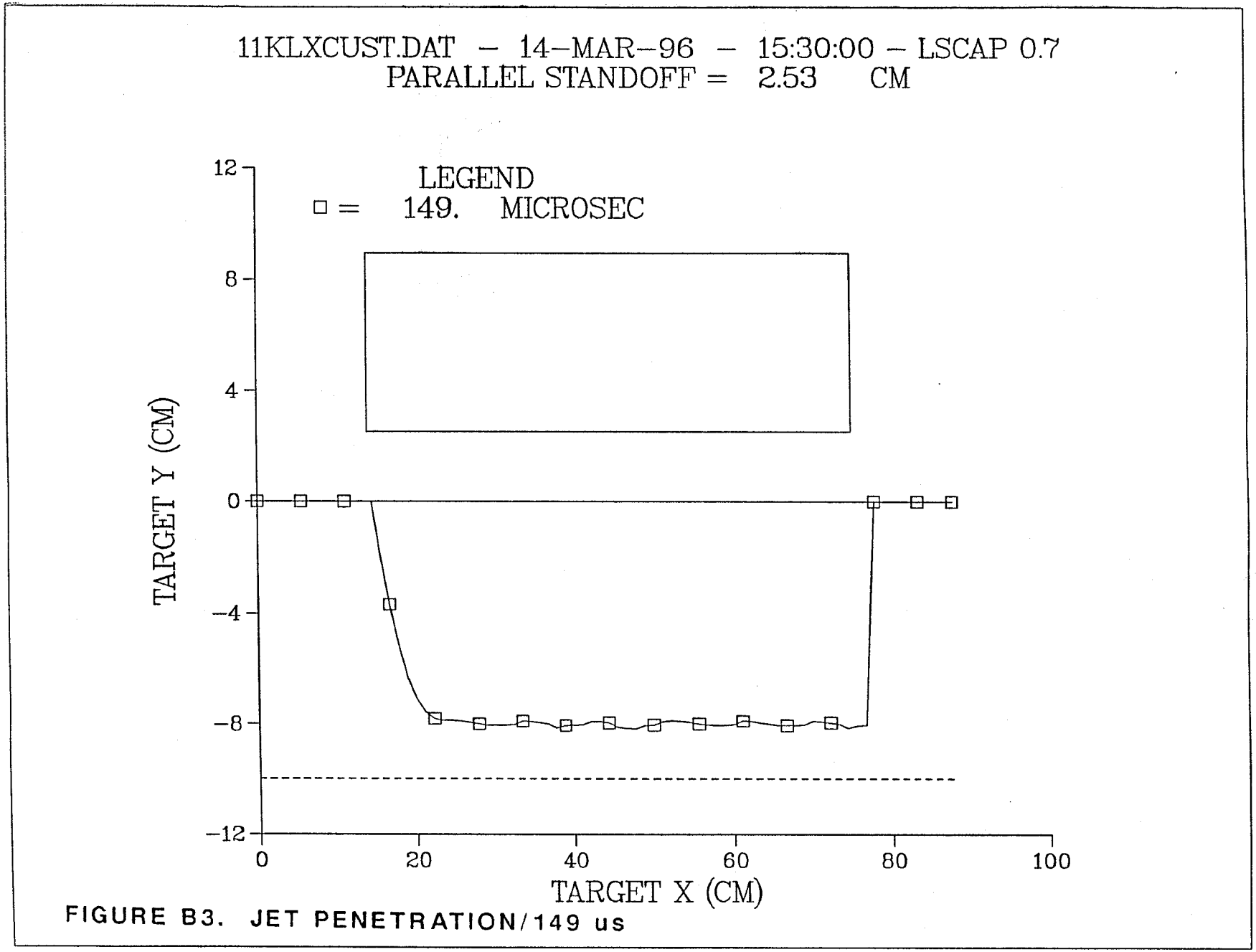

FIGURE B3. JET PENETRATION/149 us

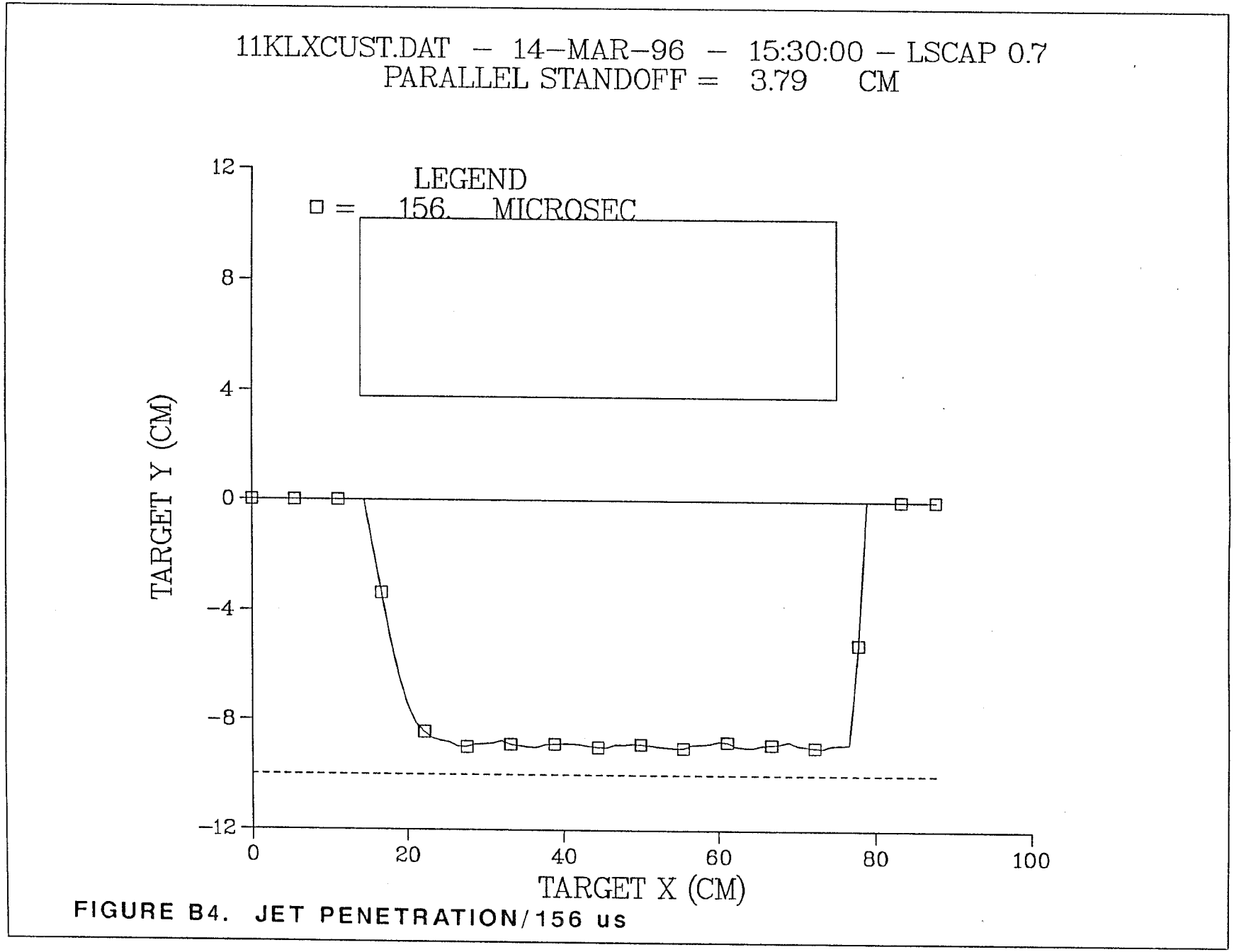

FIGURE B4. JET PENETRATION/156 us

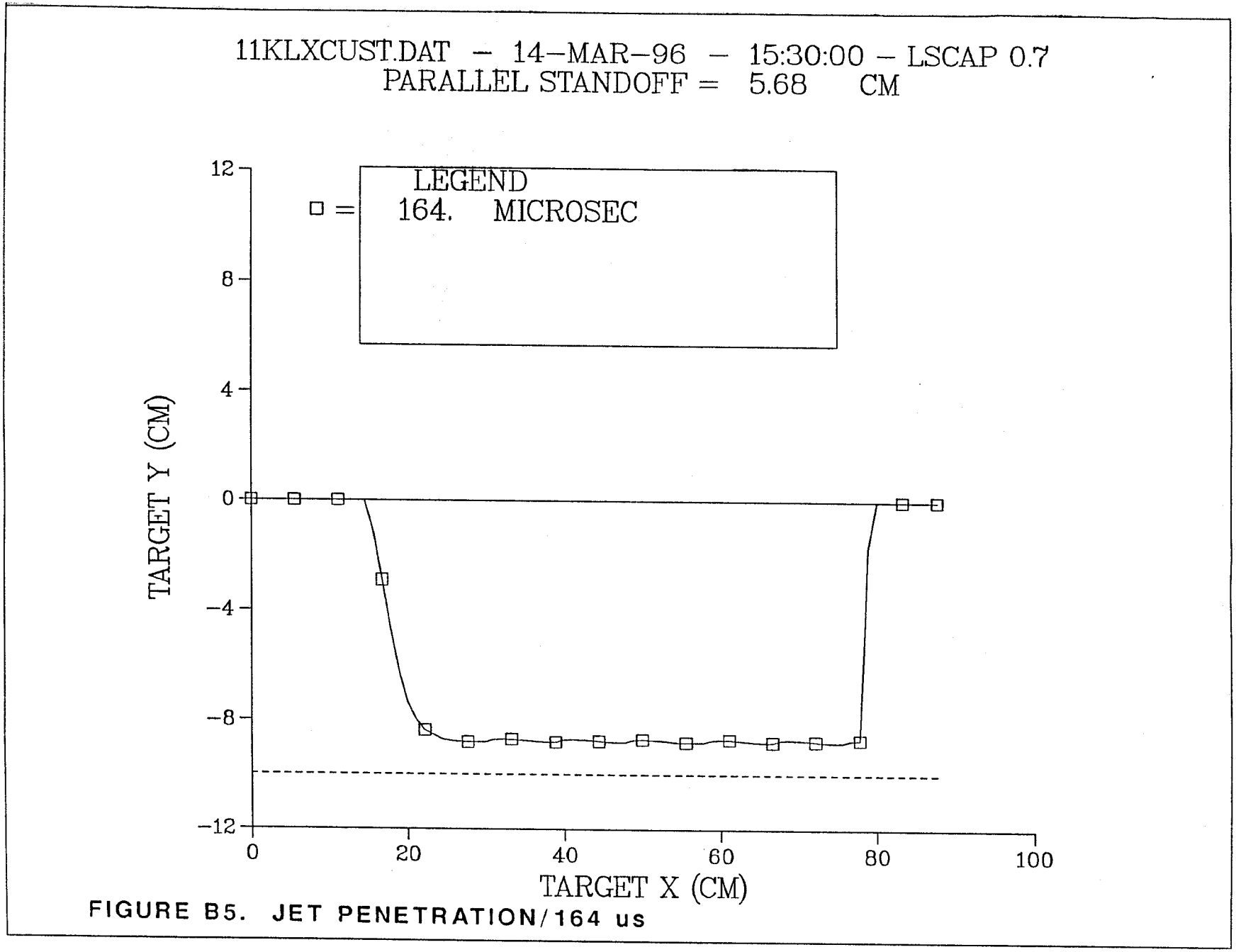

FIGURE B5. JET PENETRATION/164 us

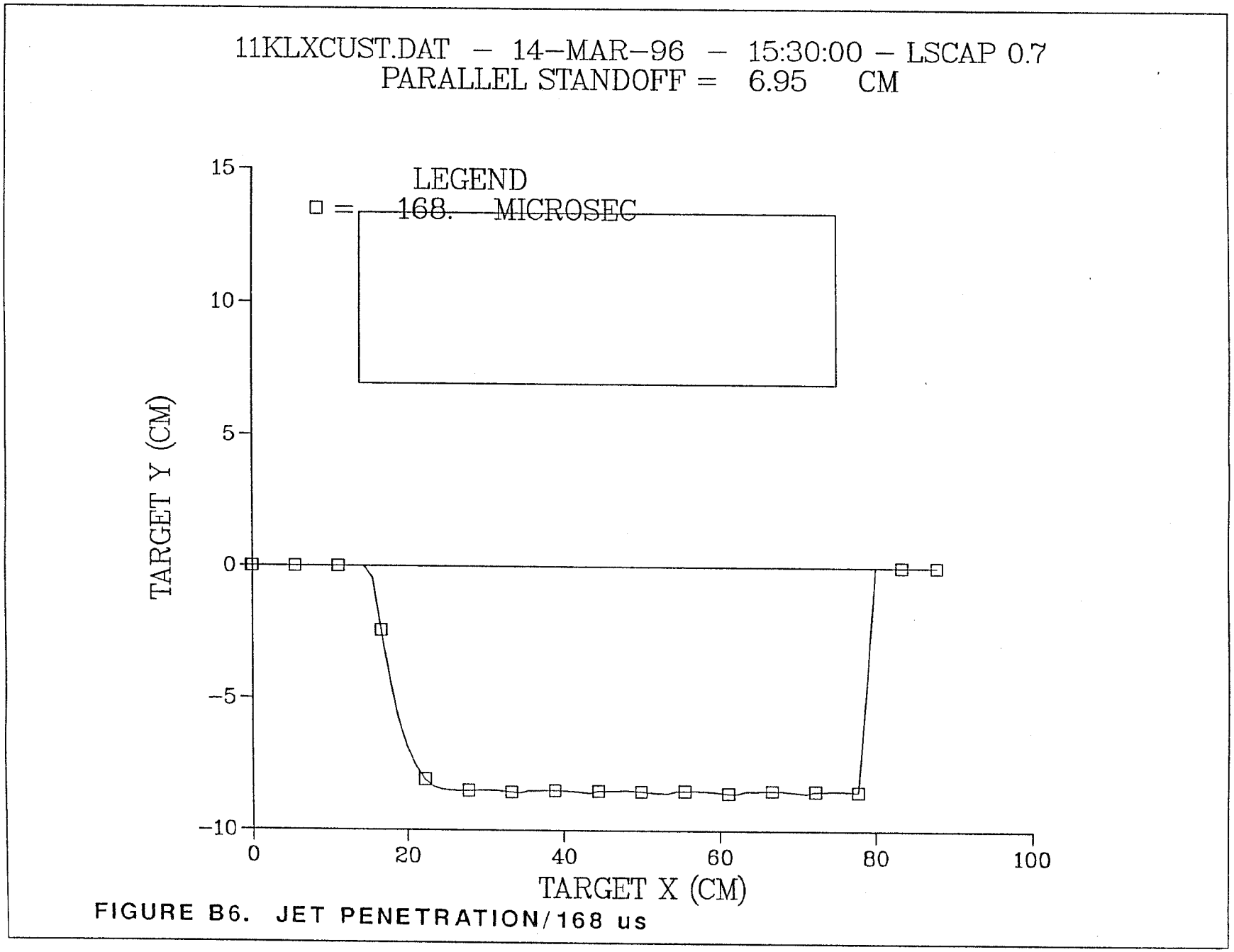

FIGURE B6. JET PENETRATION/168 us

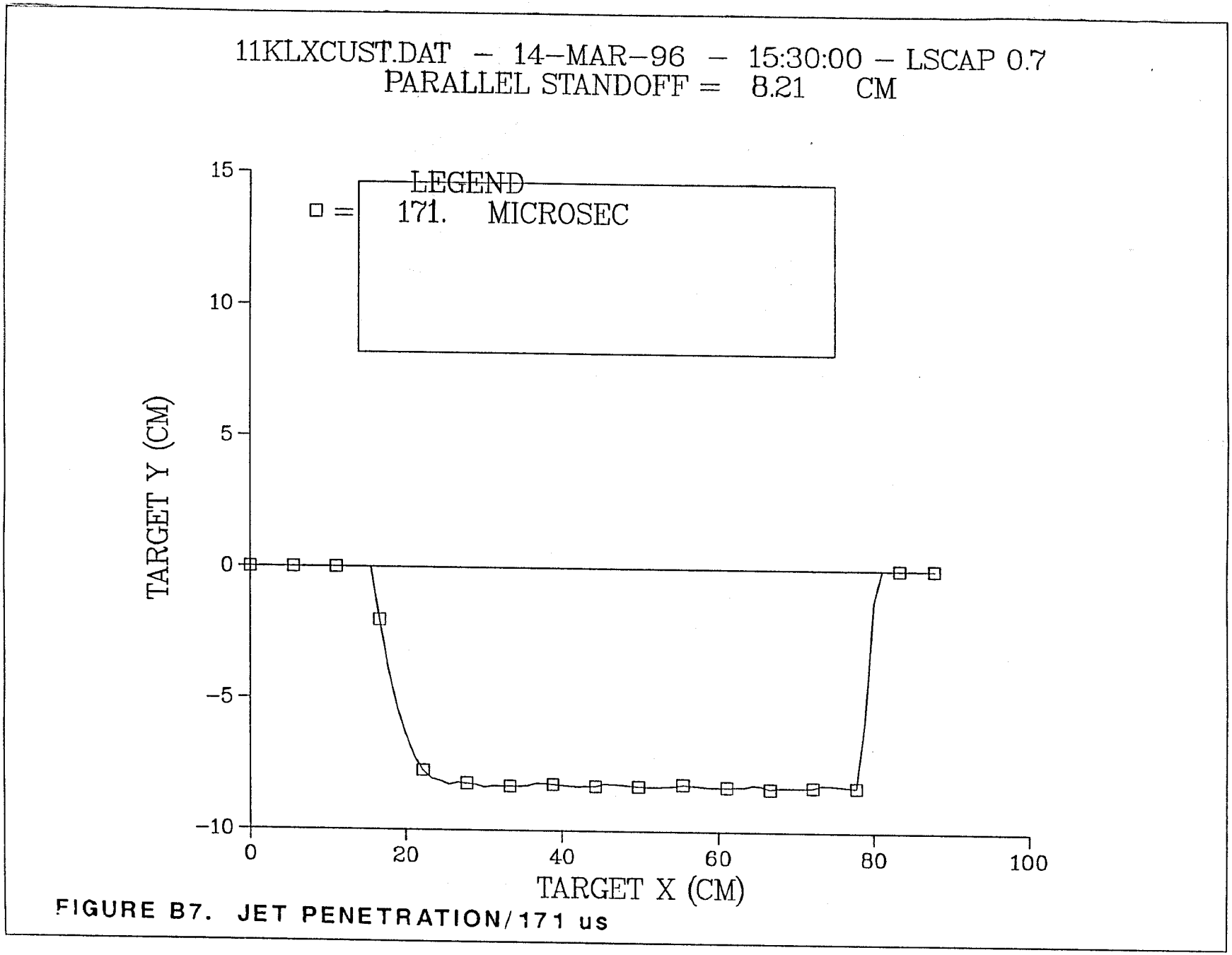

FIGURE B7. JET PENETRATION/171 us

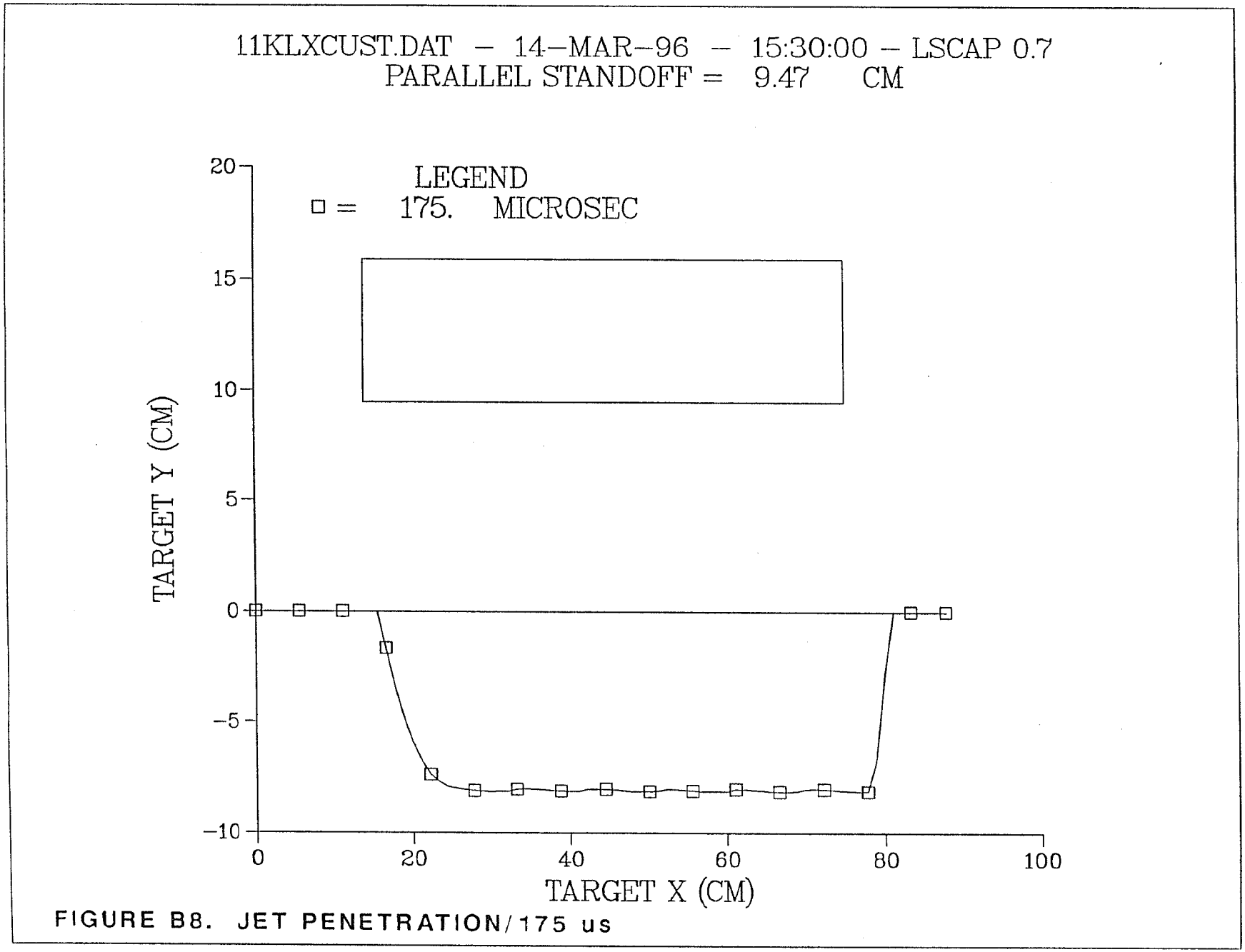

FIGURE B8. JET PENETRATION/175 us

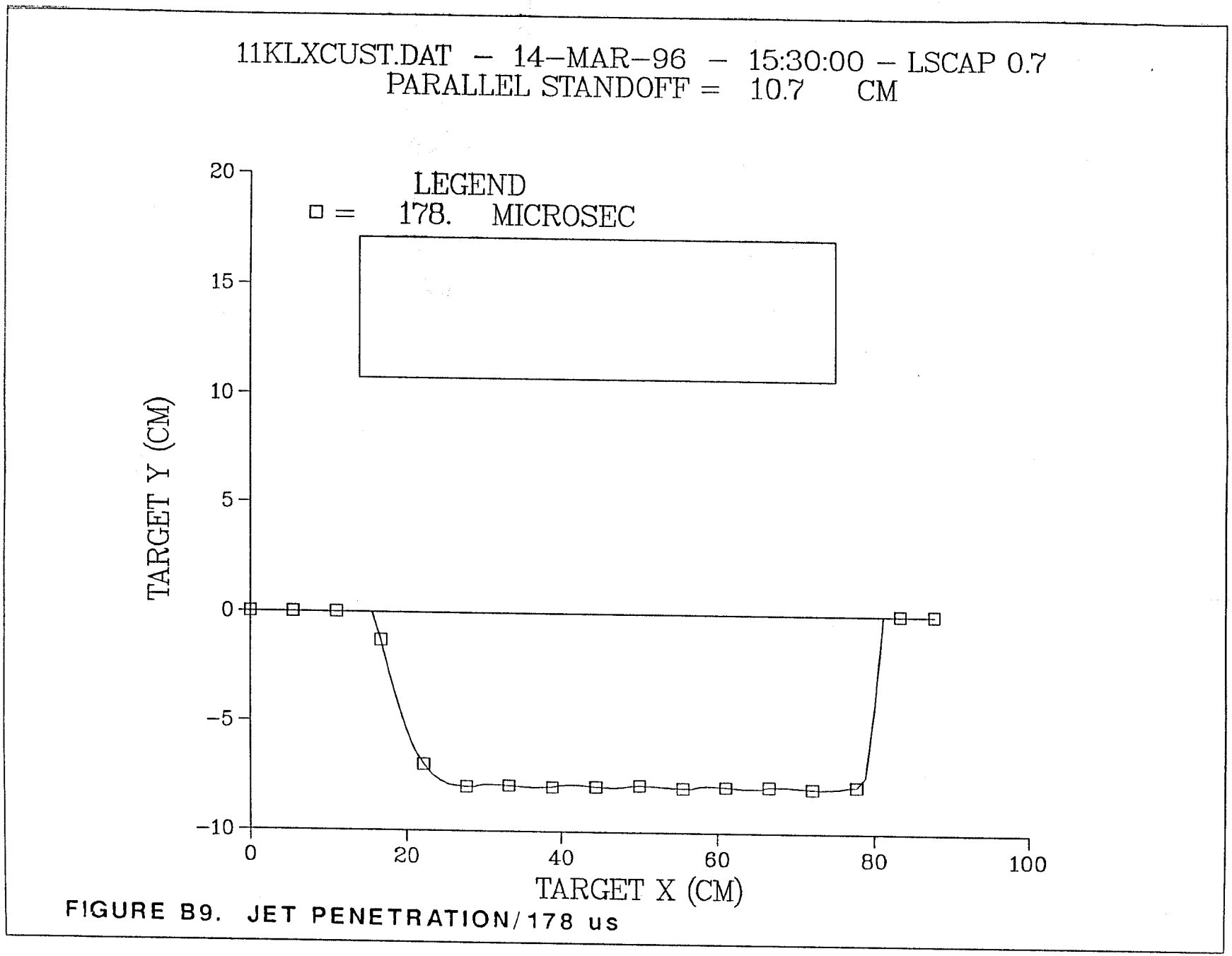

FIGURE B9. JET PENETRATION/178 us

Intentionally Left Blank

Distribution

1 Aerojet Ordnance Co.
Attn: J. Carleone
2521 Michelle
Tustin, CA 92680

1 Allied Signal Aerospace Co.
Kansas City Division
Attn: G. Oswald
P.O. Box 1159
Kansas City, MO 64141

1 Argonne National Laboratory
Attn: David B. Black
Bldg. 207
9700 South Cass Avenue
Argonne, IL 60439

1 BP Exploration, Inc.
Attn: Nick Whitehead
P.O. Box 4587
Houston, TX 77210-4587

1 Joseph Backofen
P.O. Box 1925
Washington, D.C. 20013

1 Ballistic Research Laboratory
Attn: J. T. Harrison
R. Jameson
W. P. Walter
Aberdeen Proving Ground
Aberdeen, MD 21005

1 James R. Barrett, P.E.
B&W Nuclear Environmental
Services, Inc.
P.O. Box 10548
2220 Langhome Road
Lynchburg, VA 24506-0548

1 Battelle Columbus Laboratory
Attn: D. R. Trott
505 King Avenue
Columbus, OH 43201

1 Bechtel Hanford, Inc.
Attn: Stephen K. Pulsford
Mail Stop X5-53
3350 George Washington Way
Richland, WA 99352

1 Center for Explosives
Technology Research
Attn: Per-Anders Persson
New Mexico Technical Institute
Socorro, NM 87801

1 Controlled Demolition, Inc.
Operations Headquarters
Attn: Fredrick M. Nicol
2737 Merryman's Mill Road
Phoenix, MD 21131-0326

1 Demex International, Ltd.
Attn: P. L. Marsh
P.O. Box 156
Picayune, Mo 39466

1 Dyna East Corporation
Attn: P. C. Cho
R. C. Ciccarelli
W. J. Flis
3132 Market Street
Philadelphia, PA 19104

1 E. I. DuPont de Nemours & Co., Inc.
Attn: F. C. Sawyers
3520 Pebble Beach Dr.
Farmers Branch, TX 75234

1 Ensign-Bickford Co.
Aerospace Division
Attn: L. J. Mecca
660 Hopmeadow St.
Simsbury, CT 06070

1 Exlosive Technology
Attn: M. D. Anderson
P.O. Box KK
Fairfield, CA 94533-0659

1 Halliburton
Explosive Products Center
Attn: John Regalbuto
David Leidel
8432 IH35W
Alvarado, TX 76009-9775

1 Honeywell, Inc.
Defense Systems Division
Attn: J. Houlton
5091 South County Road 18
Edina, MN 55436

1 ICI Americas, Inc.
P.O. Box 819
Valley Forge, PA 19482

1 Lawrence Livermore National
Laboratory
Attn: M. Finger
M. J. Murphy
B. Bowman
P.O. Box 808
Livermore, CA 94550

1 Lockheed Missiles & Space Co.
Attn: W. E. Moffatt
111 Lockheed Way
Sunnyvale, CA 94086

1 Los Alamos National Laboratory
Attn: M. Ginsberg, J960
R. Karpp, P940
J. Repa, J960
J. Walsh
P.O. Box 1663
Los Alamos, NM 87545

1 Mason & Hanger
Silas Mason Co., Inc.
Pantex Plant
Attn: D. Garrett
S. Hallett
P. Kramer
P.O. Box 30020
Amarillo, TX 79177

1 Naval Weapons Center
Materials Engineering Branch
Attn: G. A. Hayes
China Lake, CA 93555

1 Nobel Chemicals, Inc.
P.O. Box 1059
Jamestown, NC 27282

1 Pacific Northwest Laboratories
Attn: Suzanne Garrett, K8-18
P.O. Box 999
Richland, WA 99352

1 Picatinny Arsenal/ARDEC
Attn: Allen Epstein/SMCAR-FSM-M
Ron Karak/SMCAR-FSM-M
Picatinny Arsenal, NJ 07806-5000

1 Southwest Research Institute
Attn: A. B. Wenzel
6220 Culebra Road
San Antonio, TX 78284

1 Strategic Systems Project Office
Attn: D. Kenemuth, 27314
Department of the Navy
Washington, D.C. 20376

1 Teledyne
Attn: D. F. Elliott
3601 Union Road
Hollister, CA 95023

1 U.S. Army Armament Research
and Development Center
Attn: A. Garcia
Building 354
Dover, NJ 07801

1 University of Maryland
Mechanical Engineering Department
Attn: W. L. Fourney
College Park, MD 20723

1 White Oak Laboratory/NAVSWC
Attn: Bill Wilson
10901 New Hampshire Ave.
Silver Spring, MD 20903-5000

MS	0467	C. D. Croessmann, 5331
	0715	C. E. Olson, 6652
	0727	T. L. Sanders, 6406
	0751	D. S. Preece, 6117
	0751	J. T. Fredrich, 6117
	0761	R. V. Matalucci, 5822
	0783	M. R. Kodlick, 5511
	0783	D. J. Pedrotty, 5511
	0783	S. H. Scott, 5511
	0819	A. C. Robinson, 9231
	0820	P. Yarrington, 9232
	0834	A. C. Ratzel, 9112
	0980	L. N. Kmetyk, 5725
	1156	C. R. Cherry, 9333
	1156	P. W. Cooper, 9333
	1169	M. D. Furnish,9322
	1452	J. G. Harlan, 1552
	1452	J. A. Merson, 1552
	1452	F. J. Salas, 1552
	1453	R. A. Benham, 1553
	1453	R. W. Bickes, Jr., 1553
	1453	F. H. Braaten, Jr., 1553
	1453	S. H. Fischer, 1553
	1453	M. C. Grubelich, 1553
	1453	S. M. Harris, 1553
10	1453	M. G. Vigil, 1553
	1454	L. L. Bonzon, 1554
	1454	W. W. Tarbell, 1554
	9042	E. L. Voelker, 8742
1	9018	Central Technical Files, 8523-2
5	0899	Technical Library, 4414
2	0619	Review & Approval Desk, 12630 For DOE/OSTI